Studies on Characterization of

Hydration State of Layer-Modified Lipid Membrane

toward Design of Self-Assembly Drug

HAN JIN

MARCH 2021

Studies on Characterization of

Hydration State of Layer-Modified Lipid Membrane

toward Design of Self-Assembly Drug

A dissertation submitted to

THE GRADUATE SCHOOL OF ENGINEERING SCIENCE

OSAKA UNIVERSITY

in partial fulfillment of the requirements for the degree of

DOCTOR OF PHILOSOPHY IN ENGINEERING

BY

HAN JIN

MARCH 2021

Abstract

In this study, several guest molecules were utilized to modify lipid membrane at different region from hydrocarbon chain region to surface. The effects of these guest molecules on lipid membrane properties were investigated. Especially the hydration state of modified lipid membranes was mainly characterized to clarify how the extraneous molecules modify the hydration state of lipid membrane. The findings obtained are expect to be applied in optimizing the prodrug based self-assembly DDS by reasonable molecular structure design.

In chapter II, Quercetin (QCT) was utilized to modify the lipid membrane hydrocarbon chain region. Based on Raman spectra results, it was found that QCT could show great effect on the hydrocarbon tail region of lipid membrane, and hydrocarbon chain length and the level of unsaturation played an important role in determining the effect of QCT. For QCT, the regulation of hydration state of membrane lipid was achieved by changing the carbon chain packing density. This packing density variation of lipid membrane also affected on free radical diffusion within membrane.

In chapter III, the hydration state of lipid membrane interfacial region was modified by 2-hydroxyoleic acid (2OHOA). The effect of 2OHOA on DPPC and SM lipid membrane structure and hydration property were studied. Although there was no significant difference in overall structure between 2OHOA modified DPPC and SM lipid membrane, only 2OHOA-incorporated SM membrane polarity showed high sensitivity to pH condition and salt concentration. The reason for this difference can be attributed to the hydrogen bonding interaction of 2OHOA with SM molecules. Therefore, it is concluded that the hydration state of interfacial region can be modified by regulating the hydrogen bonding network formed by lipid molecules.

In chapter IV, Resveratrol (RES) was utilized to modify the surface polarity of heterogeneous lipid membranes, the effects of RES on lipid membrane properties were evaluated by multi-focal fluorescent probes. In each model membrane system, the incorporation of RES dramatically dehydrated the membrane surface, and this phenomenon was attributed to remove water species by hydrogen bonding formed with hydroxyl group of RES.

In chapter V, polyamidoamine amphiphilic dendrons (ADs) with multiple amide and amine groups were utilized to achieve control of superficial hydration shell modification of membrane. In this chapter, the structure and their properties of lipid/AD coassembly were characterized, and confirmed the formation of hydration shell on lipid membrane surface after G1-AD modification.

Above studies has indicated that the headgroup regulation and hydrocarbon chain density regulation are main factors to regulate the membrane hydration state. In chapter VI, the method to prepare SADDS with different hydration degree was proposed. The aryl carboxylic acid Oxaprozin was selected as a model molecule to design fatty acid-like Oxa-lipid, which is available for the control of the headgroup by pH condition and the packing density by different hydrophobic chain length.

In chapter VII, the general conclusions of this study are summarized and suggestions for clarifying relevance between the surface hydration state of carrier and its bioactivity are described as extension of this thesis.

PREFACE

This dissertation work was conducted under the supervision of Professor Hiroshi Umakoshi at Division of Chemical Engineering, Graduate School of Engineering Science, Osaka University from 2016 to 2021.

In this study, several guest molecules were utilized to modify lipid membrane at different region from hydrocarbon chain region to surface. The effects of these guest molecules on lipid membrane properties were investigated. Especially the hydration state of modified lipid membranes was mainly characterized to clarify how the extraneous molecules modify the hydration state of lipid membrane. The findings obtained are applied in proposing the method to design self-assembly drug to regulate the self-assembly properties.

The author hopes that this research would contribute to clarify the relevance between hydration state variation of lipid membrane and its influence on cellular function, and design lipid membrane targeted functional molecules. Furtherly, the insight obtained in this study is also expected to be applied in optimizing the prodrug based self-assembly drug delivery system by reasonable molecular structure design.

Han Jin

Division of Chemical Engineering
Graduate School of Engineering Science
Osaka University
Toyonaka, Osaka, 560-8531, Japan

Contents

Chapter 1

General Introduction

Lipid membranes as one of main self-assembly structures in organism do not just have a lipid-bilayer structure as barrier and contain embedded proteins. The realization that structures of these self-assembly structures are dynamic and possess their own physiochemical properties, which are also vital for understanding of their biofunction. In this chapter, some reported works, relating to the general concepts of self-assembly structure, lipid bilayer structure properties, and medical effect of self-assembly structure to shed the light on the key concepts in this study.

1. Self-assembly system for medical application

Self-assembly is a process in which a disordered system of pre-existing components forms an organized structure or pattern. The ordered self-assembled structure based on non-covalent interaction often endow it with new functionality. Especially in biological systems, self-assembly is one of the most important strategies to perform complex functions. The functionalities of macromolecule, such as protein or nucleic acid are attributed to their complex highly ordered structure, and cellular functions are usually associated with the activity of these biological macromolecules. Therefore, malfunctions of these macromolecules are normally regarded as the reasons for human pathologies, and most drugs on the market are developed to interact directly with target macromolecules. Another representative self-assembly structure in biological system is also need to be paid attention, cell membranes, which possess lipid bilayer structure self-assembled by huge variety of lipid classes and contain thousands of cellular proteins interacting with membranes in different ways. Comparison of self-assembly structure in biological system is shown in **Table 1-1**.

Table. 1-1 Self-assembly structure in biological system

	Genome (Gene)	Proteome (Protein)	Membranome (Membrane)
Element	Nucleic Acid A, T(U), G, C	Amino Acid G, A, Y, W, …	Phospholipids / Glycolipids / Cholesterol/ Fatty acid
Structure	Helix Structure Turn Structure	2nd Structure (Helix/sheet) 3rd Structure	Bilayer, Fluctuation, Microdomain etc…
Complexity	Standard	++	++++
Scientific Aspect	Clear Principle Comprehensive (Human Gene project)	Clearer Principle Structure analysis (Proteome Project)	Basic character of Pure system "Element" but not "system"
Engineering Aspect	Gene regulation RNA Interference iPS cell	Immunology Antibody Medicine Bioprocess design	Drug delivery system Cosmetic Microreactor

Membranes play an important role in defining cells and cell organelles, and various cellular processes occurred on membranes (e.g., metabolic, biochemical, signaling, biosynthetic, genetic and recycling processes). Therefore, cells with different biofunction show great difference in cell membrane composition and properties (Yeagle, *et al.*, 2005). It is also needed to point out that within a single cell membrane, coated pits, lipid rafts or synaptosomes, these locally defined (and sometimes transient) membrane domains are associated with regulation of certain proteins. Therefore, the classification of lipid types and formed membrane structures is important, and novel strategy for therapy has been developed which is named membrane-lipid therapy (Escriba, *et al.* ,2006). Different from the chemotherapy, drug molecules are expected to regulate biofunction of macromolecules. This new approach focuses on biomembrane as new target to modulate the cellular functions by regulating the self-assembled lipids bilayer structure (**Fig 1-1**). Therefore, intervention of both macromolecule and biomembrane self-assembly behavior or self-assembled structure in biological system play a dominant role for medical application.

Because the bottom-up process, self-assembly pathway offers the most realistic solution towards the fabrication of next-generation functional materials and devices, especially nano scale material. One of the main applications is development of drug delivery system. The nanometer scale is considered to be ideal to interact with cells membrane. Appropriate drug delivery vehicles can efficiently reach their target and minimizes off-target effects. Start from liposome, which is first developed as drug carrier

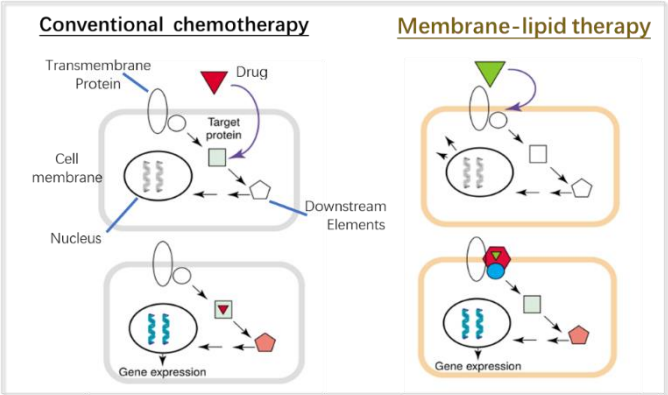

Fig. 1-1 Comparison of chemotherapy pathway and membrane-lipid therapy pathway

by mimicking cell membrane structure, molecular self-assembly has gained attention as a strategy for developing biomaterials for drug delivery applications that necessitate controlled transport, recognition, and stimuli responsiveness (Mendes, *et al.*, 2013).

With the development of self-assemble structure as drug delivery system (DDS), it is need to be noticed that besides the chemical design of these self-assembly, usually by modification of functional group on ingredient molecules, the self-assembly structure and properties also show influence on their bioactivities. Therefore, besides regulation of lipid self-assembled membrane properties, the reasonable self-assembly design is also one of main aspect to optimize the medical application of self-assembly system.

2. Biofunction and application of lipid bilayer structure

Lipids are amphipathic molecules which contain both hydrophobic and hydrophilic moieties. It is the amphiphilic nature of membrane lipids that make they can self-assembly to lipid bilayer in aqueous solution. Lipid membranes contain thousands of different lipids. (e.g., phospholipids, sphingolipids, cholesterol, isoprenoids, lysophospholipids, glycolipids, free fatty acids (FFAs), triglycerides, ceramides and cholesterol esters), each of which comprises a large number of different lipid type (**Fig. 1-2**).

From a holistic perspective, plasma membrane is delineating a membrane wall which divide the intracellular and the extracellular spaces. In addition, this “membrane wall” also worked as a matrix for various membrane proteins. In the last decade or so, it has been realized that membranes do not just have a lipid-bilayer structure as barrier and contain embedded proteins. The various lipids endow the lipid membranes with different

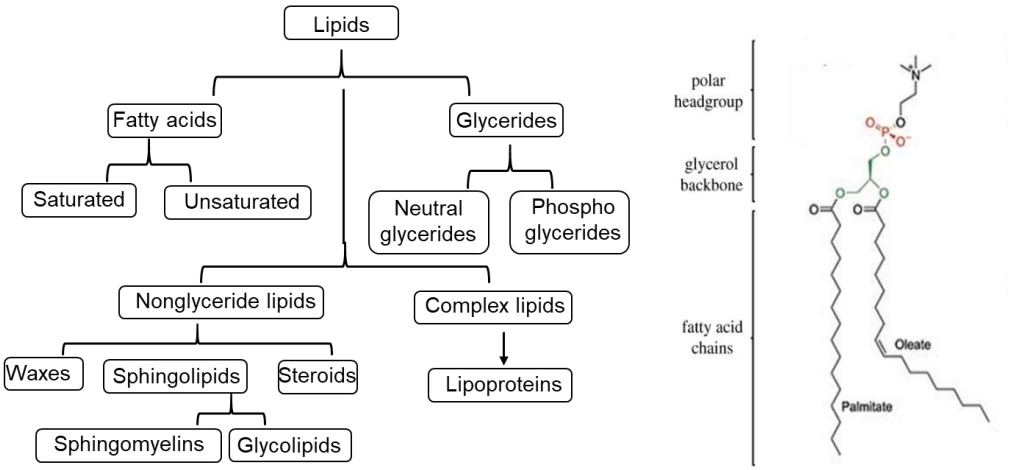

Fig. 1-2 Classification of lipid molecules and amphiphilic structure of phosphocholine

properties, especially for lipid membrane bilayer structure, lipid molecules with different structure greatly effect on membrane fluidity and nonlamellar-phase propensity properties, especially for lipid membrane bilayer structure, lipid molecules with different structure greatly effect on membrane fluidity and nonlamellar-phase propensity (**Fig. 1-3**, Harayama *et al.*, 2018). In addition, because lipids are not covalently connected in membranes, they self-assembled together and form transient arrangements dynamically whose stability can vary.

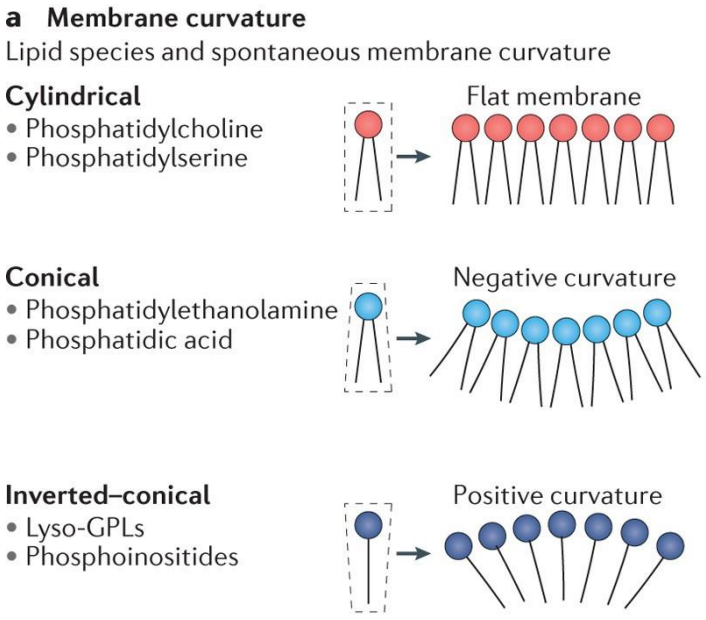

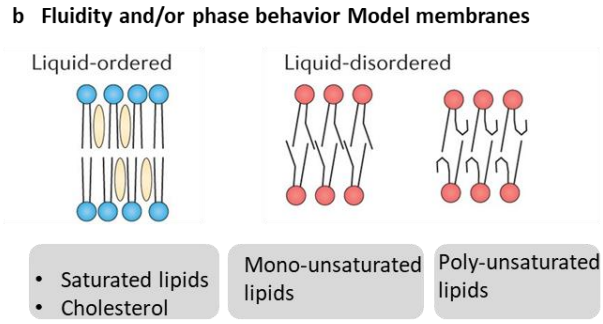

Fig. 1-3 Membranes properties resulted from the different structure of smaller components

Structures of these membranes are dynamic and contain areas of heterogeneous composition or structure which are vital for their formation, and these dynamic and heterogeneous structures have implications during stress and in relation to certain human diseases (**Table 1-2**).

Table 1-2 Human pathologies and lipid abnormalities

Disease	Membrane abnormality	Proposed molecular mechanisms	Refs
Cardiovascular (hypertension)	Changes in membrane phospholipid and cholesterol levels; changes in FA levels	Regulation of the membrane structure with concomitant alteration of membrane signaling, protein localization and activity	Escriba, P.V. et al., 2003
Cancer (pathological proliferation)	Changes in membrane FA levels	Altered cell structure and function (including cell proliferation)	Mikirova, N. et al., 2004
Neurological disorders	Reduced levels of PUFAs in brain cell membranes	Altered expression of transthyretin and other genes related to learning, cognitive and integrative functions	Puskas, L.G. et al., 2003
Infectious Diseases	Increased ceramide-enriched membrane domains	Modified membrane-lipid domains act as platforms for a wide variety of viruses, bacteria and parasite infections	Grassme, H. et al., 2005

There are some parameters that characterize these dynamic properties, such as phase state, packing state of acyl chains (membrane fluidity), hydration state (membrane polarity). On the one hand, the dynamic properties of lipid membrane are related to the regulation of the protein activity associated with cell membrane. Membrane fluidity was one of the first aspects of lipid structure shown to influence the activity of important proteins (Vessey *et al.,* 1974). the nonlamellar-phase propensity, another main property of lipids, has shown to be involved in controlling heterotrimeric G proteins for signal

transmission and amplification (Vogler, *et al.*, 2004; Escriba, *et al.*, 1997). On the other hand, the permeability, adhesion and diffusion of membrane would be influenced by variation of the lipid membrane properties (Steinkuhler *et al*., 2019). As the dynamic "platform", properties of lipid membrane in biological system are possible to be varied by diffusion of external small molecules to lipid membrane. This is also the base for membrane-lipid therapy approach. Several factors participate in integration of external (or internal) biomolecules into membrane surface, which are normally these main forces shown in **Table 1-3** (Yadav *et al.*, 2020). Among these factors, the hydrophobic interaction and hydrogen bonding usually play main role in interacting with lipid bilayer structure.

Table 1-3 Classes of distinct forces involved in self-assembly

Repulsive opposition force	Attractive driving force	Directional functional force
• Electric double layer • Solvation • Hydration • Steric	• Hydrophobic • π-π stacking • H-bond • Vander Waals • Solvation, Depletion, Bridging • Co-ordination	• Hydrogen bond • Steric repulsion • Co-odination

To investigate the role of the extraneous molecules in membranes, monitoring membrane properties *in situ* is an important task. Comparing with other methods that are capable of evaluating the properties, such as Fourier-transform infrared spectroscopy (FTIR), nuclear magnetic resonance spectroscopy (NMR) and electron paramagnetic resonance (EPR), the sensitivity of fluorescence techniques can reach to a single-molecule level and make it possible to evaluate in biological system with high complexity. In addition, based on different property of fluorescence probe, multi-focal properties of lipid bilayer system can be easily evaluated (Tham *et al.*, 2016). The evaluation of membrane fluidity can be achieved by the measurement of the fluorescence anisotropy of DPH and TMA-DPH respectively. About membrane polarity, which is the main parameter to evaluate the hydration state of lipid membrane can be evaluated by fluorescence probes with fluorescent decay kinetics depending on the dielectric constant of surrounding environment. Laurdan and Prodan are probes with environmental sensitivity that a

noticeable red-shift of their emission can be observed with increased solvent polarity due to the dipolar relaxation phenomenon (Parasassi *et al.*, 1994).

3. Role of hydration state at lipid membrane

It is known that water is a key element in a variety of structural and functional roles in membranes of living cells that takes relevance when cells suffer hydric, thermic or salt stress (Lee *et al.*, 2004). Coupling phenomena between membranes, such as adhesion, fusion, and stacking, depend on hydration forces derived from the restructuring of water (Ball *et al.*, 2008). The consideration of water as a structural component of biological membranes is relevant not only to define bilayer structural parameters in hydrated states, but mostly hydration-dehydration steps, which play a crucial role in several physiological processes. Therefore, the understanding of "water" relating to lipid membrane, namely hydration state at different located region with lipid bilayer structure of lipid membrane is crucial to clarity the effect of lipid membrane hydration property on its cellular functions.

From meso scale, namely regarding the lipid membrane structure as a whole, water around the lipid membrane can be roughly identified in a similar way as the water organized around an ion: surface bound water and bulk water. The surface bound is water excluded from the bulk water which dissolve solutes. Outside the surface coating region, solvent properties depend on the type of ions and its concentration. Water bound to the membrane is sequestered and unable to dissolve solutes. However, this region is considered to contribute to the permeability barrier. Bound water at the surface region might be related to affect the hydration properties, which is relating to govern various dynamical membrane properties such as lateral diffusion, compressibility and permeation. It is considered that specific compounds that may mimic water or with hydrogen bonding functional group can replace the surface bound water at some specific groups of lipid membrane (Disalvo *et al.*, 2008; Luzardo *et al.*, 2000).

From the micro scale, within the lipid bilayer, several regions are defined to describe the different located properties of lipid membrane, and the hydration state is one of the elements. Generally, the word "membrane surface" indicates the hydrophilic region of lipid bilayer, which behaviors as the interaction fields of hydrophilic headgroup with the

surrounding solvent water. The word “membrane interface” indicate the border region between the hydrophilic and hydrophobic moieties of the membrane, that is the region around the carboxyl group of the lipid molecules. At this region, the phosphate and the carbonyl groups of lipids are worked as the center of hydration (**Fig. 1-4**, Mencia *et al*., 2020). Some researchers made a more precise division of hydrophilic region of lipid membrane, named “membrane interphase”, which could be the region between membrane surface and membrane interface (Disalvo *et al*., 2014). The orientation of the dipolar or charged groups at the interphase region would determine the hydration state at some degree. Two important properties inherent to water and ion distribution must be considered: the surface charge potential and the dipole potential. The hydration state of phosphate, carbonyl and choline groups is mainly dependent on the adsorption of anions and anionic groups at the Stern layer (Lairion *et al.*, 2009).

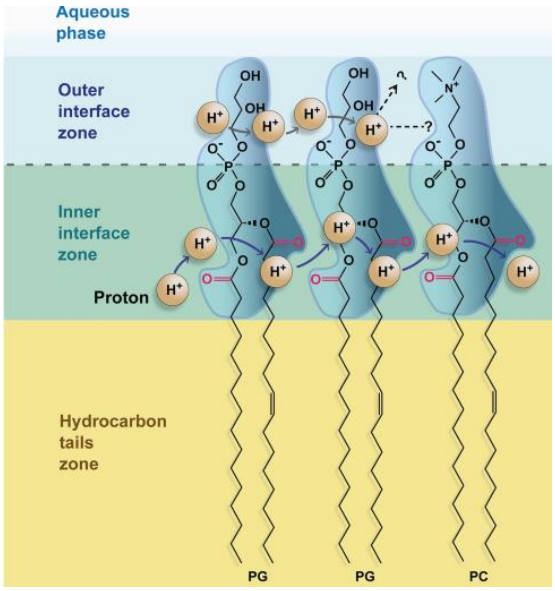

Fig. 1-4 Hydration state of lipid bilayer structure

The hydration property of lipid membrane at interfacial region has been well studied. based on multiple-components deconvolution (Watanabe *et al*., 2019). However, there are few studies about the regulation of hydration state at other region of lipid bilayer. How and which hydration levels are involved in each of the processes, such as membrane phase state variation, diffusion of radical oxidant radical (ROS), and cell uptake efficiency of some vehicle, or plasm membrane interaction is still a matter of debate. The discussion about the effect of the different hydration state arrangements within lipid bilayer structure

could make feasible the interactions is open.

4. Self-assembly structure-activity relation for drug delivery system

Self-assembly system represented by lipid membrane has been studied for many decades to be utilized as DDS. Various approaches have been developed to prepare self-assembly structure with desired performance. Different from using lipids or polymers to build carrier, recent years, self-assembly systems involving drug molecules are developed. “Prodrug” as strategy has been well established in earlier times. Prodrugs are chemically modified versions of the pharmacologically active agent that must undergo transformation in vivo to release the active drug, which provide possibilities to overcome various barriers to drug formulation and delivery. Combination the concept of prodrug and self-assembly, the prodrug self-assembled drug delivery system (SADDS) was proposed as novel approach to develop drug delivery system with higher safety and efficiency. SADDS make it possible to show high drug carrying capacity and keep almost all of the benefits of nanomedicine at the same time. In addition, the dynamic properties of the prodrugs formed SADDS may possess unique ability in tuning drug uptake and release of nanomedicine in a precise manner through molecular engineering.

Although there is still very little literature, researchers have found that the morphology and physicochemical properties of self-assembled structure have significant influence on the performance of the prodrug carriers. In addition, the self-assembly structure and self-assembly behavior control shows the difference in biological consequences (**Table 1-4**). The effects to fill this knowledge gap could greatly accelerate the development of the further rational SADDS design. For developing the SADDS, it is worth pointing out that the strategy to grasp the relevance of “molecule - self-assembly property” is an important issue for optimization of SADDS. Until now, only few studies devoted to proposal self-assembly structure control based on drug molecular design.

Among the properties of self-assembly, the hydration property is one of the key factors to improve pharmacokinetic behaviors, such as stability in the recirculation system and drug permeability from drug carrier (Komizu 2016; Poste and Papahadjopoulos 1976), the binding of macromolecules to membrane (Watanabe *et al.*, 2017) and the interaction with membrane (Bompard *et al.*, 2020). To modify the hydration properties of drug carrier,

Table 1-4. Biofunctions of self-assembly structure and behavior on its therapeutic effects

	Therapeutic agent	accessory	Morphology	Function	References
Effect of self-assembly structure	Irinotecan (Iri)	Fatty acid	Iri-5C NP (3.3 μm, 0.35 μm) Iri-8C NP (3.69 μm, 0.18 μm) Iri-12C NP (0.5 μm, 0.35 μm)	Cellular uptake Iri-12C >Iri-8C >Iri-5C>Iri	Zhang, C.Q. *et al.,* **2016**
	Capecitabine (5-FC)	Alkyl Chains	5-FCPalmityl SL NP (700 nm) 5-FCPhytanyl Cubic NP (164 nm) 5-FCOleyl Cubic NP (255 nm)	Hydrolysis rate 5-FCOleyl > 5-FCPhytanyl>5-FCPalmityl	Sagnella, S.M. *et al.,* **2011**
	Camptothecin (CPT)	β-sheet peptide	Tubular morphology mCPT-buss-Tau dCPT-buss-Tau qCPT-buss-Tau	dCPT-buSS-Tau was the most effective at inhibiting the proliferation of cancer	Cheetham, A. G. *et al.,* **2013**
Small molecules-instructed self-assembly for cell apoptosis	Metabolites		Amyloid-like structures	Induce cell apoptosis	Shira, S. N. *et al.,* **2015**
	Tetrapeptide derivative	Phosphotetrapeptide	Crescent-shaped supramolecular assemblies by Enzyme-Instructed Self-Assembly (EISA)	EISA disrupt cell membranes and target ER for selective cancer cell death.	Feng, Z. Q. *et al.,* **2018**
Transformative self-assembly structure for enhanced therapeutic effect	Doxorubicin	Acid-degradable acyclic cucurbit[n]uril	From vesicle to micelle by pH-stimulation	pH-induced conversion of supramolecular vesicles into micelles with changes in size and surface charge for promoted tumoral-cell uptake	Mao, W. P. *et al.,* **2019**

pegylation has been greatly used in previous studies.

Actually, description self-assembly structure also related to the water molecular behavior. Marsh has explored the common features of the hydrophobic effect, namely entropy and enthalpy convergence coupled with a large heat capacity for transfer from water to apolar environments, can be used to describe the self-assembly of phospholipids into micelles or membranes (Marsh 2016). Therefore, the self-assembly behavior control is greatly relating to the control of the hydration behavior in forming self-assembly structure. However, how to regulate the hydration behavior by the molecular design will is still need to be explored.

5. Overview of this study

The purpose of this study is to clarify how does functional molecules regulate the lipid membrane properties, especially the effects on the hydration state. Further, the information obtained are expected to applied in design of self-assembly with different properties by regulating its hydration property. Herein, four kinds of molecules were utilized to modify lipid membrane from hydrocarbon chain region to surface. For understanding the variation of lipid membrane properties caused by the guest molecules, the interaction between lipid membrane and the guest molecules were studied by bilayer and monolayer study (micro analysis). Finally, the findings are utilized to develop the prodrug based self-assembly drug delivery system by reasonable molecular structure design (meso design). The flame work and the flow chart of the present study are shown in **Fig. 1-5** and **1-6**, respectively.

In chapter II, Quercetin (QCT) was utilized to modify the lipid membrane hydrocarbon chain region. The interaction of QCT with various lipid membranes possessing different phase states and level of saturation were evaluated to obtain complementary information on the QCT behavior in the different lipid membranes. Based on Raman spectra, it is found that incorporation of QCT showed obvious effect on packing density, and the level of unsaturation of lipid molecule played an important role in determining the interaction of QCT within the hydrocarbon tail region of lipid membrane. For QCT, the regulation of hydration state of membrane lipid mainly was achieved by change the packing density. This packing density variation of lipid membrane contribute to inhibit free radical diffusion whin membrane.

In chapter III, the hydration state of lipid membrane interfacial region was modified by 2-hydroxyoleic acid (2OHOA). The effect of 2OHOA on DPPC and SM lipid membrane was studied to clarify the hydrogen bonding induced different effect on lipid membrane interfacial properties. For lipid membrane overall structure, based on the isotherm monolayer study of headgroup region and bilayer study of hydrocarbon chain region, there is no significant difference can be obtained between 2OHOA modified SM and DPPC membrane. However, comparing with 2OHOA-incorporated DPPC membrane, only in SM lipid membrane, the interfacial hydration state showed obvious sensitivity to pH condition and salt concentration.

In chapter IV, Resveratrol (RES) was utilized to modify the surface polarity of heterogenous membrane. The influence of RES on lipid membranes with different phase states was evaluated by utilizing membrane-binding fluorescent probes. The binding of RES lead to the membrane polarities decreasing slightly, regardless of the phase states of the membrane, while the membrane fluidities decreased only in the case of liquid-disordered phase. In each model membrane system, the incorporation of RES dramatically dehydrated the membrane surface. This dehydration effect at surface region was attributed to remove water species by hydrogen bonding formed with hydroxyl group of RES. It was been clarified that this effect of RES within lipid membrane could prevent the permeation of water-soluble materials, like ROS, and showed synergistic anti-oxidant effect.

In chapter V, it has known the hydration state of biomaterial surface play important roles in modulating biomolecular structure and function. Polyamidoamine amphiphilic dendrons (AD) contains multiple amide and amine groups, which is expected to achieve control of surficial hydration shell modification of membrane. The structure and properties of coassemblies formed by lipid and AD were characterized, especially about surficial hydration state. The results confirmed the formation of hydration shell on lipid membrane surface after G1-AD modification.

Above studies has indicated the headgroup regulation and hydrocarbon chain density regulation are main factor to regulate the membrane hydration state. Because the morphology or properties might also influence on their bioactivity, in this chapter, the method to control the SADDS self-assembly behavior by modulating its hydration degree was proposed. The aryl carboxylic acid Oxaprozin (Oxa), a primary non-steroidal anti-

inflammatory agent, was selected as a model molecule to design fatty acid-like Oxa-lipid. This prodrug design strategy achieved control of the drug self-assembly behavior, changing from micelle to fiber to solid based on pH conditions and molecular concentration.

In Chapter VII, the results obtained in this work are summarized in General Conclusions, and Suggestions for Future Works are described as extension of this thesis.

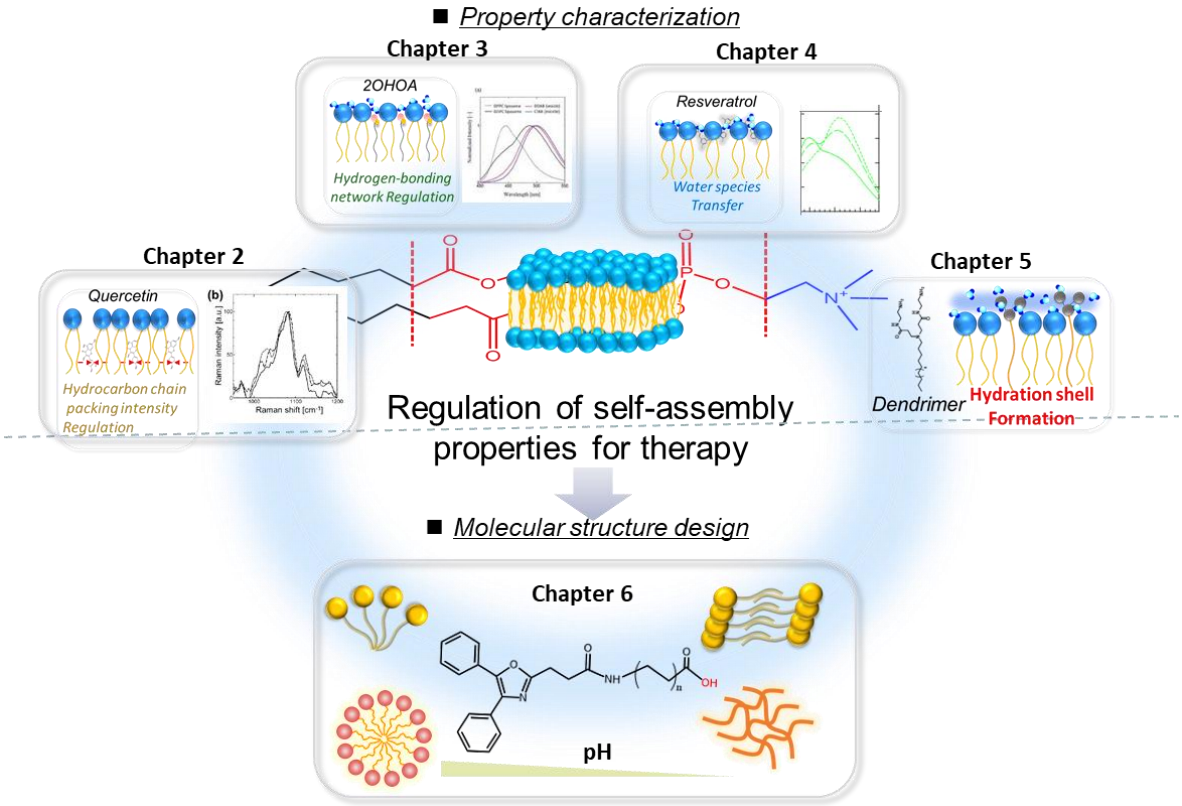

Fig. 1-5 Studies on characterization of lay-modified lipid membrane toward self-assembly drug design

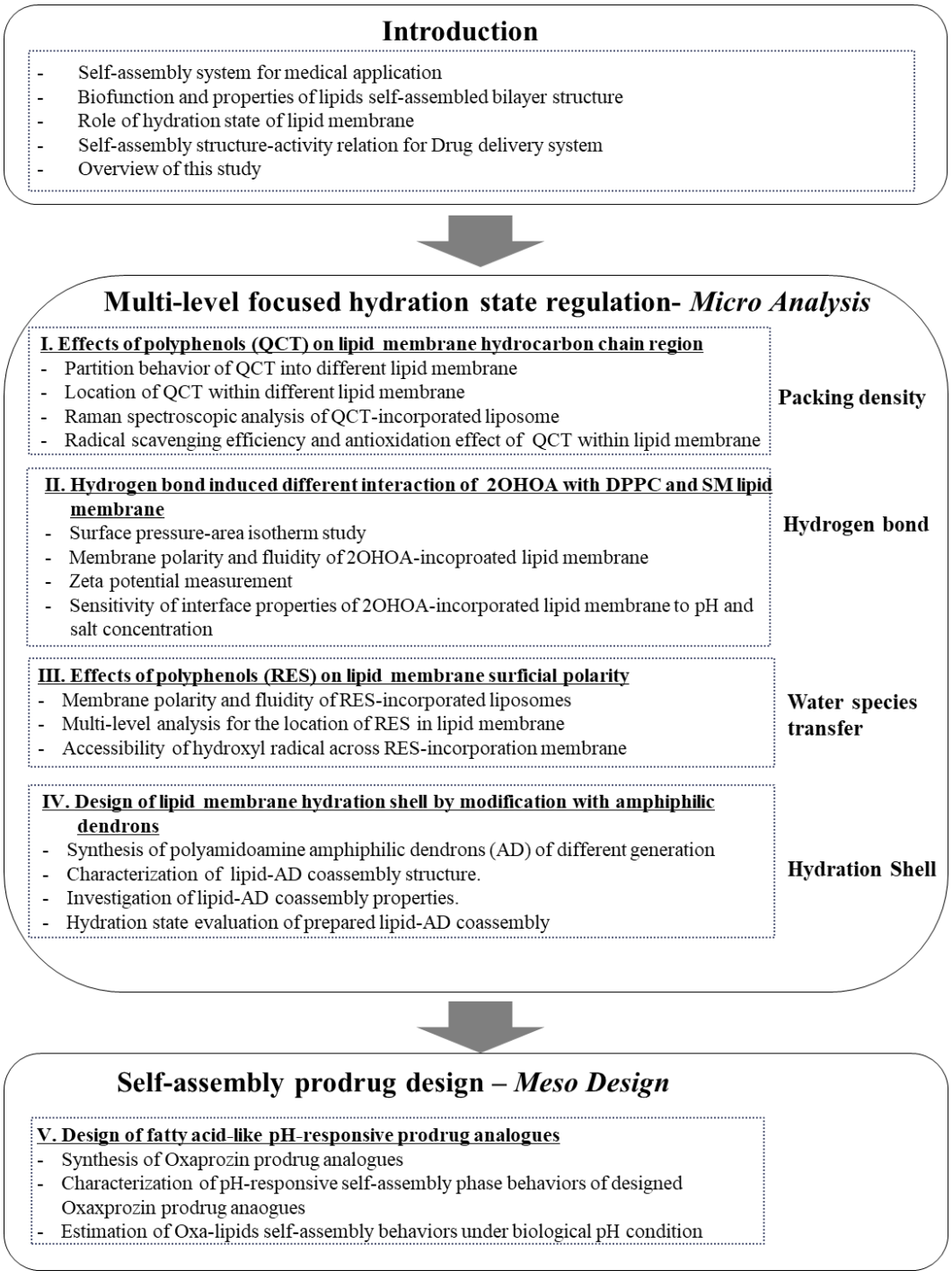

Fig. 1-6 Framework of present study

Chapter 2

Effects of Quercetin on lipid membrane hydrocarbon chain region

1. Introduction

Flavonoids are an important class of natural polyphenolic substances, which widely exist in vegetables and fruits, and constitute a major portion of human diet (Panche *et al.*, 2016). Flavonoids also show vast biological activities against oxidative stress, diabetes inflammation, cardiovascular diseases and cancer (Romano *et al.* 2013). Actually, most of these activities of flavonoids are derived from their antioxidative effects, due to multiple hydroxyl groups in their chemical structures. It has been reported that many diseases can be induced due to the imbalance between the production of oxidants such as reactive oxygen species (ROS) and the necessary antioxidant in organism, such as inflammatory diseases, Alzheimer's disease, cardiovascular diseases and cancers (Liu *et al.*, 2018). In many pathological conditions, lipid peroxidation are evidently observed, whereas the antioxidant activity of flavonoids can prevent lipid oxidation by locating at lipid membranes (Saija *et al.*, 1995; Han *et al.*, 2017). From the physiological and pharmacological view, the bioactive potential of flavonoids can be directly coupled with their interaction behaviors toward lipid membranes (Pawlikowska-Pawlęga *et al.*, 2003).

As a primary target of flavonoids, the interaction with lipid membranes has been frequently studied in recent years. A comprehensive review by Hendrich pointed out that the interaction between flavonoid compounds and lipid membranes depends on the flavonoid structures (Hendrich *et al.*, 2006). The governing factor for a flavonoid-lipid interaction seems to be the lipophilicity of flavonoid molecule (Van Dijk *et al.*, 2000). However, in addition to lipophilicity of the flavonoid molecules, the interaction (partition) between flavonoid and lipid membrane also can be affected and controlled by the membrane properties such as packing of lipid molecules, membrane polarity, *etc*. Therefore, much more attention also should be paid on interaction between flavonoids and lipid molecules for better understanding the mechanism of antioxidants by flavonoids.

Among various flavonoids, Quercetin (QCT) (3,5,7,3',4'-pentahydroxyflavone) (**Fig. 2-1**), found in common dietary sources, is one of the most abundant bioflavonols that exerts multiple pharmacological effects (Chen *et al.*, 2016). It has been reported that the flavonoids with a planar configuration such as QCT can change the membrane properties much more than non-planar flavonoids (Sanver *et al.*, 2016). In addition, QCT showed strong interaction with lipid membrane, and exhibited an enhanced antioxidant activity to protect lipid membrane from lipid peroxidation by locating within membrane. This result proved that besides the radical scavenging ability of QCT, the enhanced pharmacological potential can be obtained by QCT binding to lipid membranes. Recent studies have attempted to investigate the pharmaceutical effect of QCT at lipid membrane interferences (De Granada-Flor *et al.*, 2019; Alejandro de Athayde Moncorvo Collado, *et al.*, 2016). In these studies, attention has been mainly paid to the different interaction of QCT with lipid membrane in absence or presence of cholesterol, namely, the role and influence of cholesterol on interaction of QCT with lipid membrane. Therefore, more detail discussion is still required for distribution of QCT within lipid membrane composed by various lipid molecules, and also for how QCT differently interacts with various kinds of lipid molecules. Moreover, the detail understanding of QCT influence on lipid membrane properties should be required because the altered membrane property would also contribute to enhancing antioxidant activity.

In this chapter, we attempted to understand how and what parts in lipid membrane QCT distribute and interact with various lipid membrane. Furthermore, the influences of QCT on lipid membranes were studied for elucidation of its antioxidant activity. To attain this objective, followings were investigated: (i) the partition behaviors of QCT to the liposome membranes consisted of various lipid molecules; (ii) the localization of QCT molecules in liposome bilayer; and (iii) the effects of QCT on liposomes properties. In addition, 2,2-diphenyl-1-picrylhydrazyl (DPPH) radical scavenging assay was conducted and the prevention of DOPC oxidation by QCT was confirmed by mass spectrometry to estimate the radical scavenging efficiency of QCT in DOPC membrane. Based on these results, different interaction behaviors of QCT are discussed depending on the phase state of membrane and on lipid structure. Furthermore, it was elucidated that the antioxidant effect of QCT in lipid membrane was greatly related to its interaction with lipid molecules. Analysis of oxidation in unsaturated lipid membrane indicated altered liposomes by QCT

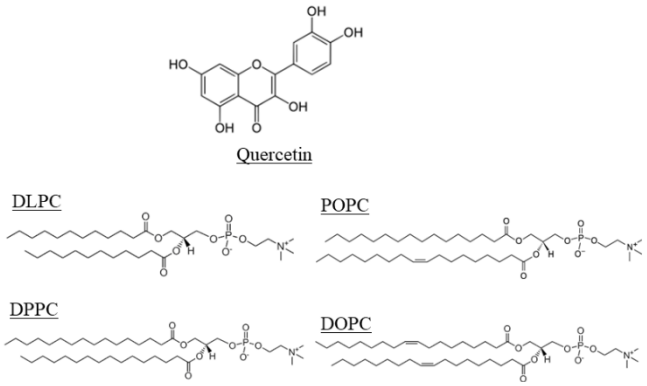

Fig. 2-1 Molecular structures of QCT and lipids used in this study

insertion also contribute to protecting unsaturated lipids from oxidation. Thus, the obtained information can be valuable and helpful for better understanding of the mechanism of QCT's antioxidant effects on biomembranes in the living organism.

2. Materials and Methods

2.1. Materials

1,2-Dioleoyl-*sn*-glycero-3-phosphocholine (DOPC), 1-palmitoyl-2-oleoyl-*sn*-glycero-3-phosphocholine (POPC), 1,2-dilauroyl-*sn*-glycero-3-phosphocholine (DLPC) and 1,2-dipalmitoyl-*sn*-glycero-3-phosphocholine (DPPC) (**Fig. 2-1)** were purchased from Avanti Polar Lipid Inc. (Alabaster, AL), and were used as received. Quercetin (QCT) and 2,2-diphenyl-1-picrylhydrazyl (DPPH) were purchased from Tokyo Chemical Industries (Tokyo, Japan). Other chemicals were purchased from Fujifilm Wako Pure Chemical Corporation (Osaka, Japan) and were used without further purification. Ultrapure water was prepared using Direct-Q® UV3 (Merck Millipore Co., Tokyo, Japan).

2.2. Liposome preparation

Liposomes were prepared by the lipid thin film hydration method as reported previously (MacDonald *et al.*, 1991). The lipids DOPC, POPC, DLPC, and DPPC were dissolved in chloroform. A chloroform solution including lipids was dried in a round-bottomed flask by rotary evaporator to yield dried lipid film. The lipid thin film was kept under high vacuum for at least 3 h, and then was hydrated at room temperature (25 ℃)

with ultrapure water. The obtained vesicle suspension was frozen at −80 °C and thawed at 60 °C. After the freeze−thaw cycle was repeated five times, the liposome suspensions were extruded 11times through polycarbonate membrane with a mean pore diameter of 100 nm using an extruding device (Liposofast; Avestin Inc., Ottawa, ON, Canada). The liposome suspensions (final lipid concentration: 20 mM) were kept in refrigerator (4 ℃) before usage.

2.3. Determination of partition coefficient

For determination of molar partition coefficient (K_p) of QCT (25 ℃, 50 mM phosphate buffer (pH 7.4)) into each liposome, the second derivative spectrometric analysis was conducted according to previous reports (Kitamura *et al.*, 1998; Kitamura *et al.*, 1995). The samples were prepared as follows, sample volume: 1 mL (including 2 vol% of ethanol); the concentration of QCT: 0.02 mM; Total lipid concentrations: 0–2.0 mM. Before measurements, samples were incubated for 3 h at room temperature (25 ℃). UV-vis spectra of QCT in the presence of liposomes were recorded with UV-vis spectrometer (UV-1800, Shimadzu, Kyoto, Japan) from 200-500 nm and the interval was 0.5 nm. The second derivative spectra were obtained by the Origin graph software (Lightstone, Tokyo, Japan) under following conditions: the cubic polynomial convolution of 15 points, and 0.5 nm interval.

K_p values is defined as

$$K_p = \frac{(f_{liposome})/[L]}{(f_{aqueous})/[W]}$$

, where ($f_{liposome}$): fraction of QCT in liposome, ($f_{aqueous}$): fraction of QCT in aqueous solution, [L]: lipid concentrations, [W]: water concentration (55.5 mol L^{-1}).

K_p values were estimated according to equation:

$$\Delta D = \frac{K_p \Delta D_{max}[L]}{K_p[L]+[W]} \qquad \text{(Eq. 2-1)}$$

where [L]: lipid concentrations, $\Delta D = {}^2D - {}^2D_0$: ${}^2D$ represents the intensity of the second derivative of flavonoid solution under the presence of liposomes and ${}^2D_0$ is the intensity

of the second derivative of QCT without liposomes at 410 nm, ΔD_{max}: the extrapolated value of the second derivative intensity when 100% of flavonoid is bound to liposomes, [W]: water concentration (55.5 mol L^{-1}). By plotting the values of [L] and ΔD, K_p values were obtained by non-linear least-squares method.

2.4. Fluorescence quenching measurements

The quenching of QCT fluorescence by iodide ion (KI) was measured to assess the location of QCT in liposomes. Liposome suspensions (1 mL) containing lipid (0.1 mM) and QCT (0.01 mM) in the presence or absence of KI in phosphate buffer solution (100 μL, KI conc. 4 mM) were incubated for 3 h at room temperature (25 °C). Then, the emission intensities (E_x=367 nm, E_m=550 nm) of liposomes suspension containing 10% QCT were recorded.

The degree of QCT fluorescence quenching was calculated as follow:

$$\text{Degree of quenching} = I_{Remained} / I_{Control} \qquad \text{(Eq. 2-2)}$$

, where $I_{Remained}$ and $I_{Control}$ represent the peak intensity of QCT in the presence and absence of KI, respectively.

2.5. Raman spectroscopic analysis

Raman spectra of QCT-incorporated liposomes suspension were recorded using a confocal Raman microscope (HR-800, Horiba, Ltd., Kyoto, Japan) with an exciting laser wavelength of 532 nm. The sample suspension was prepared as described above, wherein the initial concentrations of lipid and QCT were 1.5 mM and 0.0375 mM, respectively. QCT-incorporated liposomes were concentrated by ultracentrifugation (CS100FNX, Hitachi Koki Co., Ltd., Japan) at 50000 rpm for 2 h. Three scans were performed for each sample. The data obtained were accumulated, and then the background signals obtained from ultrapure water were removed to gain the Raman signals. The peak intensities at around 2850 cm^{-1} (I_{2850}) and 2890 cm^{-1} (I_{2890}) were recorded, and the chain packing density R was calculated as follows:

$$R = I_{2890} / I_{2850} \qquad \text{(Eq. 2-3)}$$

2.6. DPPH radical scavenging assay

Free radical scavenging ability of QCT under various liposomes was tested by DPPH radical scavenging assay. An ethanol solution including 1 mM DPPH was prepared, and 0.05 mL of this solution was mixed with 0.95 mL of liposome suspension containing QCT (total lipid concentration: 0.1 mM, total QCT concentration: 0.01 mM). The reaction mixture was vortexed thoroughly and left in the dark at room temperature (25 ℃) for 30 min. The absorbance of the mixture at 530 nm was measured. Percentage of DPPH radical scavenging activity was calculated by the following equation:

$$\%\ \text{of DPPH radical scavenging activity} = \frac{A_0 - A_1}{A_0} \times 100 \qquad \text{(Eq. 2-4)}$$

, where A_0 and $A_1$is the absorbance of DPPH in liposome suspension without QCT and of the DPPH in QCT incorporated liposome suspension.

2.7. Evaluation of DOPC oxidation by mass spectrometry

Suspensions containing 80 μM DOPC liposome and 2 μM QCT were treated with hydroxyl radicals, which was produced by mixing 100 μM Cu^{2+} and 1.2 mM H_2O_2, and were incubated for 48 h. Fast atom bombardment mass spectra of the products were obtained using a JMS-700 (JEOL, Tokyo, Japan) in the negative ion mode with 3-nitrobenzyl alcohol as the matrix and xenon gas to confirm the oxidation of DOPC molecule. Mass ranges were from *m/z* 1 to 1000.

3. Results and Discussion

3.1. The partition behavior of QCT into different liposomes

K_p is the molar partition coefficient of QCT between lipid and aqueous phases. To determine the partition coefficient K_p, separation and quantification of unbound QCT is required. However, QCT strongly binds with ultrafiltration membrane, and thus the correct quantification of unbound QCT was impossible. Therefore, the second derivative spectrophotometric analysis was conducted because this method does not require any separation and can eliminate the residual background signal effects of dispersed medium as liposomes. The representative zero order and second derivative UV-vis absorption spectra of QCT in DOPC liposomes were shown in **Fig. 2-2**. The information about four kinds of lipid molecules, formed liposomes, and partition coefficient K_p of QCT in aqueous phase / liposomes are summarized in **Table 2-1**. The obtained partition coefficients of QCT were the same order as those by Gunther and his coworkers' results (Gunther *et al.*, 2015). The K_p values of QCT indicate high partition of QCT into each liposome, and the order of K_p was as follows: DLPC >POPC >DOPC >DPPC. The higher K_p values of QCT was observed in liposomes with fluidized phase state at room temperature, indicating a preference of QCT to liquid-disordered phase rather than gel phase. Previous report also indicated a strong preference of QCT for l_d phase and showed 6.0-fold higher K_p values for l_d phase than l_o/l_d phase (de Granada-Flor, *et al.*, 2019). Among liposomes with liquid-disordered phase, compared with unsaturated lipids, DLPC showed the highest partition coefficient of QCT. These results indicated that the affinity of QCT to liposomes membrane is different due to the different lipid structures and properties.

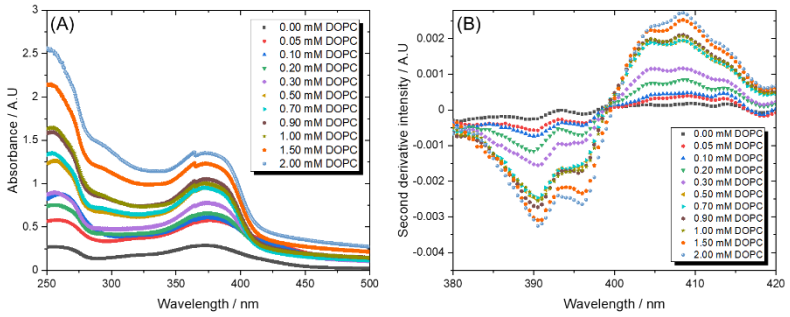

Fig. 2-2 (A)Zero order and (B) second derivative UV-vis spectrum of QCT under various concentration of DOPC liposome for estimation of K_p

Table 2-1 The summary of partition coefficient (K_p) of QCT to each liposome and the information of chemical structures and transition temperatures of each liposome.

Lipid Molecule	T_m	K_p
DOPC (18:1)	−17℃	$(8.30 \pm 1.54)\times10^4$
POPC (16:0-18:1)	−2℃	$(1.51 \pm 0.18)\times10^5$
DPPC (16:0)	41℃	$(4.46 \pm 1.46)\times10^4$
DLPC (12:0)	−2℃	$(2.39 \pm 0.49)\times10^5$

3.2. The location of QCT in different liposomes membrane

The location of QCT in various liposomes membranes was assessed by fluorescent quenching degree of QCT with iodide ion. Iodide ions are known to quench QCT fluorescence through a photoinduced electron transfer mechanism, and the quenching degree strongly depends on the distance between QCT and the quencher (KI). Almost all of KI distribute in aqueous phase, while QCT locate in liposomes due to obtained high K_p values. Thus, a higher degree of QCT fluorescence quenching by KI represents a closer distance between QCT (in membrane) and KI (in aqueous phase). In contrast, a less quenching could be evidence of the QCT location at a deeper position (hydrophobic center of bilayer). The fluorescence quenching results in different liposome membranes were shown in **Fig. 2-3**. The quenching of QCT fluorescence become significant with the order of DPPC>POPC>DOPC>DLPC, indicating the distribution of QCT varied from the membrane surface to inner region. This result means QCT prefers to be inserted into the inner region of liposome membrane with high fluidity because the lower packing site of hydrocarbon chain region is energy-stable binding site for QCT. In DPPC, the fluorescence quenching result clearly shows that QCT prefers to be located at the membrane surface, as compared to the cases of DOPC and DLPC. Therefore, it is concluded that the location of QCT in lipid membranes can be dependent on the phase state of bilayer. Furthermore, the different location of QCT within various lipid bilayer

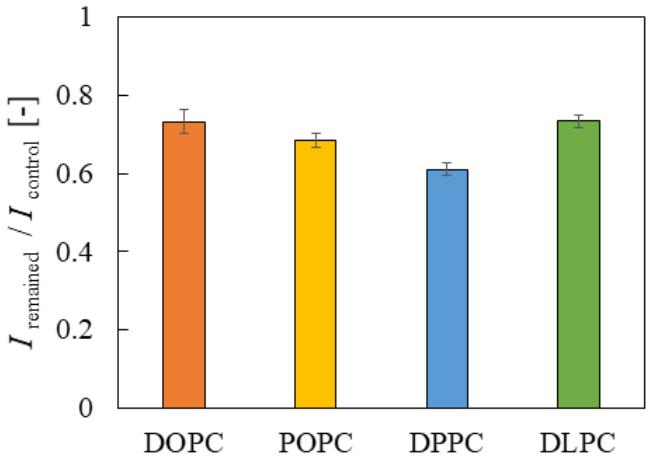

Fig. 2-3 Fluorescence quenching of QCT by iodide ion in the presence of each liposome. The error bars represent the standard deviation from the mean (n = 3).

would induce different main interaction between QCT and lipid membranes based on their own structural characteristics.

3.3. Raman spectroscopic analysis of QCT incorporated liposomes

Raman spectroscopy analysis provides information about the lipid chain packing state and chain torsion (Fox *et al.*, 2007). The Raman spectra of the liposomes incubated with 2.5 mol% QCT are shown in supporting information **Fig. 2-4**. The peaks at 2850 and 2890 cm^{-1} correspond to the symmetric and asymmetric vibrational modes of the $-CH_2-$ group, respectively. The peak intensity ratio, $R = (I_{2890} / I_{2850})$, is indicative of the hydrocarbon chain packing (Orendorff *et al.*, 2002). An increase in the peak intensity ratio indicates enhanced rotational hydrocarbon chain ordering. For pure phospholipid dispersions (liposomes), highly packed membranes, i.e., those in solid-ordered state (gel phase), show higher R values (R >1), while loosely packed membranes, i.e., those in liquid-disordered state (fluid phase), show lower R values (R <1) (Suga *et al.*, 2018). In **Fig. 2-5**, in the cases of saturated lipid systems (DLPC and DPPC liposomes), the addition of QCT decreased the R values. DPPC membrane was in highly packed state at 25 ℃, and the membrane packing was disturbed by the insertion of QCT. On the contrary, in the case of unsaturated lipid systems (DOPC and POPC liposomes), the addition of QCT increased the R values, suggesting formation of more packed states by the insertion of QCT. Compared with POPC, DOPC possessing unsaturation bond on both hydrocarbon chain

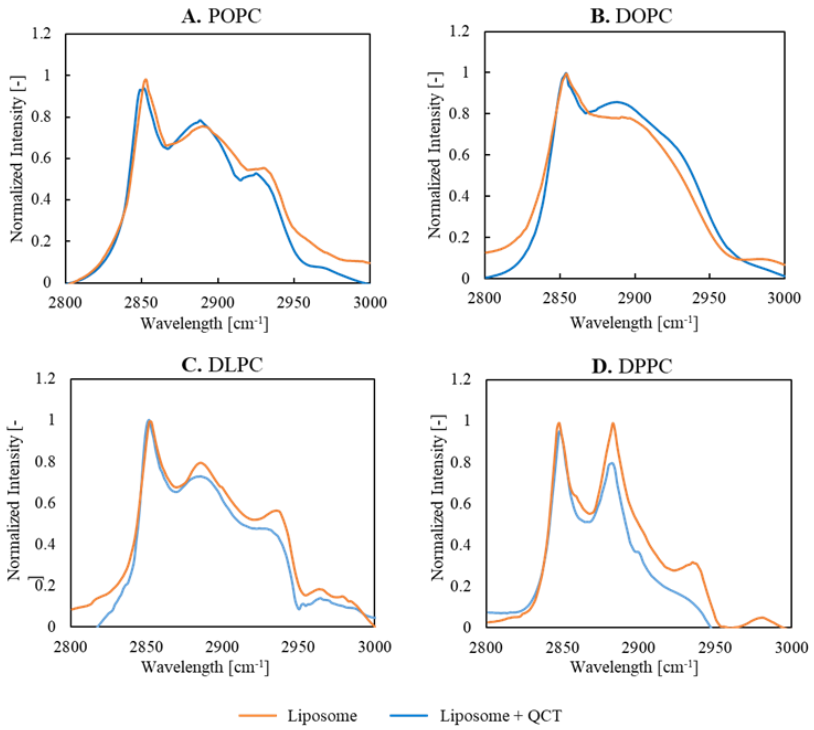

Fig. 2-4 Normalized Raman spectra of various liposome in the absence and presence of QCT.

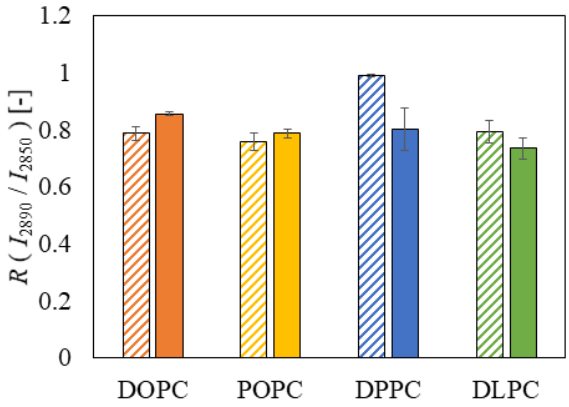

Fig. 2-5 Comparison of chain packing density values of each liposome before and after QCT incorporation. The chain packing density was calculated on the basis of Eq 3. Closed bar: the data after QCT insertion, Dashed bar: the data before QCT insertion. The error bars represent the standard deviation from the mean (n = 3).

showed more distinct compaction effect. These results indicate that QCT located near the carbon double bond and that the interaction between QCT and unsaturated hydrocarbon chain determined the effect of QCT on packing density of liposome membranes.

3.4. DPPH radical scavenging assay

The free radical scavenging ability of QCT was tested for each liposome, hereby DPPH was employed as radical reagent. The hydrogen atom donating ability of QCT was determined by the decolorization of 2,2-diphenyl-1-picrylhydrazyl (DPPH). DPPH produces violet/purple color in ethanol solution and fades to shades of yellow color in the presence of antioxidants. **Fig. 2-6** shows the radical scavenging ability of QCT at different concentration in liposomes. Under lower concentration of QCT, QCT in each condition showed almost same radical scavenging activity, because the influence of different interaction between QCT and lipid membrane is not distinct when less amount of QCT is incorporated to lipid membrane. Similarly, under high concentration of QCT, though the radical scavenging ability increased, all QCT incorporated liposomes except DPPC showed no significant difference between QCT in bulk phase without liposome. On the other hand, only QCT-incorporated DPPC membrane showed lowest scavenging activity under the higher QCT concentration.

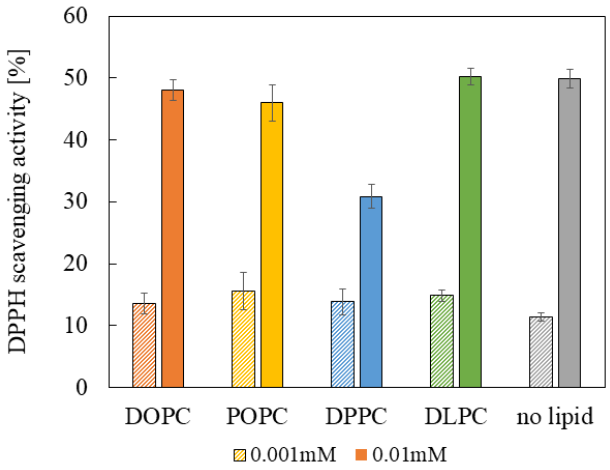

Fig. 2-6 Comparison of DPPH radical scavenging by QCT incorporated liposome and QCT. Dashed bar: QCT, 0.001 mM, Closed bar: QCT, 0.01 mM. The error bars represent the standard deviation from the mean (n = 6).

3.5. Anti-oxidation effect of QCT in liposomal membrane

Biomembranes in liquid-disordered phase state usually contain unsaturated fatty acids, which tend to be more oxidized due to presence of C=C double bond (Borst *et al.*, 2000). Herein, DOPC liposome was utilized as model of unsaturated lipid membrane to evaluate the antioxidant activity of QCT to protect unsaturated lipids from oxidation. The mass

spectra of DOPC molecules were measured in the absence and presence of QCT, after treatment with oxidant. After hydroxyl radical oxidation, new *m/z* peaks were found at 818 [M+2O], 840 [M+2O+Na^+], and 872 [M+4O+Na^+] *m/z*, which means oxidized DOPC species were generated. According to previous report, oxidized DOPC included carboxyl or aldehyde groups and showed increase of molecular weight, though it is uncertain where the carbonyl oxygen is added (Umakoshi *et al.*, 2011). This indicates that hydroxyl radical permeated through the lipid membrane, resulting in the oxidation of DOPC molecules with the extension of time. On the other hand, the mass spectra of QCT-incorporated DOPC liposome showed no evident change (**Fig. 2-7**), despite the existence of excess amount of hydroxyl radicals compared to total QCT amount. Therefore, this result proved that QCT in DOPC prevented the oxidation of DOPC molecules even under harsh conditions.

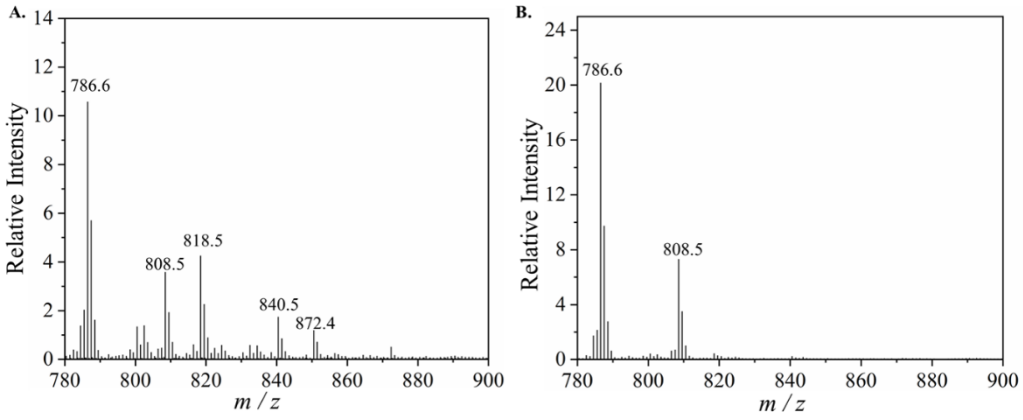

Fig. 2-7 Mass spectra of DOPC molecules from DOPC liposomes (A) dealt with oxidizing reagents and (B) incubated with 2.5% QCT and oxidizing agent.

QCT consists of two aromatic rings linked by oxygen-containing heterocyclic ring, which would show high affinity towards hydrophobic environment. However, Movileanu *et al.* demonstrated that the insertion behaviors of QCT in the membrane were pH-dependent (Movileanu *et al.*, 2000). At physiological condition (pH=7.4), deprotonated species of QCT with negative charge are predominant and log*P* is near 1.86, which means QCT is one of the less hydrophobic flavonoids compared with other flavonoids (Rothwell *et al.*, 2005). However, the K_p values of QCT for membrane-water, obtained in present

study, revealed a strong affinity to liposome membrane, which supports an aspect that lipid membranes are important target of QCT.

In the respect of K_p value, DPPC liposomes with gel phase showed the lowest K_p value among these four kinds of lipid membranes. From the analysis of QCT location in DPPC membrane, it is concluded that QCT located near the headgroup region. Other studies regarding the interaction of QCT with DPPC lipid membrane also showed consistent results that QCT prefers to locate at the membrane interface region in DPPC membrane (Shinha *et al.*, 2011; Pawlikowska-Pawlęga *et al.*, 2007; Ulrih *et al.*, 2015). As for driving force of partition, the hydrogen bonding between hydroxyl group of QCT and lipid polar headgroup of the C-O-P-O-C segment was confirmed as the main interaction between QCT and DPPC molecules by NMR and FTIR analysis in previous study (Pawlikowska-Pawlęga, *et al.*, 2014). Therefore, the lowest partition coefficient of QCT to DPPC liposome membrane could be due to the greater steric hindrance of headgroup and limited binding site at the interface. Our previous study also reported a similar result that the lipid membranes in gel phase displayed a lower adsorption capacity for small hydrophobic compound (Okamoto *et al.*, 2017).

Higher partition coefficients were observed in the liposomes in liquid-disordered phase. In these liposomes, QCT fluorescence quenching results elucidated that QCT preferentially distributed into inner region of lipid bilayer. Furthermore, K_p values revealed differences in the QCT interaction within DOPC, POPC and DLPC, even though all of these liposomes are in liquid-disordered phase. The difference of K_p values indicates that the partition behavior of QCT to liposome is not simply related to phase state of liposome, the subtle differences in chemical structure of lipids are also influential. This result suggested that the interaction between QCT and the hydrocarbon chain plays an important role in determining partition of QCT to liposomes.

About the location of QCT in DOPC and DLPC liposomes, both of which are in liquid-disordered phase, it is expected that QCT would be located in a deeper region in DOPC (C18:1) than in DLPC (C12:0), because longer hydrocarbon chains of DOPC (C18:1) can enlarge a hydrophobic space for QCT. However, the obtained result showed the quenching degree (location) was almost same in both DOPC and DLPC. Combined with Raman spectra analysis, these results reveal that the interaction of QCT with the carbon double bond of DOPC makes QCT molecules accumulated near the double bond region

and inhibits the insertion of QCT into the deeper region.

According to Raman spectra results, the disordering effect was obtained in saturated lipid systems (DPPC and DLPC), while the ordering effect was obtained in unsaturated lipid systems (DOPC and POPC). In DPPC, it is concluded that the localization of QCT at the polar headgroup region influenced the hydrocarbon chain conformation, leading to the increase of membrane fluidity. This effect can be considered as follows; the location of QCT molecules at the headgroup region increased the average area occupied by a lipid molecule, which weakened the van der Waals's force interaction between hydrocarbon chains and lowered the packing density. This result is consistent with other reports about the disordering effects of QCT confirmed by the decreasing of the main phase transition temperature of DPPC liposome (Pawlikowska-Pawlęga, *et al.*, 2007; Chulkov *et al.*, 2016). Besides, the monolayer study also indicated incorporation of QCT induced disruption of the high packing density of DPPC monolayer (Ferrreira, *et al.*, 2015).

In contrast, the ordering effect (increment of packing) of QCT was observed in DOPC with unsaturated bonds in both hydrocarbon chains. Arora *et al*. also has reported that flavonoids tend to locate in the hydrophobic core of DOPC membranes, proved by the results of significant decrease in membrane fluidity (Arora *et al.*, 2000). These results revealed that the interaction of QCT with the carbon double bond in hydrocarbon chain contribute to its ordering effects. This conclusion was also supported by the study about investigation of interaction between other planar polyphenols with DOPC liposome. Furthermore, the significant ordering effect of QCT in DOPC membrane would be one of the reasons for lower K_p value of DOPC membrane. Previous study also indicated the reasonability that increase of the bilayer thickness and decrease in the area per lipid caused the reduced by partitioning of QCT (Saha, *et al.*, 2020). Compared with the Raman results of DOPC and POPC, the incorporation of QCT to DLPC membrane decreased the packing density of hydrocarbon chains. This disordering effect might contribute to the higher K_p in DLPC than DOPC and POPC unsaturated lipid membranes.

Considering the chemical structures of the electron-donating flavonoids and the electron-accepting DPPH, it was suspected that a charge transfer complex was formed between the two species. A decrease in the absorbance was indicative of the loss of the DPPH free radical species. The DPPH free radical abstracts the phenolic hydrogen of the flavonoid molecule and this could be the general mechanism of the scavenging action of

the anti-peroxidative flavonoids. Therefore, active hydroxyl group of QCT molecule is indispensable for radical scavenging. Only QCT-incorporated DPPC membrane showed lowest DPPH scavenging activity under the higher QCT concentration. This result can be considered as follows; considering the partition coefficient of QCT to these liposomes, the amount of non-incorporated QCT was negligible ($4.18\times10-8 \sim 1.77\times10-7$mol L−1), which means almost all QCT were incorporated. Thus, the lower partition coefficient of QCT in DPPC membrane would not be the main reason but the interaction between the QCT and DPPC liposome membrane would. Different from QCT in other liposomes, QCT in DPPC located at the interfacial of lipid membrane and form hydrogen bonding between DPPC via hydroxyl group of QCT. Therefore, hydrogen bonding hindered some reaction site with DPPH and caused lowest scavenging activity of QCT in DPPC membrane. This is also supported by Saha's study, which suggested the hydrogen bonding formation between scavenger active hydroxyl groups of flavonoids and lipid molecules limited the ability to scavenge free radicals (Saha, *et al.*, 2020).

The result of mass spectrometry of DOPC molecules proved an efficient antioxidant activity of QCT in DOPC membrane, under excess amount of hydroxyl radicals over QCT for longtime incubation. As the one of reasons for this, the inserted QCT increases the rigidity of DOPC membrane (in an increased packing state), which can prevent the accessibility of free radical into the lipid bilayer. The other is that the location of QCT in DOPC membrane is close to the carbon double bond moiety. These effects could contribute to the enhancement of the radical scavenging efficiency of QCT within lipid membrane, which resulted in an inhibition of lipid peroxidation.

4. Summary

In this chapter, four kinds of liposomes were prepared as model biomembranes, and then the partition coefficient, distribution in lipid membrane and influence of the QCT on the membrane properties were evaluated. This work made following points clear; the partition of QCT to liposome membranes was affected by both liposome membrane phase state and the interference of QCT on liposome membrane properties. The location of QCT in liposome membrane was mainly determined by the stiffness of lipid membrane. The phase states of lipid membrane, sterically hindered or facilitated the interaction of QCT between the headgroup region or the hydrocarbon chain region. As for the effects of QCT on membrane packing density, the degree of unsaturation played an important role in compacting the hydrocarbon tail of lipid molecules. QCT showed higher compaction effect on unsaturated lipid membrane, which indicating QCT may possess higher affinity to carbon-carbon double bound. The different binding location of QCT in different liposome membranes would be related to show its antioxidant effects. Especially, the ordering effect of QCT in unsaturated lipid systems could inhibit the accessibility and diffusion of water-soluble ROS, which is expected to contribute to a synergistic antioxidant effect of QCT that protects lipid membrane from lipid peroxidation. Thus, our method based on membrane analysis would be also helpful and applicable for understanding the mechanism of other antioxidants effects on lipid membrane.

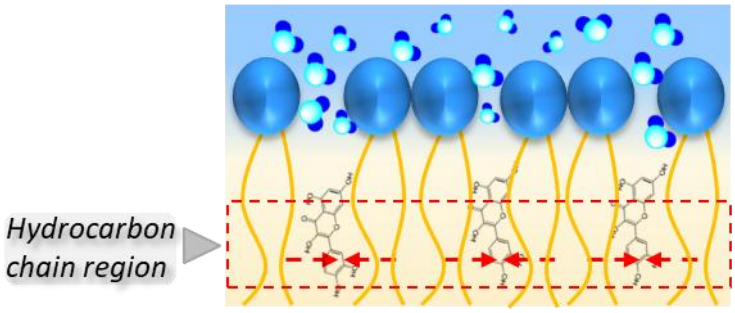

Fig. 2-8 Effect of QCT on hydrocarbon chain region of lipid membrane

Chapter 3

Hydrogen bond induced different interaction of 2OHOA with DPPC and SM lipid membrane

1. Introduction

The biomembrane existing in cell and cellular organelles possess the self-assembled lipid bilayer, which worked as flatform where lipids and proteins are organized together and involved in various important biochemical processes. The correct membrane protein activity control is required, and the lipids localized within cellular membrane are playing an important role in these processes. Thus, any alteration or modifications in the lipid membrane composition will induce both the disturbance in membrane structure and properties and in the membrane protein activities participating for example in signaling cellular processes (Escriba *et al.*, 2017). Indeed, it has been reported that it is possible for several functional compounds to act by regulating signal transduction occurred on lipid membrane through a new therapeutic approach named Membrane Lipid Therapy. Based on structure–function principles, this approach focused on the regulation of the membrane lipid organization (Escriba *et al.*, 2006).

2-Hydroxyoleic acid (2OHOA) is the first designed membrane lipid target drug molecule, which achieved the molecule of a slower metabolism and longer half-life than oleic acid (Escriba *et al.*, 2015). It has been confirmed that 2OHOA possesses antihypertension, anticancer activity (Alemany *et al.*, 2006; Teres *et al.*, 2012). The mechanism of anticancer activity of 2OHOA is complex and still under detailed verification. However, it shows that its therapeutic effects are related to both a direct influence of the composition of the cell membrane and modulate the properties of membrane, such as membrane fluidity (Barcelo *et al.*, 2004), microdomain reorganization (Ibarguren *et al.*, 2013) and the increase of the tendency to form non-lamellar structures (Yang *et al.*, 2005). However, actually the obtained effect of 2OHOA on lipid membranes showed less difference comparing with OA (Ibarguren *et al.*, 2013). From the respective of chemical structure of 2OHOA, modification of hydroxyl group to OA increased half-life of 2OHOA, however, it seems the study about the influence of modified hydroxyl group on 2OHOA-lipid inter-molecule interaction are still insufficient. It is important to

point out that lipid molecules possessing hydroxyl group usually give them special performance when interacting with other lipids, like ceramide or cholesterol (de la Arada *et al.*, 2020; Chachaj-Brekiesz *et al.*, 2019), especially interact with sphingolipids which are the major lipid species known to be associated with raft domain stability. They can form a strong intermolecular hydrogen bond with other lipid or water molecules through hydrogen binding acceptor (C=O, P=O, 3OH, or 2NH) and donor moieties (3OH or 2NH). (Slotte, *et al.*, 2016). Phospholipid and sphingomyelin are the most naturally abundant zwitterionic choline-type membrane lipids. For both of them, long saturated acyl chain allows them to packed tightly, showing same the phase transition temperature in spite of different properties of their interface (Parasassi *et al.*, 1991; Kuiika *et al*., 2001).

This chapter was aimed at explaining the different interaction of 2OHOA with saturated SM and saturated PC in the lipid membrane to clarify the influence of interfacial properties to the interaction of 2OHOA with lipids. And our systematic study allowed to conclude that the structure of interfacial properties of the lipid membrane paly important role in 2OHOA-phosphalipid interactions, while the hydrophobic region is significantly less important in this respect. From the molecular point of view, these differences can be attributed to multiply chemical interactions, especially electrostatic and hydrogen bonding.

2. Materials and Methods

2.1. Materials

1,2-dipalmitoyl-sn-glycero-3-phosphocholine (DPPC), Sphingomyelin (Egg, Chicken) (eggSM), and 2-hydroxyoleic acid (sodium salt) (2OHOA) were purchased in powder form (>99% purity, Avanti Polar Lipids, Inc., Alabaster, AL, U.S.A.). Lipid stock solutions of desired concentrations (99+% purity, ACROS Organics, NJ, U.S.A.), sodium phosphate monobasic monohydrate, and sodium chloride (NaH_2PO_4.H2O, 99.2% purity, NaCl, 99.9% purity, Fisher Scientific, Waltham, MA, U.S.A.) were used to prepare the phosphate buffer. Water used in experiments was purified with a Milli-Q Gradient water purification system with a resistivity of 18.0 MΩ·cm. For fluorescence probe, 1,6-diphenyl-1,3,5-hexatriene (DPH) and 6-dodecanoyl-2-dimethylaminonaphthalene (Laurdan) were purchased from Sigma-Aldrich (St. Louis, MO, USA). Other chemicals were purchased from Wako Pure Chemical (Osaka, Japan) and were used without further purification.

2.2. Liposome preparation

Liposomes were prepared by the lipid film hydration method as reported previously. (27) The lipids DPPC, eggSM, DPPC/2OHOA = 1/9 （3/7 and 5/5） and eggSM/2OHOA = 1/9 （3/7 and 5/5） were dissolved in chloroform/methanol (v/v = 9/1). These organic solvents containing lipids were dried in a round-bottomed flask by rotary evaporation under vacuum to yield a dried lipid film. The lipid thin films were kept under high vacuum for at least 3 h and then hydrated at room temperature with Milli-Q water. The vesicle suspension was frozen at −80 °C and thawed at 60 °C. After the freeze–thaw cycle was repeated five times, the liposome suspensions were extruded 11 times through polycarbonate membrane with a mean pore diameter of 100 nm using an extruding device (Liposofast; Avestin Inc., Ottawa, ON, Canada). The liposome suspensions with final concentration of 20 mM lipid were kept refrigerated before usage.

2.3. Investigation of the bilayer membrane fluidity

The fluidities of the bilayer membranes were determined by measuring the fluorescence anisotropy of DPH incorporated in the liposomes (lipid / fluorescence

probes molar ratio of 200:1), respectively, using the fluorescence spectrophotometer FP-6500 (JASCO, Tokyo, Japan). Liposome suspensions diluted by Milli-Q water, 0.5 mM phosphate buffer, 140 mM phosphate buffer with the final concentration of lipids is 100 μM. Fluorescence probe DPH (100 μM in ethanol) was added to liposome suspensions, and the suspensions were incubated at 25°C overnight. The samples were excited with vertically polarized light (360 nm), and the emission intensities both perpendicular ($I_{\perp}$) and parallel ($I_{/\!/}$) to the excited light were recorded at 430 nm. The polarization (*P*) of DPH was then calculated by the following formulas:

$$P = \frac{I_{\parallel} - GI_{\perp}}{I_{\parallel} + GI_{\perp}} \qquad \text{(Eq. 3-1)}$$

$$G = i_{\parallel}/i_{\perp} \qquad \text{(Eq. 3-2)}$$

where $i_{\perp}$ and $i_{\parallel}$ are emission intensities perpendicular and parallel to the horizontally polarized light, respectively, and *G* is the correction factor. The fluidity was defined as the reciprocal of polarization, 1/*P*.

2.4. Investigation of the bilayer membrane polarity

Fluorescence probe, Laurdan located near the interfacial region within lipid bilayer membrane, is sensitive to the polarity around them, which allows the membrane polarity to be determined. The sample solutions were prepared in the same way as the membrane fluidity measurements, except the fluorescence probes were Laurdan with a lipid:probe ratio of 200:1. The fluorescence spectrum of Laurdan in each liposome was recorded with excitation wavelength of 340 nm, at appropriate emission wavelengths from 400 to 600 nm at 25 °C, and the general polarization (GP_{340}) for each emission wavelength is as follows:

$$GP_{340,\ Laurdan} = (I_{440} - I_{490})/(I_{440} + I_{490}) \qquad \text{(Eq. 3-3)}$$

where I_{440} and I_{490} are the emission intensities of Laudran at 440 and 490 nm, respectively.

2.5. Monolayer surface pressure-area (π-A) isotherm measurement

A Teflon Langmuir−Blodgett trough (Type 611, Nima Coventry, UK) was used to measure lipid monolayer surface pressure−area (Π−A) isotherms. The trough experiments were carried out at a room temperature of 24.5 ± 1.0 °C on a subphase of Milli-Q water (pH of 5.7 ± 0.2). Analysis of isotherm data was shown as follows:

The behavior of 2OHOA in mixed films were determined based on the excess area per molecule A_{ex} in the mixed monolayer calculated as the following **Eq. 3-5**:

$$A_{ex} = A_{12} - (A_1x_1 + A_2x_2) \qquad \text{(Eq. 3-5)}$$

Where A_1, A_2 are mean area per molecule and x_1, x_2 are molar fractions of eggSM and 2OHOA, respectively, at the given surface pressure. A_{12} is mean area per lipid molecule in the mixed system. Additionally, partial molecular area of eggSM in the mixed monolayers were calculated at pressure at π=30 mN/m by a procedure in which tangents to the area-composition curve are extrapolated. To analyze the interaction of 2OHOA and eggSM molecules in each binary monolayer, the Gibbs free energy of mixing (ΔG_{mix}) was calculated by **Eq. 3-6**:

$$\Delta G_{mix} = \Delta G_{ex} + \Delta G_{ideal} \qquad \text{(Eq. 3-6)}$$

$$\Delta G_{ex} = \int_0^{\pi} A d\pi = \int_0^{\pi} A_{12} - (A_1x_1 + A_2x_2) d\pi$$

$$\Delta G_{ideal} = kT(x_1 ln x_1 + x_2 ln x_2)$$

Where the k is the Boltzmann constant and T is temperature.

2.6. Zeta potential measurement

A Malvern Zetasizer Nano ZS90 instrument (Southborough, MA, U.S.A.) was used to perform dynamic light scattering measurements to measure the zeta potential. Approximately 1 mL of sample (conc. = 200μM) was loaded into the cuvette and allowed equilibrate to 25 °C. Zeta potential measurements based on the electrophoretic mobility were performed to quantify the surface potential at the hydrodynamic slip plane using the Smoluchowski approximation (f(κa) = 1.5). Potential values were obtained from at least 3 independently prepared samples with at least 3 separate measurements per sample (>30 runs per measurement) for each vesicle composition.

3. Results and Discussion

3.1. Surface pressure – area isotherm studies

To evaluate the effect of 2OHOA on DPPC and SM membrane surface region, compression isotherms for pure 2OHOA and mixed with DPPC or SM were recorded. By increasing the surface pressure (π), the compression isotherms for DPPC (SM)/2OHOA mixture systems were recorded in **Fig. 3-1**, and the amount of 2OHOA was adjusted from 10, 30 and 50 mol%. The melting temperatures (T_m) of DPPC and SM are near 41 °C. In both system of the DPPC/2OHOA or SM/2OHOA mixtures, the isotherms of DPPC/2OHOA (2OHOA: 10, 30, and 50 mol%) appeared between pure DPPC (or SM) and 2OHOA isotherms. In both systems, only a slight condensation effect was observed in the lipid monolayer with 10 and 30 mol% 2OHOA.

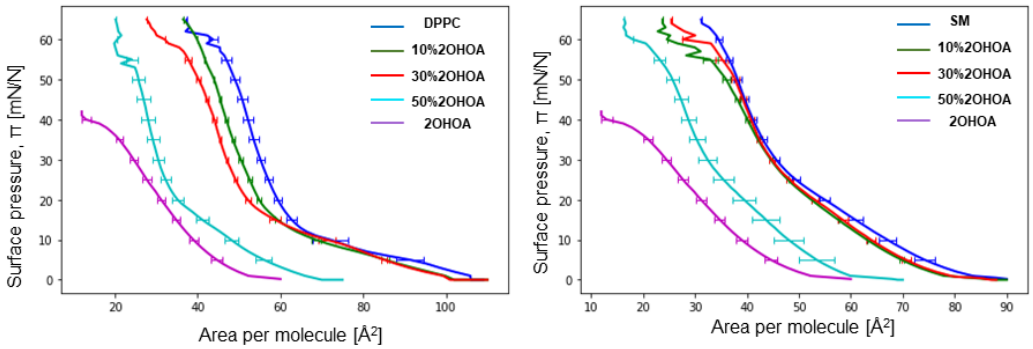

Fig. 3-1 Surface pressure – area (π-A) isotherms for pure component lipid films

Similarly, the excess area (A_{ex}) values at 30 mN/m were almost no change in both DPPC/2OHOA and SM/2OHOA system **Fig. 3-2**. However, when 2OHOA molar ratio is not more than 30%, the excess area showed almost no significant change, while the excess area decreased when molar ratio of 2OHOA is 50%, indicating high possibility that phase transition occurred, and an attractive interaction between DPPC or SM and 2OHOA with a tighter membrane packing. These similar results of 2OHOA in DPPC and SM indicated 2OHOA showed almost no different influence on DPPC and SM surficial region structure. For Gibbs free energies analysis, the Gibbs free energies of mixing (ΔG_{mix}) of DPPC/2OHOA and SM/2OHOA monolayers were all negative (**Fig. 3-3**), demonstrating that 2OHOA is miscible in DPPC and SM monolayers at least up to 50 mol%. but more less energy shown in SM lipid

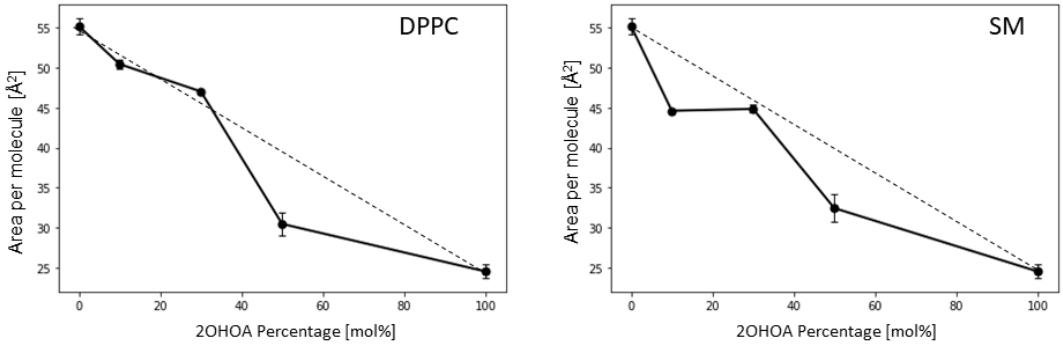

Fig. 3-2 Average molecular area of DPPC/2OHOA and SM/2OHOA Dotted lines represent ideal area at each ratio.

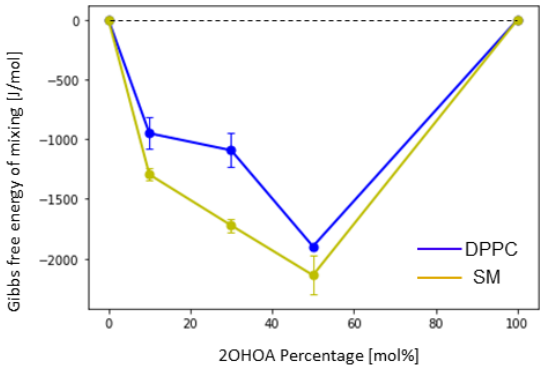

Fig. 3-3 Gibbs free excess energy of mixed monolayer at π = 30 mN/m

membrane than with DPPC. These findings suggest that 2OHOA prefers to interact with saturated SM in lipid monolayer systems.

3.2. Membrane polarity and fluidity of 2OHOA-incorporated lipid membrane

Previous work has indicated that the lipid monolayer characteristics at high surface pressure correlate with bilayer membrane properties. It is assumed that the condensation effect of DPPC(SM)/2OHOA in monolayers at π = 30 mN/m should be comparable with that in vesicular systems. To clarify the role of 2OHOA in membranes, 2OHOA-containing vesicles were prepared and characterized by fluorescent probes. The fluorescent probe, Laurdan, is widely used to characterize the polar environment in vesicle membranes. The emission peak position of Laurdan corresponds to the membrane

hydration state: a sharp peak at around 440 nm indicated less hydration state of lipid bilayer, a broader peak at 440 nm means higher hydration degree of lipid membrane.

As DPH can bind to lipid tails (acyl chains) in the membrane interior, ($1/P$) is an important indicator used to characterize the fluidity of lipid bilayers. **Fig. 3-3** displays the membrane polarity (GP_{340}) and membrane fluidity ($1/P$) as a function of 2OHOA mol%. The phase state of the membrane can be roughly estimated based on the 1/P values. Specifically, a higher 1/PDPH value ($1/P > 6$) indicates a fluid-phase membrane (liquid disordered phase, l_d), while a lower 1/P value ($1/P < 6$) indicates an ordered membrane (S_o or l_o). SM can form a strong intermolecular hydrogen bond with other lipid or water molecules through hydrogen binding acceptor and donor moieties at the interface region. Thus, SM showed less GP_{340} value than DPPC membrane although the membrane fluidity measured by DPH showed almost no difference. The Laurdan spectra of 2OHOA-incorporated DPPC lipid membrane showed no evident change comparing with pure DPPC, indicating the addition of 2OHOA did not disturb the phase state of DPPC lipid membrane. Comparing the different effects of 2OHOA in DPPC and SM lipid membrane, it can be concluded that the 2OHOA showed greater influence on interface region of lipid bilayer and almost no distinct effect on hydrocarbon tail region of lipid bilayer.

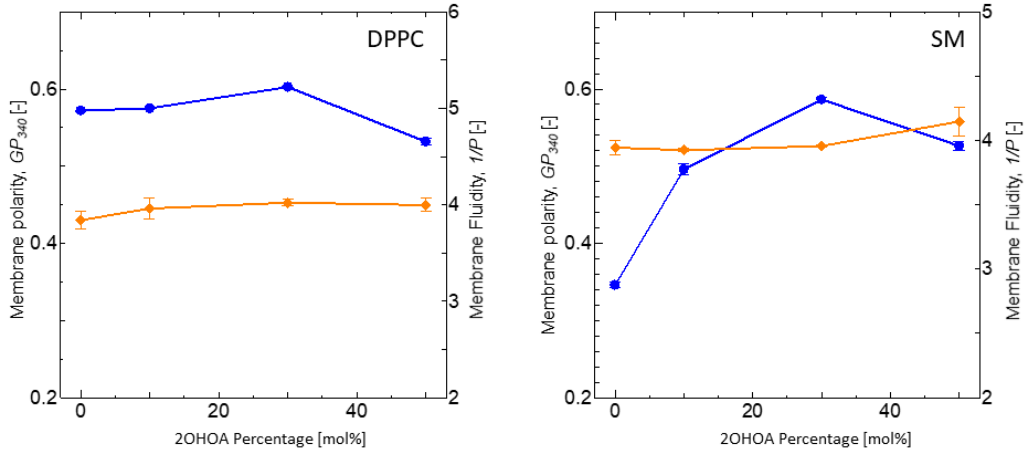

Fig. 3-3 Membrane polarity and membrane fluidity of mixed SM/2OHOA and DPPC/2OHOA vesicles in pure water.

3.3. Zeta potential measurement

Surface charges of liposome are usually determined by the head groups of lipids, which can incorporate positively charged tertiary amines or negatively charged carboxylic acid.

The surface potential of nanoparticle is an important physicochemical parameter because it determines the strength of intra-particle interactions, the adsorption of counter ions, and therefore particle stability. zeta potential of liposomes significantly depended on pH, temperature, and ionic strength of the media, adsorption of proteins (Smith *et al.*, 2017). Here, we measured the zeta potential of 2OHOA-incorporated SM and DPPC liposome (**Fig. 3-5**). With same composition and dispersion solution, the 2OHOA/SM liposomes showed higher zeta potential than in 2OHOA/DPPC system. This result indicated that the 2OHOA showed higher dissociate degree in SM than in DPPC liposome, which might be caused by the different interaction of 2OHOA with SM and DPPC.

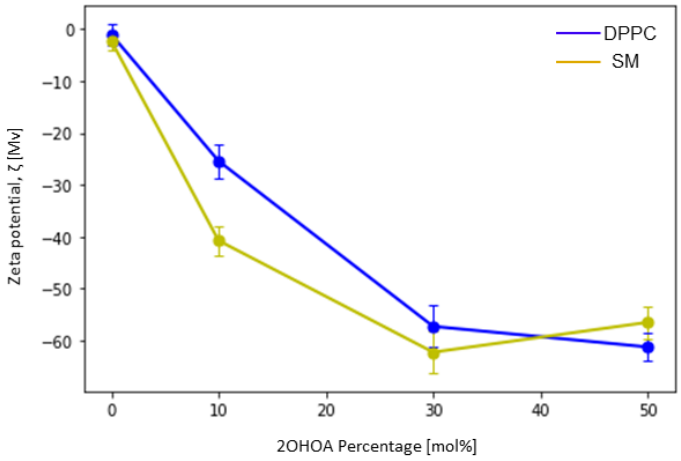

Fig. 3-5 Zeta potential measurements of mixed SM/2OHOA and DPPC/2OHOA vesicles in pure water.

3.4. Sensitivity of interface properties of 2OHOA-icorporated lipid membrane to pH and salt concentration

In order to check the effect of 2OHOA dissociation state on its interaction with lipid bilayer, we check the membrane polarity of 2OHOA-containing DPPC and SM lipid membrane under different pH conditions (pH=5.8 and pH=7.4) and salt concentration (conc.=0.5 mM and conc.=140 mM), and the results displayed in **Fig. 3-6**. From the result, the GP340 values of 2OHOA-containing DPPC system showed no variation under different pH conditions. However, SM system with 30 mol% of 2OHOA showed significant different effects under various conditions. Although addition of 2OHOA in SM membrane under 0.5 mM phosphate buffer (pH=5.8) dehydrated the membrane

significantly, the increased salt concentration and pH value of dispersion solution diminished the hydrophobic effect of the 2OHOA. However, there is no similar phenomenon was observed in membrane polarity, indicating changed pH condition and salt condition did not impact the integrity of lipid membrane structure. Besides, for pure SM, under different conditions there are also no significant influence was obtained. This different result was induced by the different interaction between 2OHOA and SM molecules under various conditions. Comparing with the result of DPPC that almost no variation under different conditions suggests the main reason for this difference is the different interfacial properties of SM and DPPC.

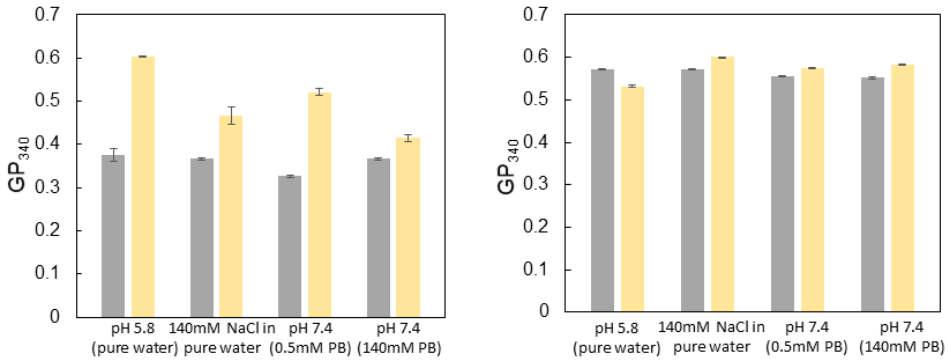

Fig. 3-6 Sensitivity of membrane polarity to pH condition and salt concentration (SM / 2OHOA (7/3) at left; DPPC / 2OHOA (7/3) at right)

The results of Langmuir isotherm monolayer study did not show distinct difference in interaction of 2OHOA with DPPC membrane and SM membrane. Under lower molar ratio of 2OHOA, addition of 2OHOA did not induced obvious disturbance on lipid membrane. Previous study showed consistent result that accumulation of OA and 2OHOA inside the membrane does not induce important structural perturbations in the bilayers. Addition of 50% 2OHOA induced much smaller surface areas at the monolayer layer. At the bilayer level, 50% 2OHOA slightly increased membrane polarity. These results indicated 50% 2OHOA might cause phase state transformation. For zeta potential measurement, liposome composed with 2OHOA and SM showed lower negative zeta potential than liposome composed by DPPC and 2OHOA. It showed high possibility that the α-hydroxyl group of 2OHOA could act as a hydrogen-bond donor with the SM amide

group like cholesterol (Ramstedt *et al.*, 2006), and this hydrogen bonding interaction induced the higher dissociation degree of 2OHOA carboxyl group. Because the amide is located significantly deeper in the bilayer than other hydrogen-bonding moieties, the 2OHOA possess high possibility to regulate the interfacial properties of SM lipid membrane. Therefore, comparing with the 2OHOA-containg DPPC membrane, the Laurdan result of 2OHOA-containg SM membrane showed sensitivity to pH condition and salt concentration. Higher pH condition will induce higher dissociation of carboxyl group, and this lipid protonation changes the water affinity of the surface polar residues. Although under lower salt concentration 2OHOA/SM liposome showed stronger negative charge than 2OHOA/DPPC liposome. Ions partly mask the effects of surface electro statics by accumulating in the counterion cloud near the charged bilayer surface. Under higher salt concentration, the higher surface charge density and polarity of 2OHOA/SM liposome can attract more counterion Na^+ to interface region of 2OHOA/SM, the water molecules surrounding the Na^+ can be brought to interfacial region at the same time. This might be the reason that the 2OHOA-incorporated SM membrane showed high sensitivity to pH condition and salt concentration. Seto and his coworkers' study indicated that the Ca^{2+} ions bind near the glycerol groups (Seto *et al.*, 2020). Comparing with the hydrate ions radius, the size of Na^+ is smaller than Ca^{2+}. Therefore, it is possible that the Na^+ can insert to amide bond region of SM lipid membrane. These results are similar with the previous report that the consequence of 2OHFA incorporation into the membranes is not restricted to a disordering of the acyl chains, but it also significantly affects the hydration and solvent relaxation dynamics (Khmelinskaia *et al.*, 2014). To confirm the functionality of α-hydroxyl group of 2OHOA molecule, the membrane polarity of oleic acid (OA) incorporated SM lipid membrane was also evaluated (**Fig. 3-7**). From the results, we can know that OA-incorporated SM lipid membrane polarity showed almost no sensitivity to pH condition and salt concentration. Thus, it is confirmed that the different interaction between 2OHOA with SM molecules can be attributed to the presence of hydroxyl. The plausible mechanism for this difference is shown in **Fig. 3-8**.

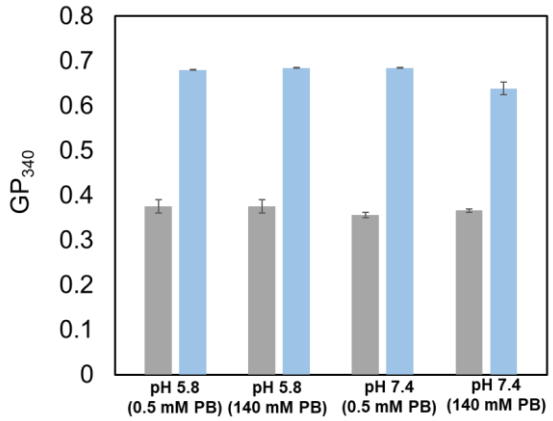

Fig. 3-7 Sensitivity of membrane polarity to pH condition and salt concentration (SM / OA= 7/3)

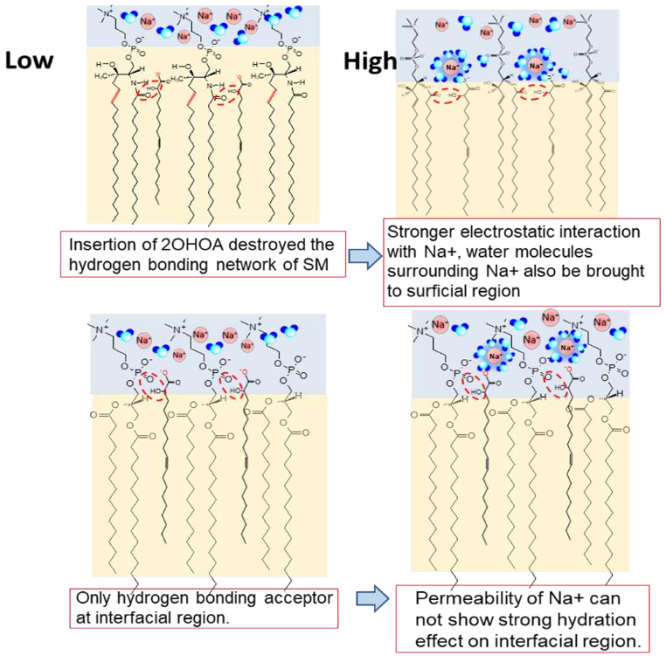

Fig. 3-8 The plausible mechanism for different sensitivity of membrane polarity to pH and salt conditions for SM membrane (up) and DPPC lipid membrane (bottom).

4. Summary

In this chapter, to clarify the functionality of hydroxyl group on lipid membrane interfacial region, the effect of 2OHOA on DPPC and SM lipid membranes, which possess different interfacial properties was investigated. The results suggested the incorporation of 2OHOA to DPPC and SM lipid membrane did not show significant influence on lipid membrane overall structure based on the isotherm monolayer study of headgroup region and bilayer study of hydrocarbon chain region. However, insertion of 2OHOA molecule to SM lipid membrane disturb the its original hydrogen bonding network at the interfacial region. Comparing with 2OHOA-incorporated DPPC membrane, 2OHOA-incorporated SM showed stronger negative surficial potential, indicating the interaction with SM molecule induced higher dissociation degree of 2OHOA. In addition, comparing with OA / SM lipid membrane, only in 2OHOA modified SM lipid membrane, the interfacial hydration state showed obvious sensitivity to pH condition and salt concentration, indicating 2OHOA molecule would show different effect on lipid membrane properties only due to one the hydroxyl group difference. Therefore, it can be concluded that the α-hydroxyl group played an important role in interacting with SM interfacial region, and this interaction greatly effect on the interfacial hydration state. The findings in this work would be also helpful for understanding the pharmacological mechanism of 2OHOA by interacting with lipid membrane.

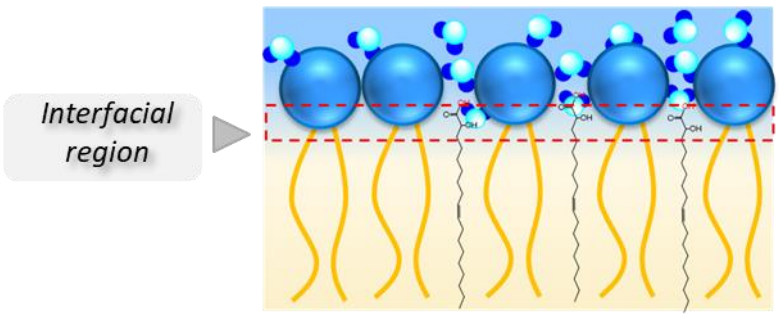

Fig. 3-9 Effect of 2OHOA on lipid membrane interfacial region.

Chapter 4

Effect of Resveratrol on lipid membrane surficial region

1. Introduction

Resveratrol (RES), chemically known as 3,5,4'-trihydroxystilene, is a naturally occurring polyphenolic compound with three hydroxyl groups present in grape peer (Gehm *et al.*, 1997). Biological and pharmacological activities of RES have been widely reported, such as antioxidant (Yao *et al.*, 2010; Lucio *et al.*, 2007; Leobard *et al.*, 2003), anti-inflammatory (Wu *et al.*, 2001), anti-carcinogenic (Athar *et al.*, 2009), cardioprotector (Bertelli *et al.*, 1999; Fearon *et al.*, 2009; Movahed *et al.*, 2012), and neuroprotector (Orsu *et al.*, 2013). The mechanism by which RES exerts its effects is thought to include multiple pathways and, furthermore, the interaction of RES with biomembranes may also play an important role in its therapeutic activity (Athar *et al.*, 2009; Britte *et al.*, 2010; Neves *et al.*, 2012), because many cellular functions usually occur in or around cell membrane, and the alterations in the types and level of membrane lipid have been described in many pathologies (Martinez *et al.*, 2005). On the other hand, lipid membranes can show different physicochemical properties in terms of fluidity, polarity, and cross-section area, when an external molecule is incorporated in the membrane. Such altered membrane properties are thought to play essential roles to maintain numerous cell functions.

There are also some reports certify that sometimes the differences in the membrane structure in more important than chemical differences (Escriba *et al.*, 2007). Therefore, it is conceivable that variation of membrane properties caused by resveratrol can contribute to the achievement of its best treatment effects through "membrane-lipid therapy" approach (Escriba *et al.*, 2006). In recent years, the interactions of RES on different kinds of lipid membranes have been widely investigated, where the results still show some controversy that RES seems to increase membrane fluidity in some liposomal models, and contrarily appears to induce stiffness on others (Brittes *et al.*, 2010; Neves *et al.*, 2016; Neves *et al.*, 2012; Wesolowska *et al.*, 2009; Sarpietro *et al.*, 2007; Neves *et al.*,2015).

Therefore, further investigation is still required to clarify the influence of RES on biomembrane properties.

The interaction of RES with the lipid membranes has been widely investigated in order to understand the mechanism by which RES exerts its therapeutic effects, while the relevance of its bioactivity to the interaction of resveratrol with lipid membranes is little characterized quantitatively. In fact, many reports on the therapeutic effects of RES can be traced back to its antioxidant activity by scavenging free radicals, so called as, reactive oxidant spices (ROS) (Yao *et al.*, 2010; Lucio *et al.*, 2007; Bertelli *et al.*, 1999; Orsu *et al.*, 2013), which play an important role as initiators or mediators involved in innumerous physiological cellular signaling processes. When describe the features of lipid membranes, the phase state of lipid membranes is one of the main characterizations. There are some kinds of phase states in lipid membranes based on their compositions: liquid disordered phase (l_d), liquid-ordered phase (l_o) and solid-ordered phase (S_o) (Yeagle *et al.*, 2005). For the l_d phase, the liposome composed of unsaturated lipid or saturated lipid at above phase transition temperature, exposures the hydrophobic region to bulk water due to less packing of their acyl carbon chain. Thus, there is high possibility for RES to interact with the lipid membranes at l_d phase to yield its pleiotropic action by change the membrane structure or modulating the activity of proteins involved in biomembranes further.

Owing to the complexity of cellular membranes, the liposomes are usually utilized to investigate the influence of bioactive compounds on biomembranes: the lipid vesicles prepared by 1,2-dioleoyl-*sn*-glycero-3-phosphatidylcholine (DOPC) and by sphingomyelin (SM), cholesterol (Ch) are used as model of l_d phase and l_o phase, respectively. Besides, Ch and SM also play a critical role in modulating the membrane fluidity and permeability of encapsulated molecule (De Almeida *et al.*, 2005; Hayashi *et al.*, 2012; Sagisaka *et al.*, 2008). While the excess ROS in cells will damage to health and easier to be converted into more reactive one, the main of which is lipid peroxide by attacking the lipids, called as lipid peroxidation. In addition, the outcomes of lipid peroxidation would damage the membrane structures (Borst *et al.*, 2000) and generate oxidized products, some of which can chemically modify the macromolecules such as DNA, resulting in diseases. RES binding to the membrane might prevent the attack of ROS, while the hierarchical location of RES within lipid bilayer and its influence on membranes properties are still unclear.

In this chapter, the critical location of RES in the liposomes in different phase states has been characterized. The DOPC liposome, DOPC/SM/Ch liposome in a molar ratio of 1:1:1, and SM/Ch liposome in a molar ratio of 1:1 were used as typical model membranes in l_d, l_d+l_o, and l_o phase, respectively. Fluorescent probes, which bind to different position in the membrane, were employed to monitor the microenvironment within the bilayer membrane at multi-level (Bui *et al.*, 2016). In this regard, the multi-level distribution of RES and its influence on each membrane property can be discussed. Towards the discussion for contribution of the interaction between RES and lipid membrane to its antioxidant bioactivity, the fluorescence quenching and mass spectroscopy analysis were carried to investigate the accessibility of hydrogen peroxide into RES-incorporated membranes.

2. Materials and Methods

2.1. Materials.

1,2-Dioleoyl-*sn*-glycero-3-phosphatidylcholine (DOPC) and sphingomyelin (SM) were purchased from Avanti Polar Lipid Inc. (Alabaster, AL), and were used as received. Resveratrol (RES) was purchased from Tokyo Chemical Industries (TCI) (Tokyo, Japan). Cholesterol (Ch), 1,6-diphenyl-1,3,5-hexatriene (DPH), 1-(4-trimethylammoniumphenyl)-6-phenyl-1,3,5-hexatriene (TMA-DPH), 6-dodecanoyl-2-dimethylaminonaphthalene (Laurdan), and 6-propionyl-2-dimethylaminonaphthalene (Prodan) were purchased from Sigma Aldrich (St. Louis, MO, USA). Other chemicals were purchased from Wako Pure Chemical (Osaka, Japan) and were used without further purification.

2.2. Liposome preparation.

Liposomes were prepared by the lipid film hydration method as reported previously (MacDonald *et al.*, 1991). The lipids with molar ratio of DOPC/SM/Ch=1/1/1, SM/Ch=1/1, and DOPC were dissolved in chloroform/methanol (v/v=9/1). These organic solvents containing lipids were dried in a round-bottomed flask by rotary evaporation under vacuum to yield a dried lipid film. The lipid thin films were kept under high vacuum for at least 3 h and then hydrated at room temperature with 3 mL of phosphate buffer (50 mM, pH=7.4). The vesicle suspension was frozen at −80 °C and thawed at 60 °C. After the freeze−thaw cycle was repeated five times, the liposome suspensions were extruded 11 times through polycarbonate membrane with a mean pore diameter of 100 nm using an extruding device (Liposofast; Avestin Inc., Ottawa, ON, Canada). The liposome suspensions with final concentration of 16 mM lipid were kept in refrigerator before usage.

2.3. Investigation of the membrane fluidity in the surface and inner membrane.

The fluidities in the superficial and inner membranes were determined by measuring the fluorescence anisotropy of TMA-DPH and DPH incorporated in the liposomes (lipid/fluorescence probes molar ratio of 200:1), respectively, using the fluorescence spectrophotometer FP-6500 (JASCO, Tokyo, Japan). Liposome suspensions diluted by phosphate buffer (Lipid: 800 μM, 1mL) were treated with 10 μL of RES dissolved in

ethanol with a final concentration of 5, 10, 20 mol% to lipids concentration, and the control also was treated with 10 μL ethanol (without RES). Then, fluorescence probe, such as DPH or TMA-DPH (100 μM in ethanol), was added to liposome suspensions, and the suspensions were incubated at 37 °C for 4 h. The samples were excited with vertically polarized light (360 nm), and the emission intensities both perpendicular ($I_{\perp}$) and parallel ($I_{/\!/}$) to the excited light were recorded at 430 nm. The polarization (P) of DPH or TMA-DPH was then calculated by the following formulas:

$$P=(I_{/\!/} \text{-G } I_{\perp})/(I_{/\!/} \text{+G } I_{\perp}) \qquad \text{(Eq. 4-1)}$$

$$G= I_{\perp}/ I_{/\!/} \qquad \text{(Eq. 4-2)}$$

where $I_{\perp}$ and $I_{/\!/}$ are emission intensities perpendicular and parallel to the horizontally polarized light, respectively, and G is the correction factor. The fluidity was evaluated on the basis of the reciprocal of polarization, $1/P$.

2.4. Investigation of the membrane polarity in the surface and inner membrane

Fluorescence probes, such as Laurdan and Prodan, are sensitive to the polarity around itself, which allows the membrane polarity to be determined. The sample solutions were prepared in the same way with the membrane fluidity measurements, wherein the fluorescence probes were taken placed by Laurdan and Prodan with lipid: probe ratio of 200:1. The fluorescence spectrum of Laurdan or Prodan in each liposome was recorded with excitation wavelength of 340 nm, at appropriate emission wavelengths from 400 to 600 nm at 37 °C, and the general polarization (GP_{340}) for each emission wavelength as follows:

$$GP_{340,\ \text{Laurdan}}=(I_{440}\text{-}I_{490})/(I_{440}+I_{490}) \qquad \text{(Eq. 4-3)}$$

where I_{440} and I_{490} are the emission intensities of Laudran at 440 and 490 nm, respectively. For Prodan, the membrane polarity ($GP_{340,\ \text{Prodan}}$) was estimated on the basis of the following equation:

$$GP_{340,\ \text{Prodan}}=(I_{437}\text{-}I_{510})/(I_{437}+I_{510}) \qquad \text{(Eq. 4-4)}$$

where I_{437} and I_{510} are the emission intensities of Prodan at 437 and 510 nm, respectively. Obtained spectra were treated by subtracting RES spectra in liposome (without fluorescent probes) to remove background signals.

2.5. Accessibility of hydroxyl radical into RES-incorporated liposomes

The accessibility of hydroxyl radical •OH to Laurdan was estimated by measuring fluorescent intensity. •OH was produced by mixing of 100 μM Cu^{2+} and 1.2 mM H_2O_2). The fluorescent intensities of Laurdan were measured in the presence or absence of oxidant. The total concentrations of lipids, Laurdan, Cu^{2+}, and H_2O_2 were 800 μM, 4 μM, 100 μM, and 1.2 mM, respectively. The samples were incubated for 8 h at 37 °C in the presence or absence of RES, and then the peak intensities (I) were measured. The degree of Laurdan fluorescence quenching was calculated as follow:

$$Quench(\%) = \frac{I_{Control} - I_{Remained}}{I_{Control}} \times 100\% \qquad \text{(Eq. 4-5)}$$

wherein I_{Remained} and I_{Control} represent the peak intensity of Laurdan in the presence and absence of Cu^{2+}/H_2O_2, respectively.

2.6. Oxidation of DOPC molecules evaluated by mass spectroscopy

DOPC liposome or RES-incorporated DOPC liposome suspensions were treated with hydroxyl radicals •OH (produced by mixing of 100 μM Cu^{2+} and 1.2 mM H_2O_2) for different incubation time (12 h and 24 h). Next, the liposome suspensions were freeze-dried for overnight. 1 mL chloroform was added to the dried sample, and then the mass spectra were obtained by JEOL JMS-700.

3. Results and Discussion

3.1. Membrane polarities of RES-incorporated liposomes

Liposome membrane is known to possess a hydrophobic gradient at nanometer scale in the vertical direction from membrane surface to hydrophobic core region (Ceve *et al.*, 1990). The fluorescent probes, such as DPH and Laurdan, have been reported to be localized at the hydrophobic region of the lipid bilayer, while TMA-DPH and Prodan can be located at the hydrophilic region of the membrane surface (Bui *et al.*, 2016). Laurdan and Prodan are usually utilized as indicators of polar environment within the lipid membrane: the existence of ordered phase (l_o or S_o) and disordered phase (l_d) was determined by the emission peak at around 440 nm and 490 nm for Laurdan (437 nm and 510 nm for Prodan) respectively. From the emission spectra of Laudan and Prodan in liposomes (**Fig. 4-1 and 4-2**), it was found that, in the case of DOPC liposome (in l_d phase), the addition of 20% RES resulted in an increase of the spectrum fraction of the emission peak at 440 nm. Regarding to liposomes possessing *l*o phase, with increasing of concentration of RES, the fluorescence intensity of Laurdan at 490nm decreased, indicating the reduce of liquid disordered phase within liposome. Identically but more obviously, the fluorescence spectra of Prodan also showed the weaker emission intensity at 510nm, but the stronger emission at 473nm with the increasing RES. Here, the GP_{340} values are employed to identify the variation of membrane polarities (Parasassi *et al.*, 1998). As shown in **Fig. 4-3**, both values of $GP_{340,\ Laurdan}$ and $GP_{340,\ Prodan}$ for DOPC were monotonically increased, revealing that RES could form the ordered (l_o) phase in l_d phase. It has also been reported that the RES could induce the formation of l_o domains, through the analysis by fluorescence quenching methods (Neves *et al.*, 2016). In the cases of DOPC/SM/Ch liposomes (heterogeneous l_o and l_o phases) and SM/Ch liposomes (l_o phase), a slight-increase in GP_{340} value was observed. The decrease of the surface membrane polarity (measured by Prodan) was also observed in DOPC, DOPC/SM/Ch, and SM/Ch liposomes (**Fig. 4-1b**). As a result of RES binding on the membrane, the affinity of hydroxyl groups to water molecules, namely, the function of RES to take away water molecules from inner region of membrane might play a key role to alter the polar environment of the liposome membrane. These results indicate that RES leads the "disordered" membrane to be "ordered" one. Different from almost of previous literatures

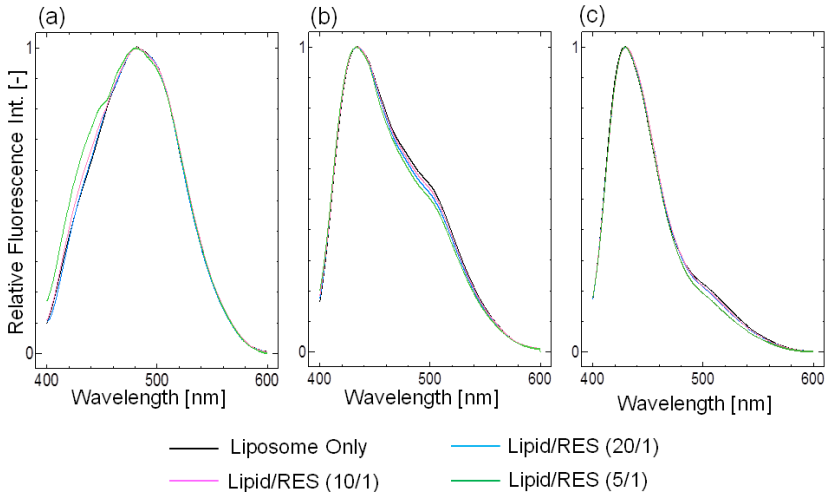

Fig. 4-1 Fluorescent spectra of Laurdan for resveratrol-incorporated liposomes. (a), for resveratrol-incorporated DOPC liposomes (b), resveratrol-incorporated DOPC/SM/Ch=1/1/1 liposomes (c), resveratrol-incorporated SM/Ch=1/1 liposomes.

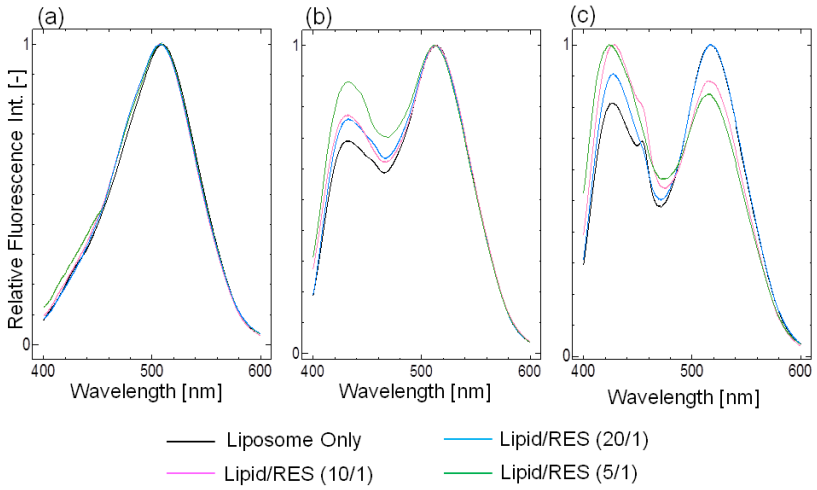

Fig. 4-2 Fluorescent spectra of Prodan for resveratrol-incorporated liposomes. (a), resveratrol-incorporated DOPC liposomes (b), resveratrol-incorporated DOPC/SM/Ch=1/1/1 liposomes (c), resveratrol-incorporated SM/Ch=1/1 liposomes.

that have paid much attention to the variations of membrane fluidity (Neves *et al.*, 2015; Neves *et al.*, 2016) caused by incorporation of RES, our results suggest that RES can subtract bound water from the inner membrane.

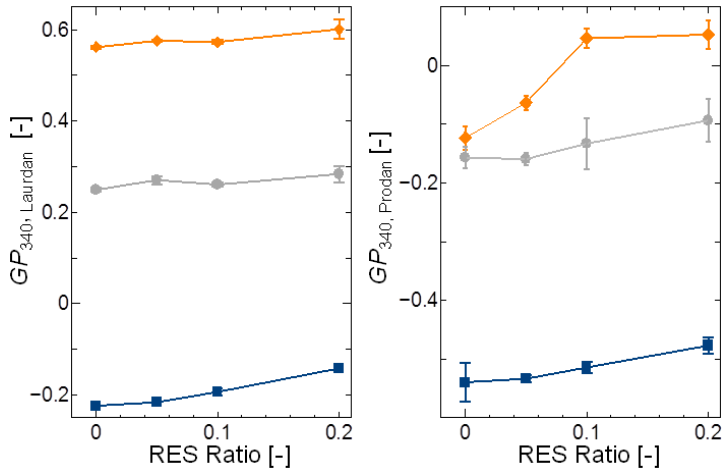

Fig. 4-3 GP_{340} values analyzed by Laurdan (a) and Prodan (b) in DOPC liposome (*blue square*), DOPC/SM/Ch=1/1/1 liposome (*gray circle*), SM/Ch=1/1 liposome (*orange diamond*) with the increasing concentration of RES. $GP_{340,\ Laurdan}$ and $GP_{340,\ Prodan}$ values were calculated based on Eqs (3) and (4), respectively.

3.2. Membrane fluidities of RES-incorporated liposomes

The fluorescence probe DPH, which binds to the acyl chain part within lipid bilayer, is widely used to evaluate the inner membrane fluidity, wherein the $1/P_{DPH}$ value varies depending on the phase state of liposome. In DOPC/SM/Ch and SM/Ch membrane systems, there is almost no variation of the inner membrane fluidity (**Fig. 4-4a**). In the case of disordered DOPC liposome, the membrane fluidity significantly decreased after the addition of RES, which is consistent with the result of Laurdan due to the formation of *l*o phase. For this reason, higher fluidity of acyl chain region in DOPC liposome allowed RES to diffuse into the inner membrane, while the tightly packed hydrophobic part in DOPC/SM/Ch or SM/Ch membrane prevent RES to be localized in the inner region. The penetration of RES into the hydrophobic core region was also verified by the log*P* value of RES: log*P* = 3.1 (Neves *et al.*, 2013). The surface membrane fluidities were investigated by another fluorescence probe, TMA-DPH, which binds to the phospholipid headgroup region. **Fig. 4-4b** shows that the addition of RES decreased the surface membrane fluidity of DOPC, although it had little effect on DOPC/SM/Ch liposomes. It is concluded that the RES binding significantly influenced the fluidity in l_d phase, while it did little influence that in the l_o phase.

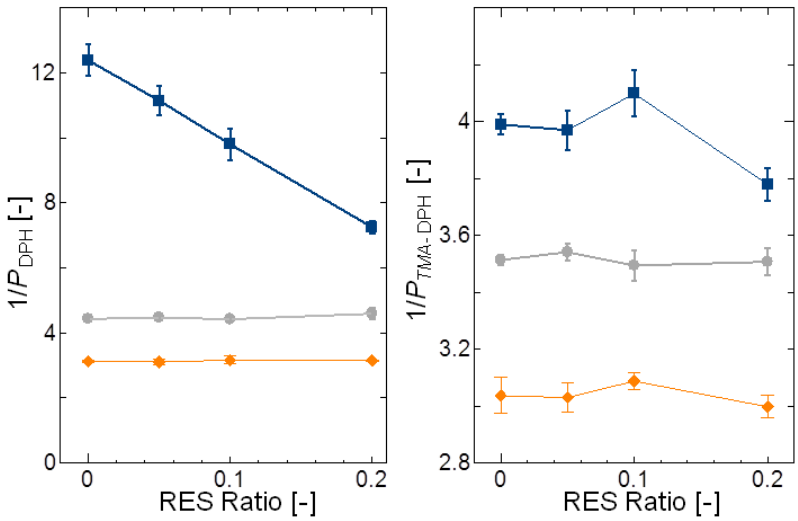

Fig. 4-4 1/*P* values analyzed by DPH (a) and TMA-DPH (b) in the DOPC liposome (*blue square*), DOPC/SM/Ch=1/1/1 liposome (*gray circle*), SM/Ch=1/1 liposome (*orange diamond*) with the increasing concentration of RES. $1/P_{DPH}$ and $1/P_{TMA\text{-}DPH}$ values were calculated based on Eq. 4-1 and Eq. 4-2.

3.3. Phase states of RES-incorporated liposomes

The inner membrane fluidity and polarity of liposome in each phase state was estimated by using DPH and Laurdan fluorescence probes. Herein, a Cartesian diagram for these three lipid membrane systems, without resveratrol and treated with 20% RES, is shown in **Fig. 4-5**, based on the membrane fluidity ($1/P_{DPH}$, *x* axis) and membrane polarity ($GP_{340,\ Laurdan}$, *y* axis). The phase state of each liposome incorporated with resveratrol was determined based on the plotted position in the diagram: the liposomes in the second quadrant ($1/P_{DPH}$ <6, $GP_{340,\ Laurdan}$ >-0.2) were in the ordered phases (l_o or s_o), and those in the fourth quadrant ($1/P_{DPH}$ >6, $GP_{340,\ Laurdan}$ <-0.2) were in the disordered (l_d) phases, respectively (Suga *et al.*, 2013). The liposomes in the first quadrant, such as DOPC treated with 20% RES, could be in a heterogeneous phase (l_d + l_o). Both of DOPC/SM/Ch and SM/Ch liposomes after the addition of 20% RES showed no phase transition, whereas the DOPC liposome after 20% RES addition showed a position shift to the 1st quadrant, which indicate the phase transition of DOPC by RES incorporation. These results also agree with the analysis of fluorescence spectra of Laurdan, because the RES-incorporated DOPC liposome showed both peaks at around 440 and 490 nm. The evident changes in both the polarity and fluidity of inner membrane indicate that RES can strongly influence

on DOPC liposome by increasing the ordered phase in the membrane. In DOPC/SM/Ch and DOPC/SM liposomes, there is almost no variations in the $1/P_{DPH}$ values, while a slight increase in $GP_{340,\ Laurdan}$ values was observed. This suggests that the membrane was dehydrated by the presence of RES, in heterogeneous phase and l_o phase, although the change in the membrane fluidity was little.

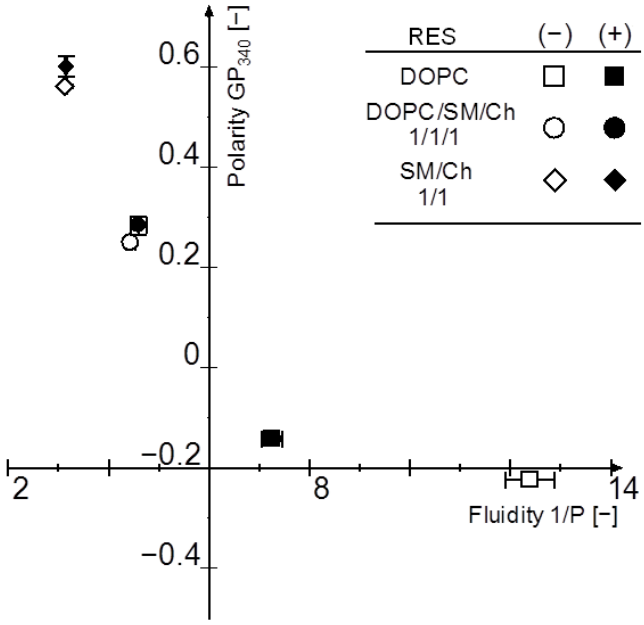

Fig. 4-5. Cartesian diagram for liposomes in the absence (open symbols) and in the presence of 20% RES (*closed symbols*), in DOPC, DOPC/SM/Ch=1/1/1, SM/Ch=1/1. The $1/P_{DPH}$ and $GP_{340,\ Laurdan}$ values were measured at 37 °C.

3.4. Multi-level analysis for the location of RES in liposome membranes

The influence of RES on the interior region of lipid membranes can be shown by Cartesian diagram. However, the interaction of RES with lipid headgroup (hydrophilic region) has not been clarified. Fluorescence probes, such as TMA-DPH and Prodan, were utilized to investigate the membrane properties in hydrophilic region (**Figs.4-3b and 4-4b**). Especially, in DOPC/SM/Ch and SM/Ch liposomes, the decreases of surface membrane polarity were more evident for the location of RES at membrane surfaces rather than inner region, suggesting that RES binding on the membrane replaced the bound water at the surface. In the case of DOPC, which is in l_d phase, RES prefers to penetrate into the inner membrane, resulting in drastic alteration in inner membrane rather than in the membrane surface.

The affinity of hydroxyl groups of RES with lipid headgroup, which alternatively replaced water molecules, must play an important role in increasing the surface membrane polarity in ordered phase. In a report by Wesolowka *et al.*, the Pordan generalized polarization of RES and piceatannol were investigated. Piceatannol (3,3',4,5'-tetrahydroxyl-trans-stilbene) possesses one additional hydroxyl group, the effect of which was more pronounced than the case of RES in liquid crystalline states. It has also been reported that the addition of RES on DPPC liposome abolished the pretransition completely at RES >5mol% (Longo *et al.*, 2016), indicating that the influence of RES on DPPC membrane surface was stronger than that on DPPC membrane interior. It is suggested that both compounds studied here interacted with the membrane head-group region more strongly than the deeper parts of the bilayer. In the present study, different from DPPC (gel phase), the interspace could be existing in DOPC/SM/Ch or SM/Ch membrane (partially or completely in *l*o phase), coupled with high hydrophobicity of RES, it is conceivable that RES can exit in such an interspace to be eliminated from bulk aqueous phase, similar with the "umbrella model" for existence of cholesterol in membrane (Huang *et al.*,). The inserted RES was able to gather the water molecules that existed in the hydrophilic and hydrophobic interface, resulting in the increase of membrane polarity. As we investigated, one of the functions of RES in lipid membrane systems is to act as an umbrella in the membrane surface, and replace water molecules away from the membrane. According to our findings, plausible location of RES and fluorescent probes are summarized as **Fig. 4-6**. Thanks to the less polar environment provided by RES binding, it is expected that water-soluble ROSs (i.e., hydroxyl radical) lose an accessibility into the inner membrane region.

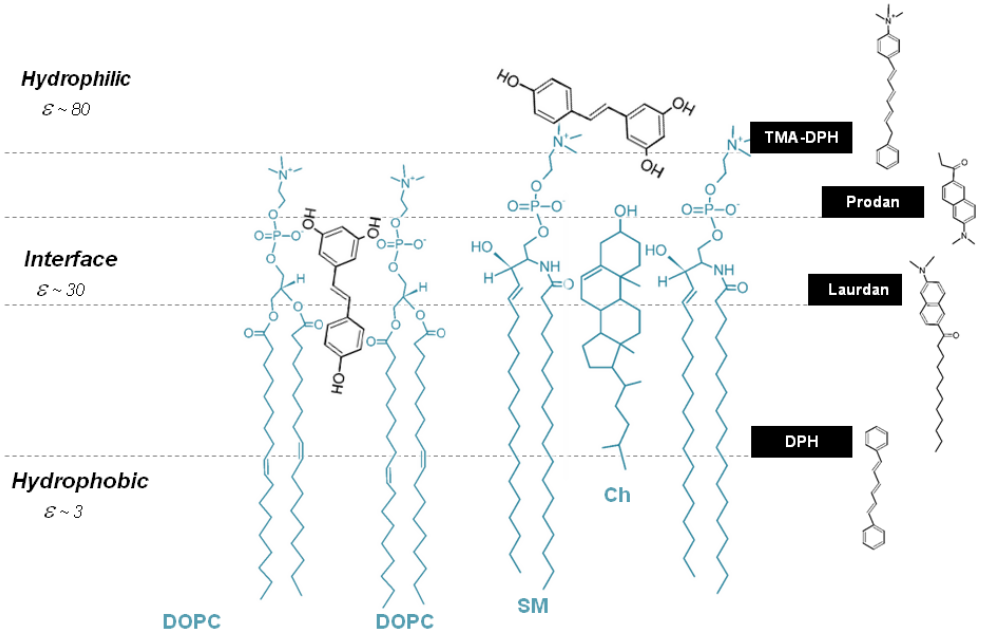

Fig. 4-6 Plausible location of RES and fluorescent probes in model biological membranes.

3.5. Accessibility of hydroxyl radical across the RES bound membranes

Because double bonds of polyunsaturated fatty acid chains are the main target of ROS, DOPC molecules could be oxidized easily. In general, a radical molecule quenches fluorescent probe if they are close to each other. Using DOPC liposomes, the fluorescence quenching of Laurdan was evaluated to determine whether oxidant could be accessible to inner membrane region or not. As shown in **Fig.4-7**, the RES-incorporated DOPC liposome reduced the quench of Laurdan (the percentage of remaining fluorescence intensity increased to 57% from 43%), revealing that less hydroxyl radical access to the inner part of DOPC liposome. Based on the above results, the addition of RES increased the stiffness and decreased the polarity of the DOPC liposome. The rigid and less polar membrane state might contribute to inhibit the accessibility of hydroxyl radicals, due to the decrease of the diffusion rate of hydroxyl radicals. Although literatures have reported that RES is effective on the inhibition of the lipid peroxidation of cellular membrane by scavenging the hydroxyl radicals, the outer vertical location of Laurdan than RES restricted RES to scavenge hydroxyl radical before it quenched the fluorescence of Laurdan. According to Lúcio, the RES might locate in the deepest region of lipid bilayer because of the high lipotropy of RES and high fluidity of acyl carbon chain part in unsaturated liposome. It has also reported that tea catechins, a kind of polyphenol

compounds, show the inhibition effect on the lipid peroxidation (Kubota *et al.*, 2007). This effect could be due to i) catechin compound itself acting as radical scavenger, and ii) the catechin-incorporated membrane property which decrease the accessibility of radicals permeating across the membrane. In fact, the amount of H_2O_2 was much higher than that of RES. Therefore, we conclude that the dehydrated environment caused by RES slightly affected on the inhibition of accessibility of hydroxyl radicals, showing the possibility to prevent and control lipid peroxidation of the membranes.

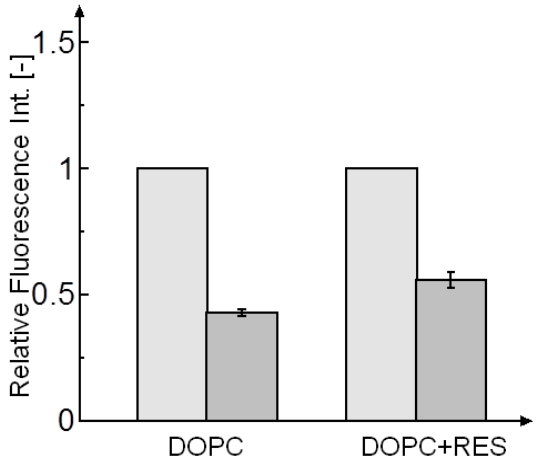

Fig. 4-7 Relative fluorescence intensity of Laurdan in liposome of DOPC (total lipid: 800 μM) without (*gray bar*) and with (*black bar*) the oxidative system Cu^{2+} and H_2O_2 at 37 °C. The total concentrations of RES and H_2O_2 were 200 μM and 1.2 mM, respectively.

3.6. Prevention lipid oxidation in the presence of RES

Because C=C double bonds of unsaturated fatty acid chains are the main target of ROS, lipid membranes in liquid-disordered phases more inclined to be oxidized. Thus, we used the model membrane prepared by DOPC molecules to evaluated the degree of lipid membrane peroxidation by ROS. The mass spectra of DOPC molecules were measured before and after the oxidation treatment of oxidized agent. After hydroxyl radical oxidation, new m/z peaks were found at 802, 818, 832, and 850 m/z, suggesting that oxidized DOPC spices were generated. According to previous report, oxidized DOPC includes carboxyl or aldehyde groups and showed increase of molecular weight, although it is uncertain where the carbonyl oxygen is added (Umakoshi *et al.*, 2011). From the mass spectra result, shown in **Fig. 4-8b**, DOPC molecules were oxidized more strongly by the incubation time 24h, This indicates that a greater number of hydroxyl radical permeated trough the lipid membrane, resulting in the oxidation of DOPC molecules with

the extension of time. However, the mass spectra of DOPC extracted from RES-incorporated DOPC liposome showed no evident change regardless of the oxidation time (**Figs 4-8c, d**), although an excess amount of hydroxyl radicals could be existed as compared to total RES amount. Therefore, we conclude that the prior binding of RES to the lipid membrane reduced the accessibility of the hydroxyl radical thanks to the change of lipid membrane structure. Herein, the alteration in the membrane properties also contributed to the protection biomembrane from peroxidation for a long time. Based on the above results, the addition of RES increased the stiffness and decreased the polarity of the DOPC liposome. The rigid and less polar membrane state provided a synergistic effect to inhibit the accessibility of hydroxyl radicals, due to the decrease of the diffusion rate of hydroxyl radicals. Although literatures have reported that RES is effective on the inhibition of the lipid peroxidation of cellular membrane by scavenging the hydroxyl radicals, excess hydroxyl radicals than RES and longtime incubation did not result in further oxidization of DOPC molecules. Besides, there is also report that radical scavenger antioxidant will act more efficiently in a fluid lipid bilayer.[4] Therefore, we conclude that the dehydrated environment caused by RES affected on the inhibition of accessibility of hydroxyl radicals, showing the possibility to prevent and control lipid peroxidation of the membranes.

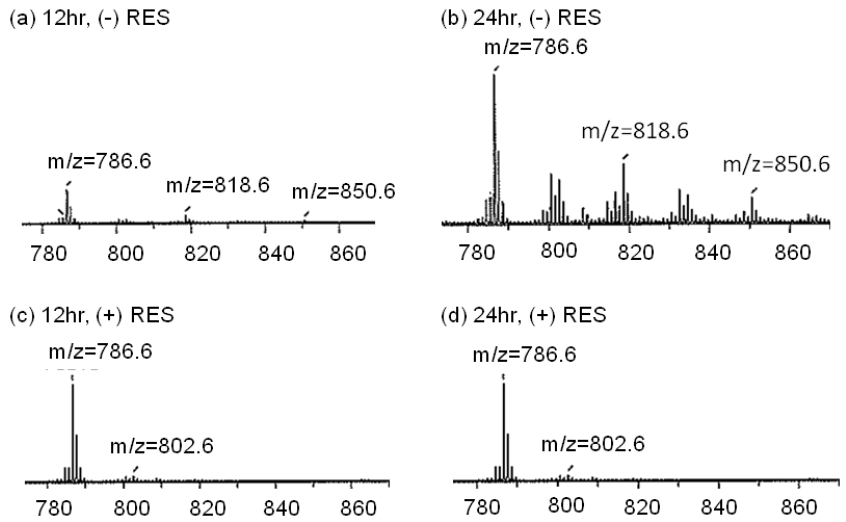

Fig. 4-7. Mass spectra of DOPC molecules. **a** and **b** are the mass spectra DOPC molecules extracted from oxidized DOPC liposome and RES-incorporated liposome respectively for 12h. **c** and **d** are the mass spectra DOPC molecules extracted from oxidized DOPC liposome and RES-incorporated liposome respectively for 24h.

Unsaturated lipid membranes, e.g., DOPC, possess high membrane fluidity and their membrane surfaces are hydrated. It can enable the water-soluble ROS to permeate across the membrane, resulting in the lipid peroxidation (**Fig. 4-8**). On the other hand, the RES incorporation into DOPC liposomes drastically prevented the lipid peroxidation. Based on the obtained result, possible roles of RES on the lipid membrane are suggested as follows (**Fig.4-9**): 1) the RES, locating at the surface region of the lipid membrane, itself can act as radical scavenger; 2) the RES incorporation leads the membrane ordered. The ordered membrane provides a less polar environment around C=C double bond; 3) synergistic effect can be obtained. Because the altered membrane by RES can be packed and dehydrated, which prevents the access of ROS, even if the presence of less amount of RES.

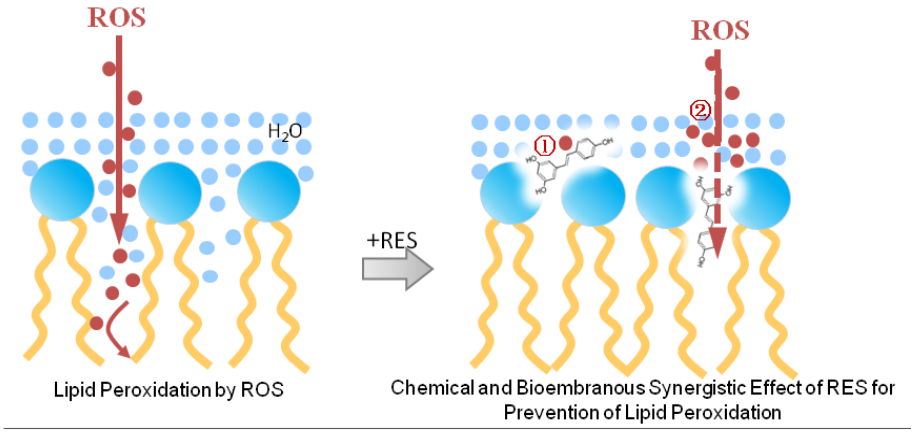

Fig. 4-9 Plausible role of RES on antioxidation.

4. Summary

In this chapter, three different types of liposomes with different phase states were prepared as model cell membranes, and then the influence of the incorporation of RES on their membrane properties was evaluated by utilizing membrane-binding fluorescent probes. The binding of RES lead to the membrane polarities decreasing slightly, regardless of the phase states of the membrane, while the membrane fluidities decreased only in the case of liquid-disordered phase. In each model membrane system, the incorporation of RES dramatically dehydrated the membrane surface, which could prevent the permeation of water-soluble materials. This view is also supported by results about fluorescence quenching of Laurdan, which indicated less accessibility of hydroxyl radial into the inner region of the RES-incorporated membrane. As conclusion, this new finding brought more clarification on influence of RES within biomembranes, which is explained by the affinity of hydroxyl groups in RES structure to water molecules in or surrounding the lipid membranes. In addition to the antioxidant effect of RES itself, the altered membrane properties provided by the RES incorporation can provide a synergistic effect to prevent the permeation of oxidant across the lipid bilayer, due to the less polar environment of RES-incorporated membranes. Besides, the pharmacological activity of RES could be enhanced through its location and this function within the biomembrane.

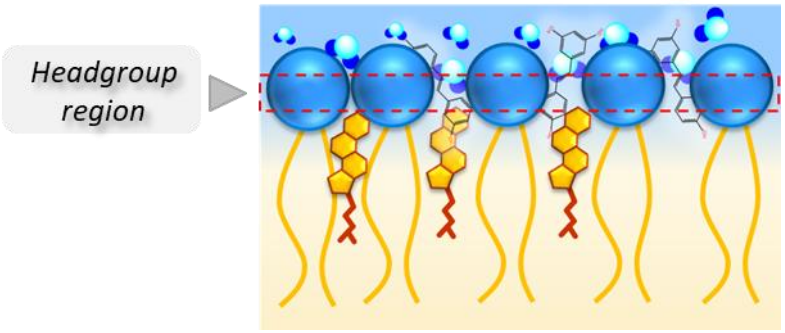

Fig. 4-10 Dehydration effect of RES at headgroup region of heterogenous lipid membrane

Chapter 5

Design of lipid membrane hydration shell by modification with amphiphilic dendrimers

1. Introduction

Dendrimer molecules have attracted the researchers of drug delivery by virtue of their unique radial structure and numerous terminal functionalities. Polyamidoamine (PAMAM) dendrimers, originally developed by Tomalia as protein mimics, have been the most extensively studied dendrimer for biomedical applications, especially for gene delivery and transfection (Liu *et al.*, 2014). The amide functionalities in the interior and primary amine terminals on the surface with positive charge enhance the interaction with nucleic acid molecules and cell membrane. In addition, those amine groups suppress the lowering of pH in endosomes and lysosomes by adsorbing protons, and prohibit the degradation of DNA in lysosome. These advantages of amino and amide group of PAMAM contribute a lot to show good performance in gene delivery or gene-infection. However, their strong electrostatic interaction and hydrogen bond interaction with biomembrane are related to their disruptive effects toward biomembrane, which brings out issues connected with their low biocompatibility and high cytotoxicity (Peetla *et al.*, 2009). Besides, the limited loading capacity also hinders its further biomedical application.

More recently, amphiphilic dendrons (AD), constructed from long hydrophobic alkyl chains and PAMAM dendrons, have emerged as new materials in the drug delivery field. They have shown potential to possess more effective delivery capacity than traditional dendrimer even at low dendrons generation due to formation of some specific self-assembly structure. However, this strategy still faces great challenges because of the difficulties to control the self-organization structures, properties and the function (Márquez-Miranda *et al.*, 2016; Cao *et al.*, 2017; Yu *et al.*, 2012).

Different from dendrimer, liposome have been extensively used as drug delivery carrier. One of its features is the inimitable high biocompatibility and stability (Bulbake *et al.*, 2017). Therefore, the design of new carrier by incorporating ADs into lipid membrane could be one of most effective and possible way to enhance the performance of drug delivery carrier. In addition, the hydration state of biomaterials also plays important roles in modulating biomolecular structure and function, and in regulating adhesion among biomaterials (Levy *et al.*, 2006; Laage *et al.*, 2017). PAMAM dendrons contains multiple amide and amine groups, and their number can be easily modulated by changing the generation of AD. Therefore, it can be expected that hydration degree in coassembly (lipid-AD) also can be easily controlled by AD generation and the composition ratio.

In this chapter, we focused on these coassemblies, and characterized the structure and properties of coassembly constituted with different generation of ADs and phospholipid, especially focusing on hydration degree of the formed coassemblies (**Fig. 5-1**).

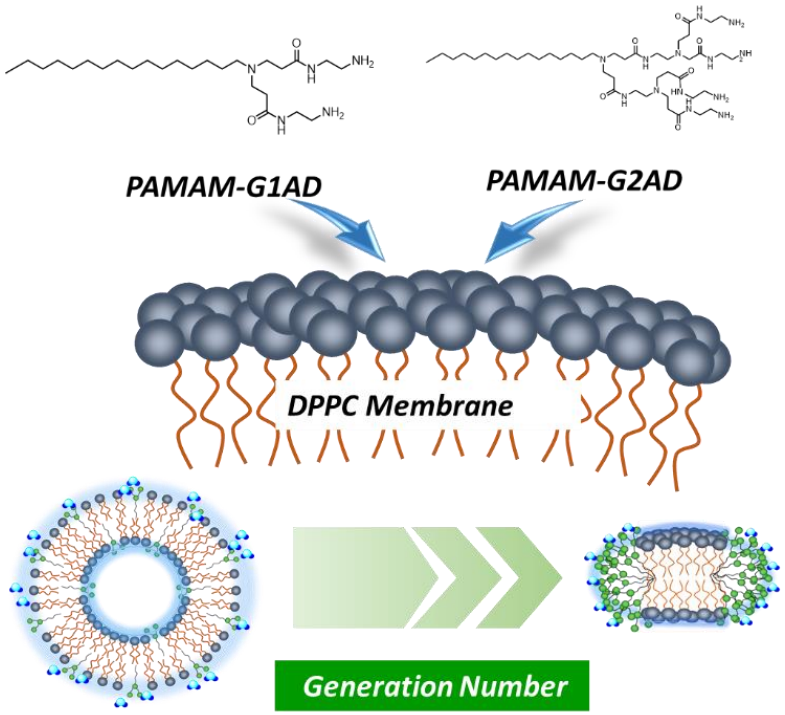

Fig. 5-1 Concept of this study

2. Materials and Methods

2.1. Materials

1,2-Dipalmitoyl-*sn*-glycero-3-phosphocholine (DPPC) was purchased from Avanti Polar Lipid Inc. (Alabaster, AL). Hexadecylamine, methyl acrylate and sodium chloride were obtained from Tokyo Chemical Industry Co., Ltd. (Tokyo, Japan). Methanol, ethyl acetate, and diethyl ether were purchased from Kanto Chemical Co., Inc. (Tokyo, Japan). 6-Lauroyl-2-dimethylamino naphthalene (Laurdan), 2-(Dimethylamino)-6-propionylnaphthalene (Prodan), and 1,6-Diphenyl-1,3,5-hexatriene (DPH) were bought from Wako Pure Chemical (Osaka, Japan). Ethylenediamine was purchased from NACALAI TESQUE, INC (Kyoto, Japan). Ultrapure water was prepared using Direct-Q® UV3 (Merck Millipore Co., Tokyo, Japan).

2.2. Synthesis of amphiphilic dendrons (AD)

Amphiphilic Dendron (AD) constituted of polyamidoamine dendrons as hydrophilic part and alkyl chain as hydrophobic part was synthesized by the following steps (**Scheme 5-1**). As for G1-AD precursor synthesis, hexadecylamine (4 mmol) was dissolved in methanol (20 mL), and methyl acrylate (1.30 mL, 14.4 mmol) was added dropwise under nitrogen atmosphere. The reaction mixture was then stirred at 30 °C for 48 h (**Scheme 5-1-1)**. After evaporation of the reaction solution, ethyl acetate and NaCl aqueous solution were used for extraction. Ethyl acetate phase was collected, and ethyl acetate was removed with an evaporator. The highly viscous transparent liquid after evaporation was dried in vacuum for more than 3 hours.

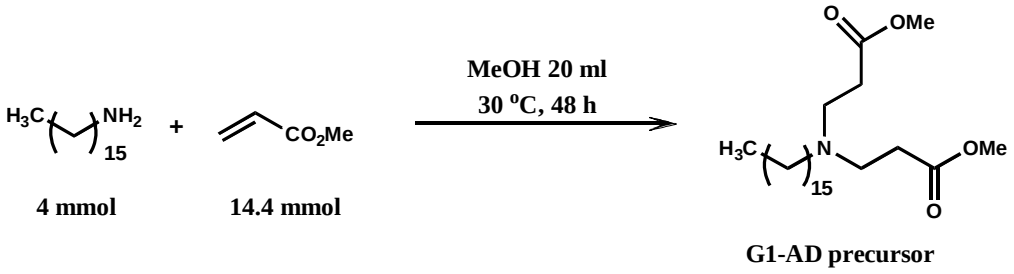

Scheme 5-1-1 Synthetic route of G1-AD precursor

As for G1-AD synthesis, G1-AD precursor was dissolved in methanol (5 mL) and ethylenediamine (5.00 mL, 75.0 mmol) was added under nitrogen atmosphere. The reaction mixture was stirred at 30 °C for 48 h (**Scheme 5-1-2**). After evaporation of the reaction solution, the residue was purified by precipitation with methanol/diethyl ether three times. The final yield was 50%.

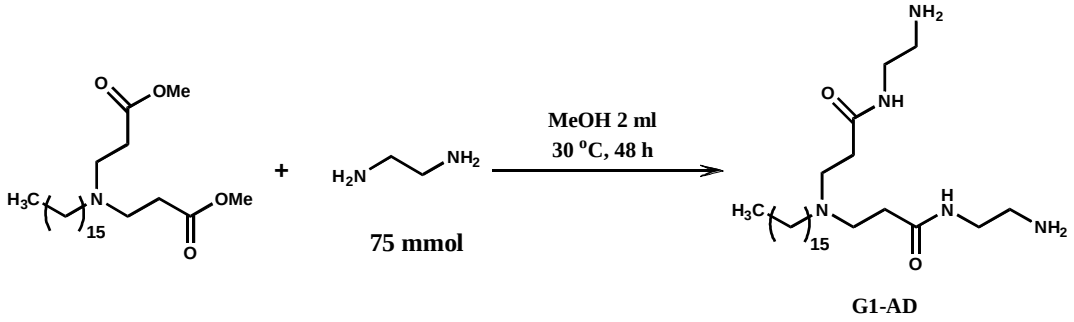

Scheme 5-1-2 Synthetic route of G1-AD

As for G2-AD synthesis, the same procedures as the above were carried out with G1-AD as substrate. The synthetic root was shown as **Scheme 5-2.** The final yield was 25%.

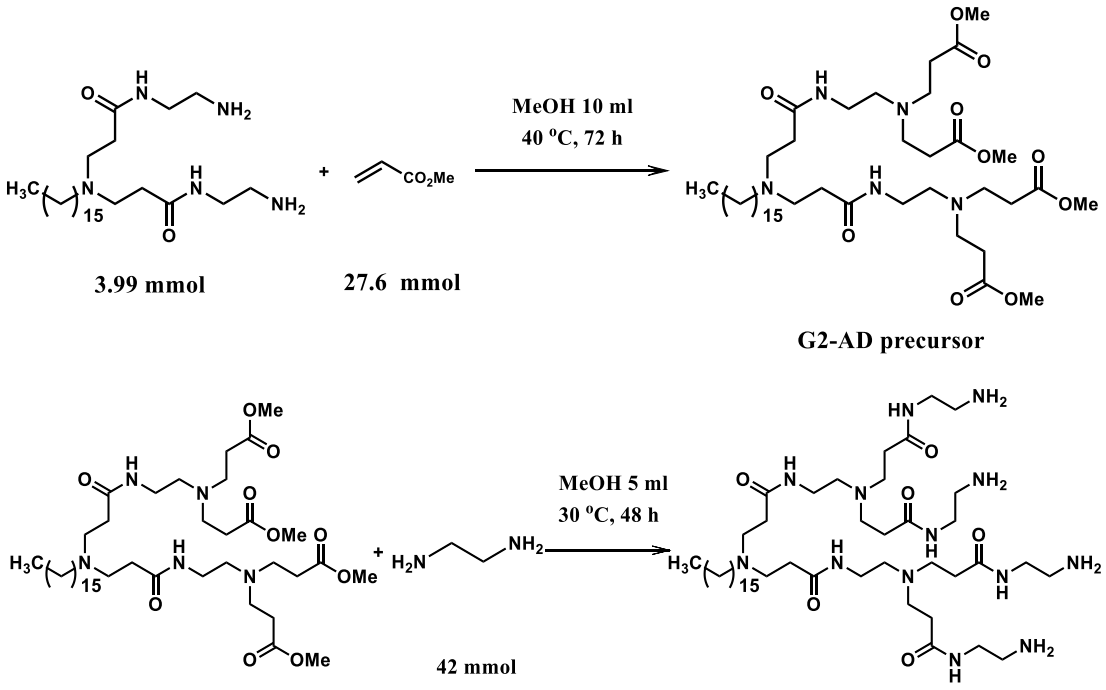

Scheme 5-2

Fast atom bombardment mass spectra of the products were obtained using a JMS-700 (JEOL, Tokyo, Japan) in the negative ion mode with glycerol as the matrix and xenon gas to confirm the synthesized amphiphilic dendrons. Mass ranges were from *m/z* 10 to 2000.

2.2. Dynamic Light Scattering (DLS) measurement

Size distributions of lipid-AD coassemblies were measured by the dynamic light scattering (DLS) (Zetasizer Nano, Malvern Instruments Ltd., Tokyo, Japan). Samples of lipid-AD suspension (1 mmol/L) were used for measurement at 25℃.

2.3. Differential Scanning Calorimetry (DSC) measurement

Thermal analysis of lipid-AD coassemblies were carried out with differential scanning calorimeter (DSC-60; Shimadzu, Kyoto, Japan) operating with Pyris software to determine phase transition temperature. The sample pan for measurement was sealed with 20 μL of 50 mM lipid-AD sample and the sample pan containing pure water was used to calibrate temperature and heat flow. The measurement was performed from 0 ºC to 70 ºC under a temperature rising condition of 1 ºC/min in nitrogen gas environment with a purging rate of 60 mL/min.

2.4. Analysis for membrane hydration state of lipid-AD coassemblies

The hydration states of lipid-AD were estimated with fluorescent probes Laurdan and Prodan. The final concentrations of Lipid, Laurdan, and Prodan were adjusted to 100 μM and 1 μM, respectively. After incubation for 30 minutes in the dark, the fluorescence spectra of Laurdan and Prodan excited at 340 nm were measured from 400 nm to 550 nm with a fluorescence spectrophotometer FP-6500 (JASCO, Tokyo, Japan). Hydration state in more hydrophobic part of lipid-AD was evaluated with Laurdan.

$GP_{340\ \mathrm{Laurdan}}$ values of Laurdan, which is defined as follows:

$$GP_{340\ \mathrm{Laurdan}} = (I_{440} - I_{490}) / (I_{440} + I_{490}) \qquad \text{(Eq. 5-1)}$$

, where I_{440} and I_{490} are fluorescence intensity of Laurdan at 440 nm and 490 nm, respectively.

Similarly, hydration state at surface region was also evaluated with $GP_{340\ Prodan}$ values of Prodan, which is defined as follows:

$$GP_{340\ Prodan} = (I_{437} - I_{510}) / (I_{437} + I_{510}) \qquad \text{(Eq. 5-2)}$$

, where I_{437} and I_{510} are fluorescence intensity of Prodan at 437 nm and 510 nm, respectively.

2.5. Evaluation of lipid-AD coassemblies fluidity

The sample suspension was prepared in the same way as the hydration state measurements, except the fluorescence probe was changed to DPH. The membrane fluidity (1/P) is reciprocal values of the polarizability (P) and was calculated according to the following formula:

$$P = (I_{//} - GI_{\perp}) / (I_{//} + GI_{\perp}) \qquad \text{(Eq. 5-3)}$$

$$G = i_{\perp} / i_{//} \qquad \text{(Eq. 5-4)}$$

, G is the correction coefficient.

2.6. Circular Dichroism (CD) spectral measurements

The CD spectra at 300 – 400 nm were obtained at various temperatures by using a JASCO J-820 SFU spectropolarimeter (JASCO, Tokyo, Japan), and the induced CD intensity of DPH was measured at 360 nm. In ICD experiments, the total concentrations of lipid and DPH were 20 mM and 80 μM, respectively.

3. Results and Discussion

3.1. Structure confirmation of synthesized amphiphilic dendrons

PAMAM dendron-bearing lipid, which structures are shown in **Fig. 5-1**, were synthesized by repetition of exhaustive Michael addition with methyl acrylate using hexadecylamine as the core material (Morita-Imura *et al.*, 2014) and subsequent exhaustive amination with ethylene diamine (Takahashi *et al.*, 2003). Mass spectrum of G1-AD and G2-AD were shown in **Fig. 5-2**. The peaks at 470.4 (G1-AD, [M + H^+]) and 926.8 (G2-AD, [M + H^+]) were found and indicate the successful synthesis of G1-AD and G2-AD. 350.3 *m/z* in G1-AD mass spectra might be the molecular weight of G1-AD that lose two ethanediamine groups at the headgroup. 866.7 *m/z* in G2-AD mass spectra is derived from the G2-AD losing one ethanediamine groups at the headgroup.

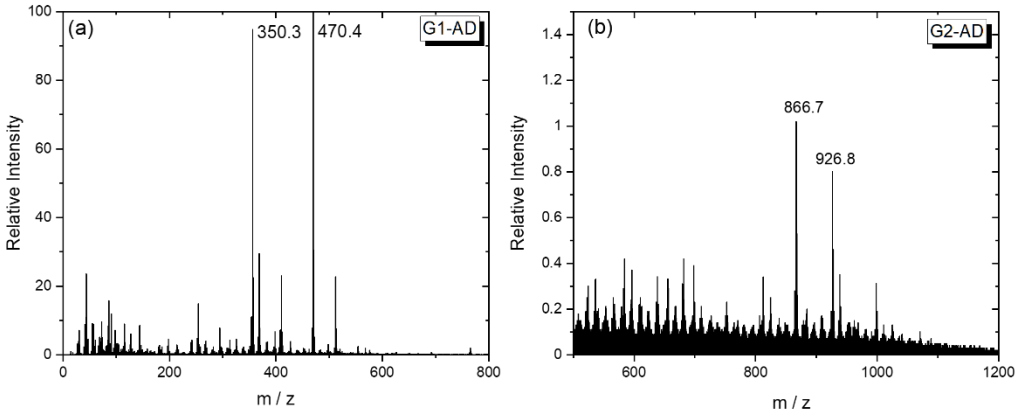

Fig. 5-2 Fast atom bombardment mass spectra of (a)G1-AD and (b) G2-AD

The ^{1}H nuclear magnetic resonance (JNM-ECS400; JEOL) analysis was carried out at room temperature with CD_3Cl as solvent. ^{1}H NMR ($CDCl_3$): δ 0.88 (t, $\mathbf{CH_3}(CH_2)_{15}$), 1.22 (br, $CH_3(\mathbf{CH_2})_{14}$), 2.40 (t, $NCH_2\mathbf{CH_2}CO$), 2.34 (t, $\mathbf{CH_2}N$), 2.81 (t, $N\mathbf{CH_2}CH_2CO$), 2.71(t, $NHCH_2\mathbf{CH_2}NH_2$), 3.28(t, $NH\mathbf{CH_2}CH_2NH_2$)^{1}H NMR spectra of G1-AD and G2-AD were shown in **Fig. 5-3**.

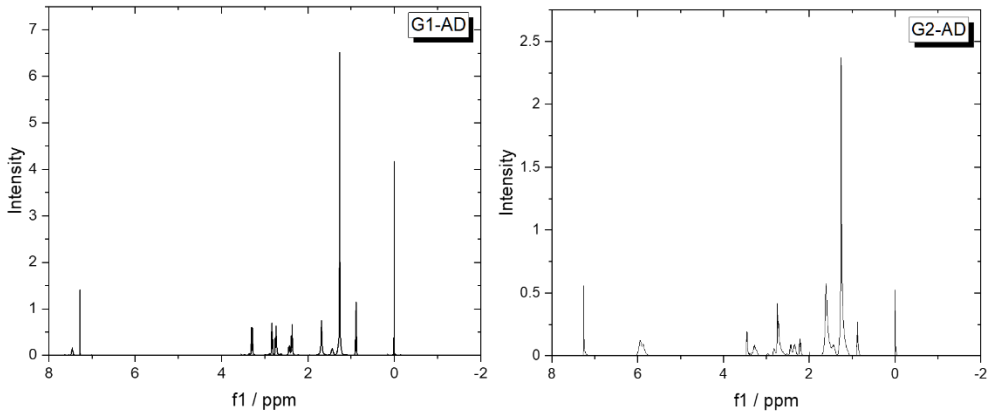

Fig. 5-3 ^{1}H NMR spectra of (a)G1-AD and (b) G2-AD

3.2. Structure and properties characterization of lipid / G1-AD formed self-assembly

Depending on the generation (G*i*, *i* = 1, 2) of PAMAM dendron, ADs were named as G1-AD and G2-AD, respectively. The synthesized ADs were mixed with 1,2-dipalmitoyl-*sn*-glycero-3-phosphocholine (DPPC) at the molar ratio 20% and 40%. The properties and structure of the formed coassemblies were characterized by differential scanning calorimetry (DSC) analysis and dynamic light scattering (DLS). In addition, the fluidity and hydration state in hydrophobic region of coassembly were evaluated with 1,6-Diphenyl-1,3,5-hexatriene (DPH) (Lentz *et al.*, 1989) and 6-Lauroyl-2-dimethylamino naphthalene (Laurdan) at 25℃. The surface hydration degree of the coassembly was evaluated with 2-(Dimethylamino)-6-propionylnaphthalene (Prodan) at 25℃.

First, the coassembly constituted of G1-AD and DPPC was characterized. The size of coassemblies formed by mixing DPPC and 20 mol% G1-AD was measured by DLS, and showed distribution near 93 nm (**Fig. 5-4a**). This result is consistent with the pore size of extrusion and DPPC liposomes. In the case of 40mol% G1-AD, its size was about 500 nm, showing small aggregation (data not shown here). Pure DPPC liposome shows the phase transition from gel phase to liquid crystalline phase at 42°C (Leekumjorn *et al.*, 2007). From DSC results, G1-AD (20 and 40mol%) modified DPPC coassemblies showed similar phase transition temperature of DPPC, suggesting the gel-like bilayer structure was maintained after G1-AD modification (**Fig. 5-4b**). From results of DLS and

DSC, it can be concluded that the vesicle structure of DPPC liposome was not destroyed by even incorporation of 40mol% G1-AD. This retention of lipid bilayer structures is also supported by Hinman's report (Hinman *et al.*, 2017). In addition, G1-AD formed the coassembly with DPPC because free G1-AD micelle (ca.10 nm) could not be detected by DLS.

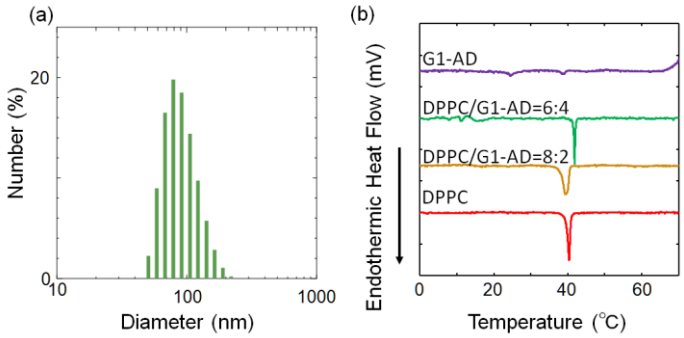

Fig. 5-4 (a) Size distribution of 20mol% G1-AD modified DPPC lipid membrane. (b) DSC thermograms of coassemblies constituted by different ratio of DPPC and G1-AD.

Next, the effects of G1-AD on DPPC membrane properties were evaluated in the respect of fluidity and inner hydration state. As a result, it was found that there was no significant change in fluidity of coaasemblies after AD modification (**Fig. 5-5a**). The interposition of single alkyl chain did not disturb the molecular interactions in DPPC hydrophobic regions. Inner membrane hydration state analysis was performed on the DPPC/G1-AD coassembly by using the fluorescent probe Laurdan, which prefers to locate at glycerol backbone in lipid bilayer and is sensitive to hydration state around Laurdan. As a result, it was found that the GP_{Laurdan} value decreased after 40 mol% G1-AD modification (**Fig. 5-5b**), indicating the incorporation of G1-AD slightly increased the hydration state(hydrophilicity) of coassemblies. The amount of PAMAM parts contributed to this membrane hydration state variation. In conclusion, the above results inferred that the addition of G1-AD did not disturb the DPPC membrane original integral structure.

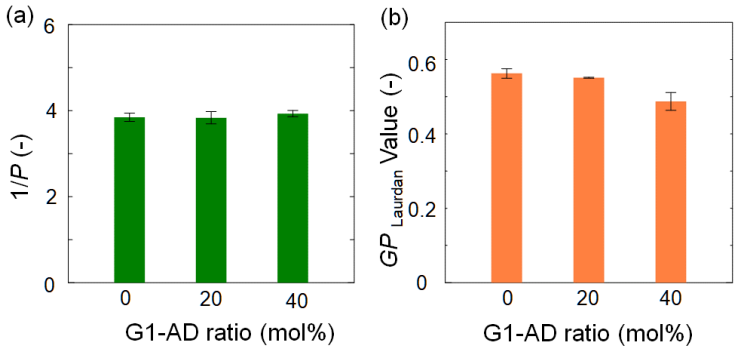

Fig. 5-5. Effect of G1-AD on (a) fluidity and (b) hydration state (polarity) of coassemblies prepared by different ratio of DPPC and G1-AD. The error bars represent the standard deviation from the mean (n=3).

3.3. Structure and properties characterization of lipid / G2-AD coassemblies

Coassemblies prepared with DPPC and G2-AD were also characterized about the effects of AD generation on structure and properties of the coassembly. For G2-AD, the average hydrodynamic diameter of the coassembly was 9 nm in the incorporation of 20mol% G2-AD (**Fig. 5-6a**). On the other hand, 40mol% incorporated coassembly showed a little smaller diameter near 6.5 nm (data not shown here). This several nano size is similar with that of bicelle structure in previous study (Mineev *et al.*, 2016). Moreover, the existence of weak phase transition was confirmed by DSC (**Fig. 5-6b**). These results indicate that bilayer structure of DPPC were preserved in the small size coassembly. This implies that "bicelle", a disc-shaped molecular self-assembly was formed by mixture of 20 mol% or 40 mol% G2-AD with DPPC molecules.

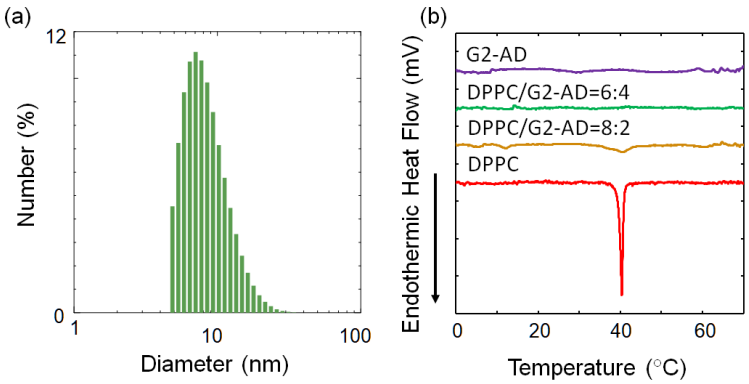

Fig. 5-6. (a) Size distribution of 20mol% G2-AD modified DPPC lipid membrane. (b) DSC thermograms of coassemblies constituted by different ratio of DPPC and G2-AD.

To confirm the formation of bicelle-like structure, induced circular dichroism (ICD) of DPH molecules was measured. ICD spectrum of DPH molecule can be utilized to confirm the formation of bicelles and to evaluate the lipid membrane ordering properties in bilayer membrane. Although DPH itself is an achiral molecule, its CD can be induced when it orients in chiral molecules such as phospholipid (Walde *et al.*, 1997). In addition, the ICD of DPH can be significantly enhanced only in the bilayer with gel phase. By CD measurement of coassembly composed of DPPC and G-2AD at 25°C, the ICD signal intensity (360 nm) of DPH was obtained in both coassembly with 20mol% and 40mol% G2-AD (**Fig. 5-7**). By the way, research about bicelle formed with 1,2-dimyristoyl-*sn*-glycero-3-phosphocholine (DMPC) and 1,2-dihexanoyl-*sn*-glycero-3-phosphocholine (DHPC) demonstrated that in bilayer system, the ICD intensity reflected the molecular ordering state of the lipids in the bicelle bilayer and the ICD intensity of DPH in bicelles is more significant than that in the DMPC vesicle (Suga *et al.*, 2020). Based on this report, the ICD signal of DPH of DPPC/G2-AD coassembly was compared with that of DPPC liposome. In addition to the small size (9 nm and 6.5 nm), the stronger ICD signal of DPPC/G2-AD than DPPC liposome supported the insight that the bicelle structure was constructed. In regards to effect of the G2-AD ratio, the more ordered bilayer structured was formed by 20mol% G2-AD with DPPC compared to that by 40mol% G2-AD modification. The reason for this structure change from liposomes to bicelle-like structure is considered as following; Increment of generation (PAMAM parts) change the hydrophobic-hydrophilic balance of AD. G2-AD with bulky hydrophilic group resembles DHPC. Thus, wedge-shape of G2-AD molecules tend to aggregate and form micelle-like cluster. These clusters destabilized lipid bilayer, and at the same time form bicelle-like structures by locating at the edge of bilayer structure to prevent exposed hydrocarbon chains from contacting water, which is the energetically unfavorable situation (Kessi *et al.*, 1994).

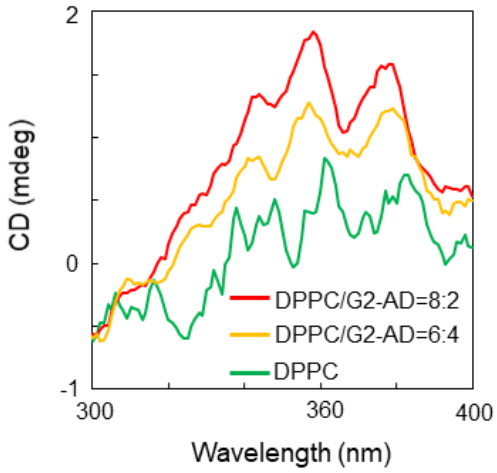

Fig. 5-7 Comparison of ICD spectra of DPH in DPPC liposome and DPPC/G2-AD coassemblies

As for the fluidity and hydration state at hydrophobic site, incorporation of 20mol% AD showed no variation, while that of 40mol% showed increment of fluidity and hydration (**Fig. 5-8**). This can be considered as follows; these probes are also distributed in the rim part, which shows higher fluidity and hydration compared to bilayer (Hinman *et al.*, 2017). Thus, obtained numerical values are the sum of rim and lipid bilayer parts. As the ratio of AD increases, the parts of rim increased and attributed to increment of fluidity and hydration degree.

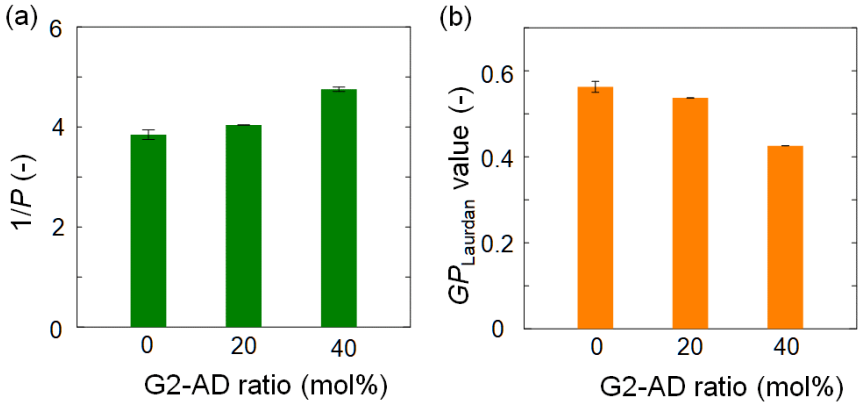

Fig. 5-8 Effect of G2-AD on (a) fluidity and (b) hydration state (polarity) of coassemblies prepared by different ratio of DPPC and G2-AD. The error bars represent the standard deviation from the mean (n=3).

3.4. Surface hydration degree evaluations of lipid / AD coassemblies

Finally, the surface hydration degree in coassembly surface was analyzed with the fluorescence probe Prodan (**Fig. 5-9**), which is suitable for evaluation of hydration state at surface region (Bui *et al.*, 2016). In G1-AD modified DPPC liposomes, the remarkable decreasing of GP_{Prodan} was observed by increasing ratio of G1-AD. This indicates that incorporation of G1-AD can greatly increase hydration degree in the surface region. This is because amine groups at the head group of PMAMA dendron attracted water molecules by hydrogen bonding and significantly changed the surface hydration of coassembly. Compared with G1-AD modified DPPC lipid membrane, the surface of DPPC/20mol%G2-AD formed coaseembly showed significantly higher hydration at the surface, which is probably due to much more PAMAM dendrons at the surface.

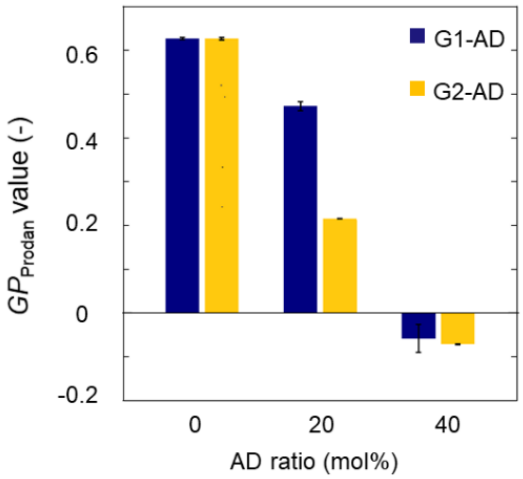

Fig. 5-9 Effect of G1-AD and G2-AD on the surface hydration state of coassemblies. The error bars represent the standard deviation from the mean (n=3).

4. Summary

In this chapter, we focused on the advantages of liposomes and ADs, and attempted to prepare the coassembly of liposome and AD, which could be one of effective and possible way to enhance the performance as drug delivery carrier. To investigate the structure and properties, especially hydration state, various coassemblies were prepared by changing different generation and different composition of PAMAM ADs. Our results demonstrated that the coassemblies were prepared by ADs and DPPC, and that the coassembled structure and surface hydration could be controlled by the generation of the dendrons and composition ratio of ADs. For G1-AD, the incorporation of G1-AD into DPPC liposomes did not disturb the vesicle morphology, but greatly improved the surface hydration degree. However, the incorporation of G2-AD induced bicelle-like structure because the bigger hydrophilic headgroup region of G2-AD make it easier to form the rim part of bicelle-like structure. Thus, our work and method would become an index for modifying the surface hydration state of lipid membrane and construction and understanding of lipid-AD coassembly.

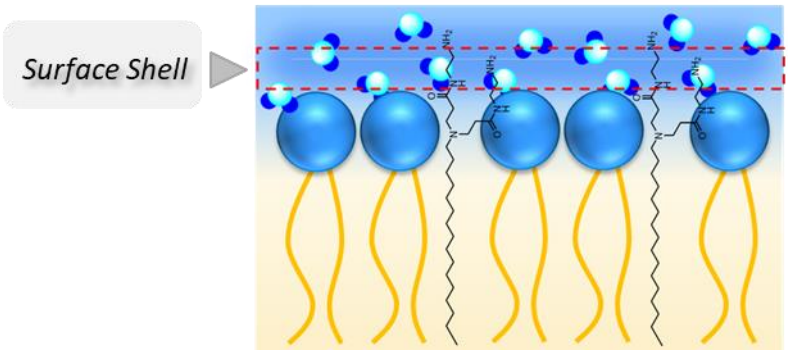

Fig. 5-10 Lipid membrane surface hydration shell formation by modification with G1-AD

Chapter 6

Design of fatty acid-like pH-responsive prodrug analogues for regulation of their self-assembly behaviors

Strategy

Inspired from lipid membrane, self-assembly is evolving as an appropriate strategy to create a variety of complex architectures, especially in the field of drug delivery. The self-assembly properties are hence expected to be used as the index for design of drug carrier.

Studies have indicated hydration property of carrier is crucial for the regulation of the pharmacokinetics. The representative one is pegylation effect, namely modification of carrier surface with poly (ethylene glycol) (PEG). The hydration layer at the surface results in escape from the engulfment of macrophage and dominantly extends the drug half time in the blood. However, the PEG-modified liposome showed reduced cell uptake, which was attributed to the less nonspecific hydrophobic interaction of liposome with cell membrane (Klibanov *et al.*, 1990). Another example is PE-incorporated liposome. Phosphoethanolamine (PE) has a small head group which preferentially provide a flat membrane surface almost no curvature, possessing thinner hydration layer at the surface than PC. PE-incorporated liposome usually can cause membrane fusion (Bompard *et al.*, 2020). The different surface hydration property might be one of the reasons to explain its different membrane-related behavior. Therefore, the hydration property of carrier possesses great potential to effect on each step during drug delivery process, which is needed to be considered as a key factor when design prodrug-based SADDS.

As one of representative self-assembly system, it is known that the hydration state of lipid membrane is related to its lipid headgroup, packing states of acyl chains, lateral interaction of lipids etc. For lipid self-assembly, because of diversity of lipid molecules, the hydration state of lipid self-assembly can be regulated by modulating the lipid composition to modulating the hydration state. For prodrug based self-assembly, the diversity of aggregate structures arises from an interplay of various molecular forces that drives the self-assembly. Therefore, self-assembly design is essentially the design of molecular structure. How to regulate the hydration state is still an uncharted territory, because of the less strategy about how to reflect and regulate the influencing factors in the molecular design to regulate the mesostructured formation.

Based on the above results in this study, we summarized the location, phenomenon and effect on variation of hydration degree by the fours molecules studied, and found the regulation of hydrocarbon chain packing density and headgroup properties would be efficient pathway to regulate the self-assembly hydration state. For chain packing density, the 'hydrophobic effect' worked as main force to bring the molecules closer together, while at the headgroup region, the 'solvation' or electrostatic interaction of the head groups tends to be important factors to regulate the interaction of headgroup. Manipulation these two molecular level interactions might be the possible way to regulate prodrug based self-assembly hydration state.

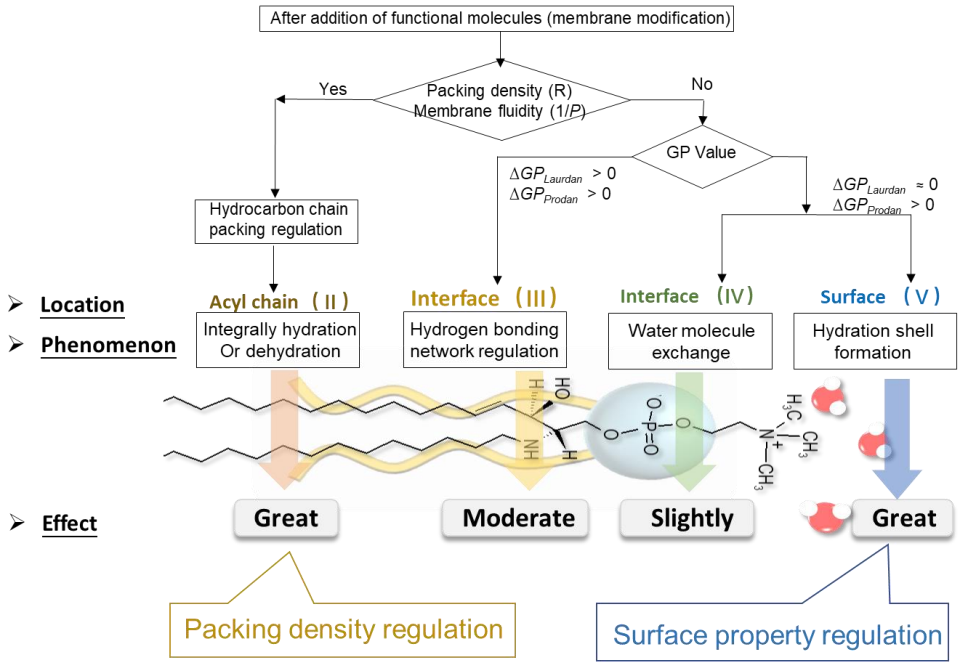

Scheme 6-1. Summary of effects of functional molecules on regulation of lipid membrane hydration state

Therefore, in this chapter, we would like to propose a molecular design strategy to regulate self-assembly hydration state by focusing on modulating the balance of hydrophobic effect and 'solvation' effect of headgroup.

1. Introduction

In recent years, various carrier-assistant drug delivery systems (DDSs), such as liposomes, micelles, and hydrogels, have been extensively studied to reduce side effects and enhance therapeutic potential (Tiwari *et al.*, 2012; Patra *et al.*, 2018) However, further development of DDSs has been impeded by factors like low drug carrying capacity, carrier-induced toxicity, and immunogenicity. To address these issues, self-assembly drug delivery systems (SADDSs) have been proposed as a novel paradigm to carry out intracellular delivery without the help of drug carriers (Jin *et al.*, 2006). The main strategy to build SADDSs is prodrug-based self-assembly (Nasa *et al.*). Prodrugs are prepared by bioreversible modification of a drug into a masked, inactive form with more desirable physicochemical properties, and are usually classified into bioprecursor prodrug and carrier prodrugs. SADDSs can be designed by carrier prodrug based on their ability to form self-aggregation structure. Therefore, SADDSs involve pre-existing systems that the active drugs participate in via cleavable linkers to form nanostructures that achieve high loading and delivery at the same time. This prodrug-based SADDS strategy has also introduced the possibility of regulating the self-assembly structure in a precise manner through molecular structure design (Malhotra *et al.*, 2009; Wang *et al.*, 2015).

For SADDSs, almost all reports have focused on exerting therapeutic effects derived from parent drugs (Cheetham *et al.*, 2017). However, it has been reported that the structure and property of self-assembly, such as the shape, size, surface charge density, and so on, usually plays important roles in uptake efficiency (He *et al.*, 2016; Tree-U dom *et al.*, 2015) and controlled release (Caldorera-Moore *et al.*, 2010), which also influences exertion of the therapeutic effects of the parent molecule. All of these works emphasize efforts to clarify the structure-activity link that will contribute to further effective design of prodrug-based SADDSs. Aside from clarification of the structure-activity relationship, efforts dedicated to the molecule-structure association are also indispensable. Nonetheless, the strategy regarding how to design prodrugs to obtain various self-assembly structures and be controlled under different biophysical microenvironments remains lacking.

In this chapter, fatty acid-like prodrugs were designed, and their self-assembled prodrug systems were investigated with a focus on controlling self-assembly behavior via pH change. These prodrug structures were inspired by fatty acids (FAs). It is known that FAs are amphiphilic molecules with hydrocarbon chains and hydrophilic carboxyl groups whose assembling behaviors strongly depend on the hydrocarbon chain length as well as the ionization state of the polar head group (Suga *et al.*, 2016). Until now, oleic acid has been widely applied to design a pH-sensitive carrier for delivering hydrophobic drug

molecules (Salentinig *et al.*, 2010; Gontsarik *et al.*, 2018). Here, Oxaprozin (Oxa) (Maestrelli *et al.*, 2009), as a representative of the aryl carboxylic derivatives, which are a primary kind of non-steroidal anti-inflammatory agent possessing high hydrophobicity, was chosen as model molecule to design Oxa prodrug analogues (Oxa-lipids). Due to the presence of phenyl groups in the Oxa structure, there is a high possibility of forming a fiber structure. These designed prodrug molecules possess a carboxyl group as the head group and different hydrocarbon chain lengths as linkers. Thus, they achieved control of prodrug self-assembly behavior, changing from micelles to fibers to solids depending on different prodrug molecular structures, pH conditions, and concentrations. Therefore, this variation in self-assembly structure depending on pH would be helpful for the development of a biological microenvironment-sensitive SADDS.

2. Materials and Methods

2.1. Materials

The following agents were purchased from Tokyo Chemical Industry Co., Ltd. (Tokyo, Japan): Oxaprozin (Oxa), *N,N'*-carbonyldiimidazole (CDI), and sodium methoxide (CH_3ONa). Dimethyl formamide (DMF) and ethyl acetate were purchased from Kanto Chemical Co., Inc. (Tokyo, Japan). Methyl 6-aminohexanoate hydrochloride and 8-aminooctanoic acid were purchased from Sigma-Aldrich (St. Louis, MO, USA). All other reagents employed in the Oxa-lipid synthesis, purification, and preparation or evaluation of self-assembly structures were purchased from Wako Pure Chemical Industries (Osaka, Japan). Both 8-aminooctanoic acid and 12-aminododecanoic acid were applied to 4N-HCl/dioxane, which were purchased from Watanabe Chemical Industries, Ltd. (Hiroshima, Japan), to obtain methyl 8-aminooctanoic acid and methyl 12-aminododecanoic acid, respectively. All chemicals were used without further purification.

2.2. Prodrug synthesis

Condensation reagents CDI and Oxa were mixed at a molar ratio of 1:1 and dissolved in 5 mL of DMF. The reaction was conducted at 65 ℃ for 8 h with stirring for carboxylic acid activation. After that, 1 mmol methyl 6-aminohexanoate hydrochloride, methyl 8-aminooctanoic acid, or methyl 12-aminododecanoic acid was added to react for 24 h at 65 ℃. The reaction mixture was finally treated with 10 mL saturated solution of Na_2CO_3 and extracted twice with 10 mL ethyl acetate. The ethyl acetate phase was washed with water two times, and the product was collected after evaporation. Next, demethylation of the obtained product was performed. 1 mmol of product and 1.5 mL of 5 mmol/L CH_3ONa in methanol were dissolved in 2 mL methanol before the mixed solution was stirred for 24 h at room temperature (25 ℃). Separation and purification were carried out with 2 mol/L NaOH solution and ethyl acetate to remove undermethylated reactants. After products were extracted from the neutralized NaOH solution by ethyl acetate, the final pure solids were obtained by evaporation of the ethyl acetate. These final solids, the amphiphilic pro-drug Oxa-lipids, were named Oxa-C6, Oxa-C8, and Oxa-C12. The synthetic procedure is shown in **Scheme 6-2**.

Scheme 6-2. Synthesis of Oxaprozin-based lipid prodrugs

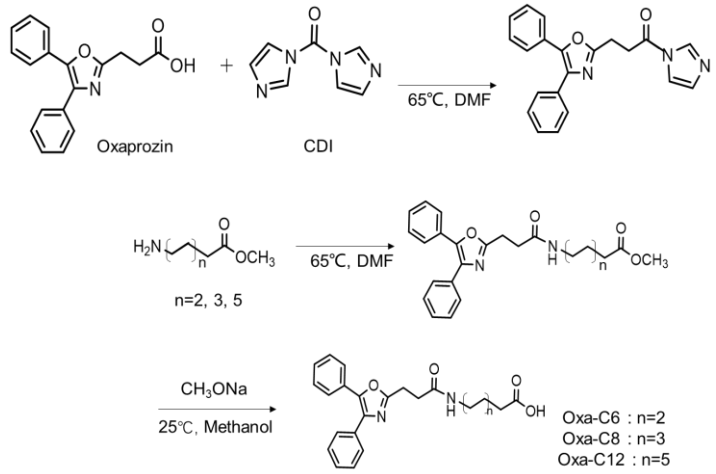

2.3. Chemical structural confirmation of Oxa-lipids by ^{1}H NMR spectroscopy

The ^{1}H nuclear magnetic resonance (NMR) (JNM-ECS400; JEOL) analysis was conducted at room temperature (25 ℃). Dried Oxa-lipids (30 mg) were mixed with 0.7 mL of CD3Cl in 1.5 mL Eppendorf. Mixed solutions were transferred into NMR tube after Oxa-lipids dissolved completely. The NMR experiment for each sample was acquired in 3.53 min for 8 scans with a relaxation delay of 5 s, respectively. Phasing and baseline correction of NMR spectra were done using Alice software (Version 6, Tokyo, Japan) for all samples.

2.4. Hydrophobicity evaluation by high-performance liquid chromatography (HPLC)

The hydrophobicity of the synthesized Oxa-lipids was determined by HPLC. 200 μg/mL of Oxa-lipids were prepared by dissolving in mobile phase solution (methanol: H_2O=75:25 volume ratio). The same molar weight was calculated for the other Oxa-lipids. The analytical column used was a reversed-phase C18 (ODS) column (GL Sciences Inc., Tokyo, Japan). 10 μL of the solution was injected into the mobile phase with a 0.5 mL/min flow rate for HPLC analysis. The analysis was performed using the Waters 1515 Isocratic HPLC Pump and Waters 2489 UV/Vis Detector system (Waters, Milford, MA, USA). The detection wavelength was set at 254 nm to evaluate the retention time for each Oxa-lipid. The log *P* values of the Oxa-lipids were predicted

with chemical drawing software from PerkinElmer (Waltham, MA, USA).

2.5. pH titration and turbidity measurements

The Oxa-lipid analogues were added to ultrapure water. After the pH was adjusted to near 12 by the addition of 10 μL of 5 mol/L NaOH (pH=11.74 for Oxa-C6, pH=11.75 for Oxa-C8 and pH=11.21 for Oxa-C12), the sample solutions were titrated with 500 mmol/L HCl and stirred at room temperature. The initial solution volume and concentration of each Oxa-lipid for pH titration were 10 mL and 30 mmol/L, respectively. After pH titration, the final concentrations of the Oxa-C6, Oxa-C8, and Oxa-C12 solutions were 28.46, 28.90, and 28.85 mmol/L, respectively. Thus, the influence caused by this concentration difference was negligible.

The solution pH was measured using an alkali-resistant pH electrode (LAQUA; Horiba, Ltd., Kyoto, Japan). The turbidities of the sample solution (OD_{440}) under various pH conditions were measured using UV-Vis spectroscopy (UV-1800; Shimadzu Corporation, Kyoto, Japan).

It has previously been reported that the pK_a values of acid compounds are defined by the Henderson−Hasselbalch equation (Kanicky *et al.*, 2003; Rendon *et al.*, 2012) as follows:

$$X_{HA} + X_{A-} = 1$$

$$\mathrm{pH} = \mathrm{p}K_a + \log_{10}\frac{X_{\mathrm{A}^-}}{X_{\mathrm{HA}}} \qquad \text{(Eq. 6-1)}$$

where X_{HA} and X_{A-} represent the molar fractions of the protonated Oxa-lipids and ionized Oxa-lipids, respectively.

2.6. Cryo-transmission electron microscopy (Cryo-TEM)

Cryo-TEM experiments were carried out using a JEM-3100FEF microscope (JEOL Ltd., Tokyo, Japan). The measured samples were Oxa-C6 at a concentration of 30 mM and pH 12±0.1 over the inflection point, pH 7.5±0.1 near the inflection point, and pH 6.5±0.1 during the pH titration process. A thin layer of sample solution was rapidly frozen to prevent rearrangement of water molecules into a crystalline form. A little solution was placed on an electron-microscopy microgrid. The excess solution on the grid was drained

off with a piece of a filter paper. The grid was immediately plunged into liquid ethane maintained at approximately 100 K in an immersion cryofixation apparatus (Leica, EM-CPC; Leica Microsystems; Wetzlar, Germany). It was placed in a cryotransfer holder (Gatan, 626; Gatan Inc.; California, USA) and transferred to the TEM (JEOL, JEM-3100FEF; JEOL; Tokyo, Japan). The liquid nitrogen cryotransfer holder keeps specimens around 100 K.

2.7. Estimation of critical micelle concentration (CMC) and critical aggregation concentration (CAC)

The CMCs of the Oxa-lipids were determined by fluorescence with Nile Red. Fluorescence spectra were recorded on a fluorescence spectrophotometer (FP-6500; JASCO, Tokyo, Japan). The experiments were carried out by adding 10 μL of 4×10^{-5} mol/L stock ethanol solution of Nile Red to 1 mL Oxa-lipids to create the final concentrations (from 0.1 to 10 mmol). The measured sample solution was first dissolved in carbonate buffer (pH=9.0; 50 mmol) and diluted under various pH conditions. The maximum intensity of the emission peak (excitation at 550 nm) of Nile Red was in the 600–650 nm region, which was used to determine the CMCs.

Here, the CAC of the fiber structure was confirmed by its self-fluorescence properties, namely the aggregation-induced emission (AIE) phenomenon. These fluorogens are non-emissive in the dissolved state but strongly emissive in the aggregate state, which is attributed to the restriction of intramolecular rotations. Thus, the maximum fluorescence intensity (E_x: 550 nm; E_m: 640 nm) was plotted to determine the CAC of the fibroid self-aggregated structure.

3. Results and Discussion

3.1. Prodrug synthesis

We synthesized a series of Oxa-lipids with different hydrocarbon chain length as hydrophobic moieties with carboxyl groups as the head group. These FA-like Oxa-lipids were expected to form various self-assembly structures by controlling the balance of their hydrophobic and hydrophilic parts. The prodrug molecular structures were confirmed by ^{1}H nuclear magnetic resonance (NMR) in $CDCl_3$ (JNM ECS-400, JEOL Ltd., Tokyo, Japan). The number of proton atoms on the methylene groups (ppm < 4) and ring structure (ppm > 7) was calculated to confirm the Oxa-lipid molecular structures. The precise proton ratios of 14:10, 18:10, and 26:10 for Oxa-C6, Oxa-C8, and Oxa-C12, respectively, proved that the products were obtained through the aforementioned synthetic procedures. The Oxa-lipid molecular structures and NMR results are summarized in **Fig. 6-1.**

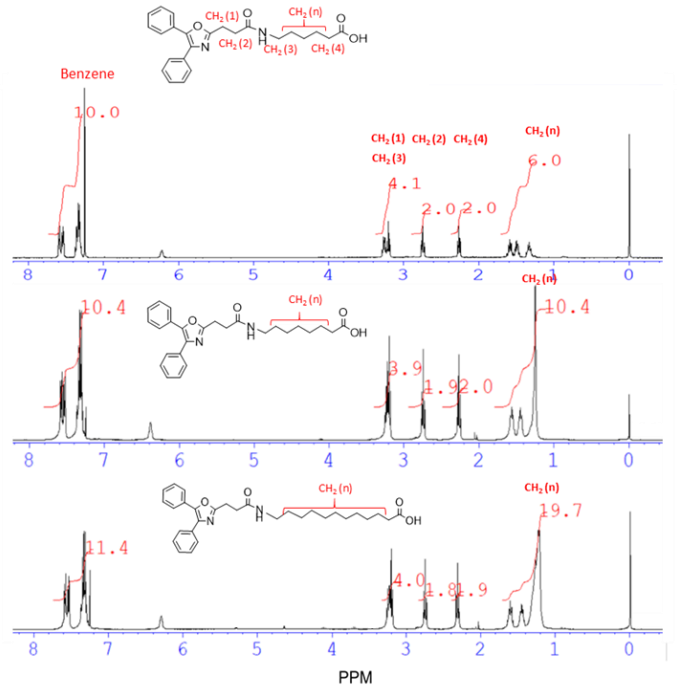

Fig. 6-1 ^{1}H NMR spectra of Oxa-C6, Oxa-C8, and Oxa-C12.

The hydrophobicities of the prodrug analogues were evaluated by HPLC in reversed-

phase mode (ODS column). It is known that reversed-phase chromatography is typically used to analyze the hydrophobicity of compound based on relative retention time (Sharma *et al.*, 2016; Chen *et al.*, 2017): a compound with longer hydrocarbon chain results relatively longer elution time in reversed phase-HPLC. The retention times for Oxaprozin, Oxa-C6, Oxa-C8, and Oxa-C12 were 4 min, 6 min, 8 min, and 18 min, respectively (**Fig. 6-2**). From these results, we conclude that increasing lengths of the alkyl carbon chain enhanced the hydrophobicities of the Oxa-lipids. This result is similar to many other report (Zhang *et al.*, 2016). For Oxa-C6 and Oxa-C8, the retention times were not largely different. However, when the number of carbon atoms increased to 12, the retention time increased significantly, indicating that hydrophobicity changed significantly in Oxa-C12. These results also corresponded to simulative log *P* values. The log *P* values of Oxa-C6 and Oxa-C8 were 4.17 and 4.18, respectively. While this difference was negligible, the log *P* value of Oxa-C12 was near 6.31. Thus, the length of modified hydrocarbon chain can alter the hydrophobicities of the Oxa-lipids, which empowered the Oxa-lipids to form self-assembled structures.

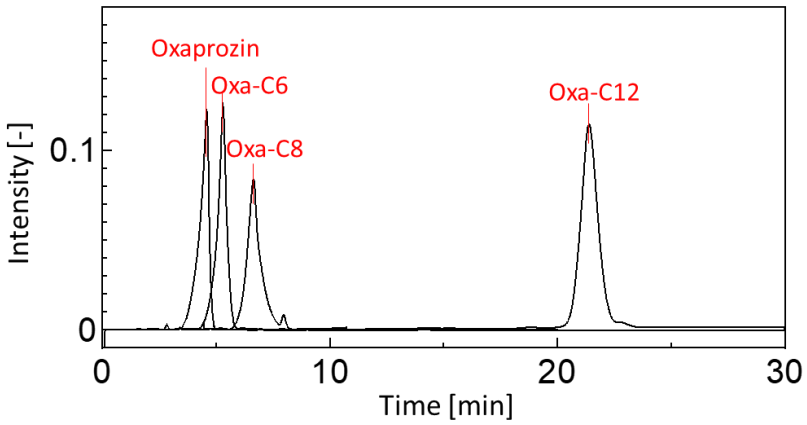

Fig. 6-2 Retention time analysis of each Oxa-lipid for estimation of hydrophobicity by reversed-phase chromatography.

3.2. Characterization of pH-responsive self-assembly phase behaviors of designed Oxaprozin prodrug analogues

The self-assembly phenomenon and behavior are strongly determined by molecule structural properties. In general, the concept of molecular packing parameter is widely

employed in the literature to explain, rationalize, and even predict molecular self-assembly in solutions (Hayashi *et al.*, 2017). The molecular packing parameter is defined as V_0/al_0, where V_0, l_0, and a are the volume of surfactant tail, length of the surfactant tail, and equilibrium area per molecule at the aggregate surface, respectively (Nagarajan *et al.*, 2002). For the amphiphilic molecules in this study, the carboxyl group can behave as hydrophilic head group. Therefore, the self-assembly structure can be altered by regulating the head group size, namely the "*a*" value in the molecular packing parameter, through controlling the protonation degree of the carboxyl group. It has been reported that oleic acid can form various self-assembly structures depending on pH conditions. Similar to oleic acid, the synthetic Oxa-lipids in this study were also expected to show pH-responsive self-assembly behavior. To observe the morphological alterations in Oxa-lipid self-assembly depending on the balance between hydrophobic and hydrophilic moieties, pH titration and monitoring of solution turbidity were performed (Suga *et al.*, 2014). Here, pH-responsive self-assembly phase behavior was analyzed with Oxa-C6. Based on the solution turbidity variation of Oxa-C6 **(Fig. 6-3a**), the OD_{440} value was near zero at pH=10. Therefore, Oxa-C6 was dissolved or formed a micelle. With the addition of HCl solution (60 μmol), the OD_{440} value greatly increased from 0 to 0.505. From the pH titration curve (**Fig. 6-3a**), the point of obvious change was observed near pH=7.5, which was higher than the normal pK_a value of the carboxyl group (near 4.8). At the same time, the phase transition was confirmed by the change of transparency from soluble to turbid. This much higher apparent pK_a value indicates that some tiny aggregates exist when the pH is higher than this distinctly changed point. Due to the existence of a self-assembly structure during the titration process, the protons accumulate on the aggregate surface and promote protonation of head groups while leaving the bulk solution with a lower proton activity (higher pH).

The morphology of this tiny assembled structure under different phase states was also confirmed by cryo-TEM images (**Fig. 6-4a** and **4b**). At 25 ℃, a non-distinct image with the recognizable aggregation was obtained, and the observed dots in the image are considered to be frost formed at low temperatures. This is consistent with the observed transparent bulk phase state and the near-zero OD_{440} value. Despite the absence of detectable images, the increased pK_a value mentioned above and the detectable CMC value indicated the existence of a tiny aggregation structure even though the size of this

structure is too small to be observed. Based on these results, the micellar structure can be confirmed when the pH condition is higher than the apparent pK_a.

For the turbid state, the fiber-like structure was observed at pH=6.5 as shown in **Fig. 4c**. Similar to Oxa-C6, all three Oxa-lipids formed two kinds of assembled structures before the final solid formed under low pH conditions: a tiny assembled structure and a fibrous structure. Given the Oxa-lipid molecular structures, this pH-dependent self-assembly behavior can be explained by the repulsive interaction between deprotonated head groups and cooperative interactions between tails. At a high proportion of ionized species, the electrostatic repulsion between negatively charged head groups makes the size of the head groups effectively larger. On the other hand, the hydrophobic interactions between the tails do not seem strong enough to form a distinct hydrophobic core due to intermolecular distance. Therefore, the micelle structure can be formed. With increased protonation of the carboxyl group, the electrostatic repulsion between negatively charged head groups is weakened. The hydrophobic interactions of the tails start to play the main role in deciding the self-assembly structure. It has been reported that molecules containing aromatic rings without ionized groups usually govern their ability to self-assemble through aromatic π-π stacking with a distinct hydrophobic core. In fact, such interaction can be regarded as a robust hydrophobic interaction (Tobe *et al.*, 2002; Lu *et al.*, 2019). However, unlike common hydrophobic interactions, the π-π stacking is always directional and can induce directional growth due to the ordered stacking of benzene rings, which makes it easier to form tubes or fiber structures (Lin *et al.*, 2010). Consequently, when the ionization degree is lower than the ionized degree at pH = the apparent pK_a, the fiber structure is formed based on the dominant hydrophobic interaction. The formation of fiber solids can also be confirmed by the sudden slight increase in pH as illustrated in the pH titration curve. With the increased protonation of the Oxa-lipids, more fiber-like solids were formed, and the fiber structure was gradually conjugated together. This inference is also supported by the unchanged pH value despite the addition of HCl. Finally, the fully

a. b.

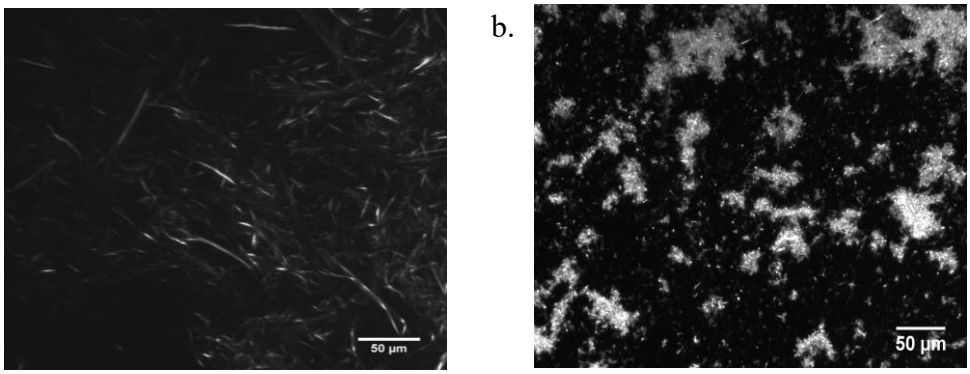

Fig. 6-3 Dark field microscope images for a. turbid state and b. insoluble solid state

protonated prodrug molecules formed an insoluble solid state, and the dark field microscope images for the turbid and insoluble solid states are shown in **Fig. 6-3**.

Among the three Oxa-lipids, different molecular structures were associated with differing degrees of pH responsiveness (**Fig. 6-4b** and **6-4c**). With greater hydrocarbon chain length, the stabilization of the aggregated surface induced an increase in the apparent pK_a value (Oxa-C6: pH=7.5; Oxa-C8: pH=8.0; Oxa-C12: pH=10.0). For Oxa-C6 and Oxa-C8, the apparent pK_a did not demonstrate obvious change, which indicates that the two carbon atoms difference in hydrocarbon chain length has little effect on self-assembly behavior. This trend is also consistent with the results of the hydrophobicity evaluation by HPLC. On the other hand, the hydrophobicity increased greatly with 12 carbon atoms in the alkyl chain, and the apparent pK_a value was also much higher than those of the other Oxa-lipids. Since the hydrocarbon chain of Oxa-C12 is much longer, the molecules may be packed more densely in its assembled structure than the other Oxa-lipids when the pH value is over the inflection point. The higher density of the negatively charged carboxylate may attract protons more strongly, thus resulting in a higher apparent pK_a. Furthermore, the higher hydrophobicity of Oxa-C12 may also contribute to a larger pK_a value. Based on the pH titration results, the pro-drug analogues with different carbon chains showed different self-assembly behaviors depending on pH, suggesting that the behaviors can be regulated both by pH conditions and molecular structures. In addition, this pH dependence of self-assembly structures is reversible from an insoluble solid state to a micellar structure with increasing pH value. Thus, the pH-responsive self-assembly behavior of these synthetic Oxa-lipids demonstrate potential as a pH-sensitive SADDS for parent drug molecules.

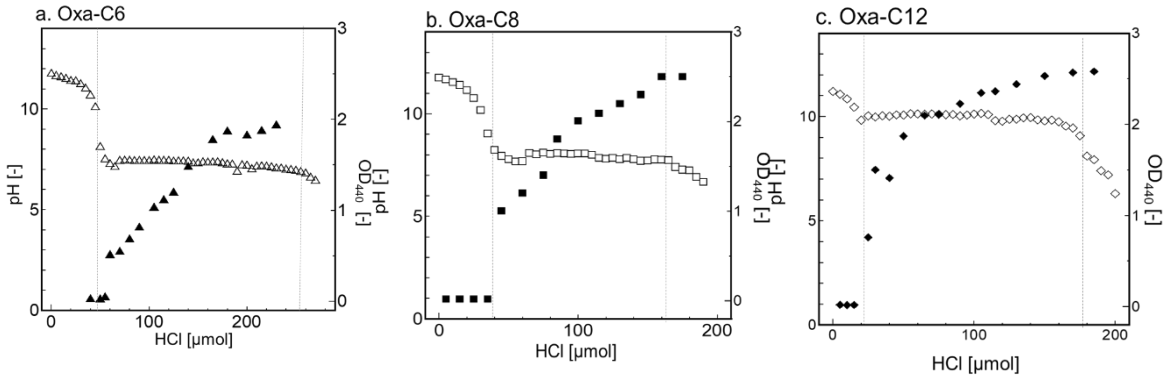

Fig. 6-4. Phase state analysis of Oxa-lipids by pH titration. a) Triangle for Oxa-C6, b) square for Oxa-C8, and c) diamond for Oxa-C12 from left to right, respectively. The open marks stand for pH variation, and the closed ones represent turbidity variation.

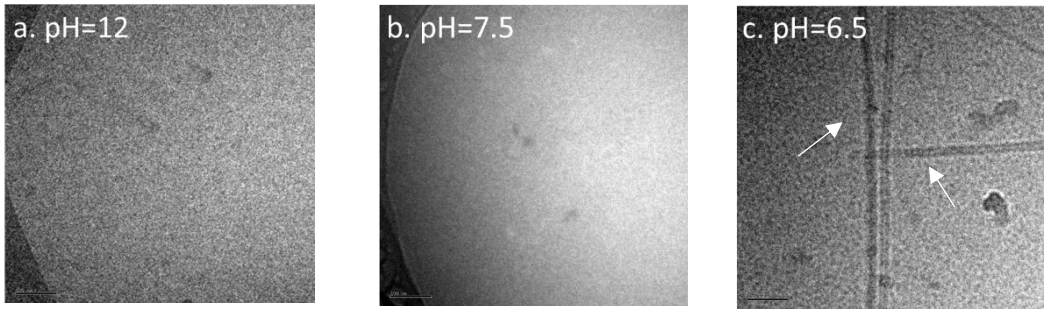

Fig. 6-5. Transmission electron microscopy **(**TEM) images of Oxa-C6 self-assembled structures under different pH conditions (pH=12, 7.5, and 6.5). The scale bar is 100 nm.

3.3. Estimation of Oxa-lipid self-assembly behaviors under biological pH conditions

The above results showed that different formations can be obtained by our fatty acid-like prodrug design under various pH conditions. In addition, we evaluated the influence of prodrug concentration on self-assembly behaviors under biological pH conditions. On the one hand, gastrointestinal tract as the main digestive and absorptive organ, the pH in the gastrointestinal tract has been shown between 2 and 8.5. Different organs function at their optimal level of pH (Aron-Wisnewsky *et al.*, 2012). The enzyme pepsin requires low pH to act and break down food, while the enzymes in intestine require high pH or alkaline environment to function (Solovyev *et al.*, 2015). The pH-responsive variation of self-assembly structures will induce different drug metabolism rate.

On the other hand, there is also difference in the normal tissue and diseased tissue.

Usually, the inflammatory site or the cancerous site shows lower pH. The pH-responsive variation of self-assembly structures can influence on the accumulation and uptake of the drug at diseased region. Here, the pH conditions as follows were selected to imitate the different pH environment stressors within biological organisms: pH=9 (carbonate buffer, 50 mmol/L), pH=7.4 (phosphate buffer, 50 mmol/L), and pH=6 (acetate buffer, 50 mmol/L). In this study, the associations between self-assembly behaviors and concentrations of the Oxa-lipids under different pH environments were evaluated.

As described previously, the transparent solution under high pH conditions was considered to be a micellar structure. Here, the CMC of the formed micellar structure was determined using Nile Red as a fluorescence probe. This probe is almost non-fluorescent in water or other polar solvents but strongly fluorescent in less polar environments, showing an intense emission peak in the 600–650 nm region (Coutinho *et al.*, 2015). The maximum fluorescence intensity of Nile Red at the emission peak was plotted with different concentrations of the Oxa-lipids to estimate the CMC. **Fig. 6** shows the results of CMC analysis for Oxa-C6 under pH=7.4. At low concentrations, the fluorescence intensity of Nile Red was also low, indicating that Nile Red detects a purely hydrophilic environment. However, when the Oxa-C6 concentration increased above the CMC near 5.2 mM, the intensity increased significantly. This change indicates that the amphiphilic Oxa-C6 is now self-organized into micellar-like structures where the parent Oxaprozin molecule and alkyl chains form the hydrophobic core and the anionic carboxyl groups form the hydrophilic corona, thus stabilizing the system in water. As a consequence, Nile Red is now solubilized in the hydrophobic region of the formed micellar structures and "senses" a hydrophobic microenvironment. At a pH=9 condition, both Oxa-C6 and Oxa-C8 can form micellar structures. However, the CMC of the Oxa-lipids decreased from 4.5 mM to 4.0 mM as the hydrocarbon chain length increased, which indicates that the longer hydrocarbon chain enhances intramolecular hydrophobic interaction and thus the formation of micellar structures at low concentrations. This decrease in the CMC value with increased hydrophobicity is consistent with previous reports [17].

The CAC of the fiber structure of Oxa-C8 observed by dark field microcopy images was confirmed by the self-fluorescence properties of the ring structure within the Oxaprozin molecular structure (**Fig. 6-7a**). **Fig. 6-7** presents the CAC measurement result of Oxa-C8 when pH=7.4. By increasing the concentration of the Oxa-lipid, the

fluorescence intensity at 640 nm showed a sharp enhancement near 1 mM. When the molecules were dispersed in solution, they could move freely and showed low fluorescence intensity. On the other hand, when the molecules aggregated together following protonation of the molecules, the fluorescence increased because of the low mobility of the fluorophore. This phenomenon is usually referred to as aggregation induced emission (AIE) (Hong *et al.*, 2009). This AIE effect is thought to be caused by the restriction in the intramolecular rotation (IMR) process of the luminogen. A similar situation was observed in tetraphenylethene; the formation of a crystalline microfiber structure can induce efficient fluorescence emission while the soluble state quenches its emission because its four phenyl rings undergo an active IMR process (Dong *et al.*, 2007). Although the exact explanation for this phenomenon still needs to be confirmed, alteration of the phase state due to increased concentration can be proven. Therefore, the CAC can be confirmed by its self-fluorescence, which is near 0.75 mmol/L for Oxa-C8 (pH=7.4) and 0.6 mmol/L for Oxa-C6 (pH=6). Under the acidic condition of pH=6, the high protonation degree induced high hydrophobicity of Oxa-C8, so the molecules precipitated and separated from the bulk solution.

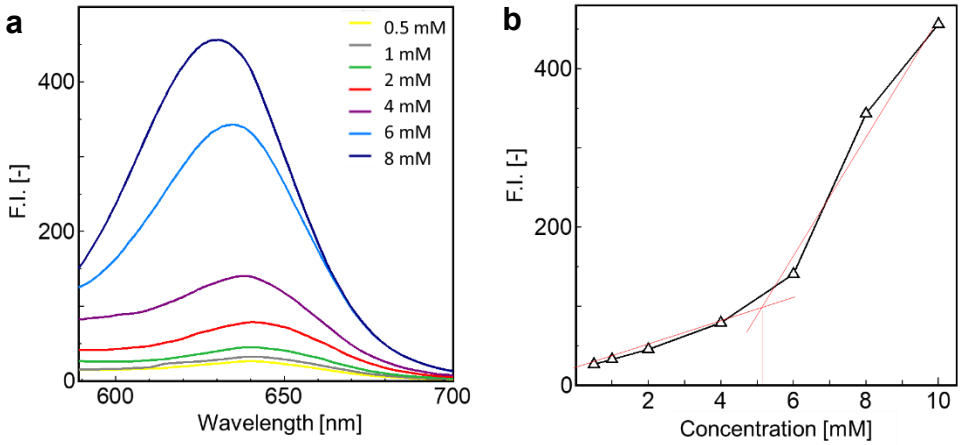

Fig. 6-6 Estimation of the critical micelle concentration (CMC) of Oxa-C6 with Nile Red in 50 mmol/L phosphate buffer (pH=7.4). (a) Fluorescence spectra of Nile Red and (b) the relationship between Oxa-C6 concentration and fluorescence intensity.

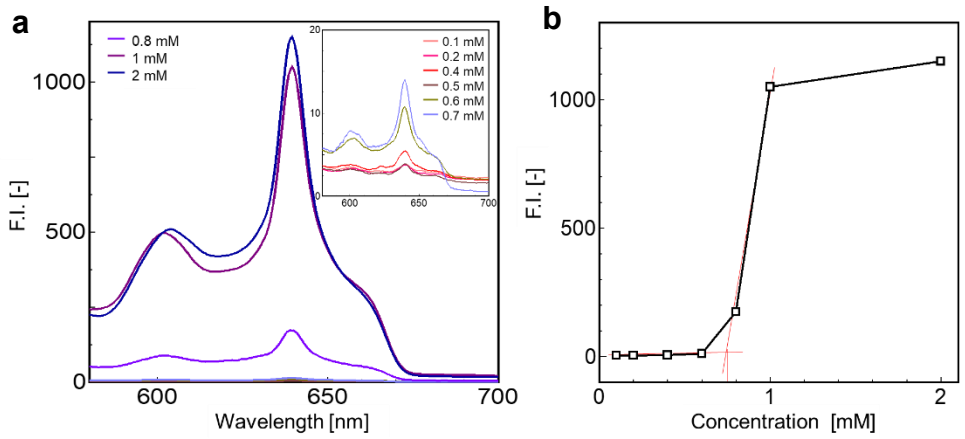

Fig. 6-7 Estimation of the critical aggregation concentration (CAC) of Oxa-C8 by self-fluorescence in 50 mmol/L phosphate buffer (pH=7.4). (a) Fluorescence spectra of Oxa-C8 at various concentrations and (b) the relationship between Oxa-C8 concentration and fluorescence intensity.

Here, the associations between the self-aggregation behaviors and concentrations of Oxa-lipids under different biological pH environments were evaluated and summarized in Table 1. At higher pH conditions (pH=7.4 and pH=9), Oxa-C6 formed a micellar structure with CMCs of 5.2 mmol/L and 4.5 mmol/L, respectively. When the pH decreased to 6, Oxa-C6 will form a fiber structure when the concentration increased to 0.6 mmol/L. For Oxa-C8, a micellar structure could be formed at pH=9 while a fiber structure appeared at pH=7.4. At pH=6, a solid structure was developed because of low solubility. In the case of Oxa-C12, no self-assembly structures could be formed because of the high hydrophobicity. Thus, the formation of Oxa-lipids can be regulated by controlling pH and Oxa-lipid concentrations as well as the design of Oxa-lipid structures. Therefore, our strategy contributes to the possibility of developing a pH-sensitive DDS and it is expected this method can be extended to modify other aryl carboxylic derivatives as non-steroidal anti-inflammatory agents.

Table 1. Summary of the formation and CMC or CAC of Oxa-lipids under different pH conditions

	pH=6	pH=7.4	pH=9
Oxa-C6	Fiber (CAC=0.6 mM)	Micelle (CMC=5.2 mM)	Micelle (CMC=4.5 mM)
Oxa-C8	Insoluble	Fiber (CAC=0.75 mM)	Micelle (CMC=4.0 mM)
Oxa-C12	Insoluble	Insoluble	Insoluble

* The CMC or CAC value was estimated at the described pH condition

4. Summary

In this chapter, based on acknowledge obtained from above studies, a molecular design strategy to regulate self-assembly structure by focusing on modulating the balance of hydrophobic effect and 'solvation' effect of headgroup was proposed. Headgroup of prodrug molecules were regulated by utilizing pH sensitivity of carboxyl headgroup. And the packing density was regulated by change the hydrocarbon chain length of amphiphilic prodrug molecules. Namely, fatty acid-like Oxaprozin prodrugs, Oxa-lipids, were synthesized to enable the control of drug self-assembly behaviors depending on pH conditions and molecular structures. This prodrug design strategy achieved control of the drug self-assembly behavior, changing from micelle to fiber to solid based on pH conditions and molecular structure. The results indicated that prodrug molecules with shorter hydrocarbon chain length (lower packing density) and higher pH condition (higher solvation headgroup) could be highly hydrated to form micelle structure. Reversely, combination of lower pH condition and shorter hydrocarbon chain length is difficult to be hydrated, forming fiber-like structure. Although further evaluation *in vivo* is necessary, this method for designing fatty acid-like prodrugs provides new insight into a potential approach for fine-tuning and optimizing drug loading as well as the physicochemical properties of SADDSs in a precise manner through molecular engineering. In addition, this variation in self-assembly structure depending on pH may also be helpful for the development of a biological microenvironment-sensitive self-assembled DDS.

Chapter 7

General Conclusion

It is known that hydration state of lipid membrane structure plays an important in regulating its biological function. In previous reports, the interactions between lipid membrane and small molecules have usually been considered to induce the change of bulk-phase thermodynamics. In this study, to clarify how do lipid membrane targeting molecules regulate the cellular function by hydration state modification of lipid membrane, the variation of lipid membrane properties by several guest molecules is investigated. Finally, the findings obtained are applied in developing the prodrug based self-assembly drug delivery system by designing fatty-acid like prodrug analogues.

In chapter II, the interaction of Quercetin (QCT) with various lipid membranes possessing different phase states and level of saturation were evaluated to obtain complementary information on the QCT behavior in the different lipid membranes. It is found that incorporation of QCT showed obvious effect on packing density, and the level of unsaturation of lipid molecule played an important role in determining the interaction of QCT within the hydrocarbon tail region of lipid membrane. QCT can regulate hydration state of membrane lipid mainly by change the packing density. And this packing density variation of lipid membrane contribute to inhibit free radical diffusion whin membrane.

In chapter III, interaction of 2-hydroxyoleic acid (2OHOA) on DPPC and SM lipid membrane was studied to clarify the hydrogen bonding induced different effect on lipid membrane interfacial properties. For lipid membrane overall structure, based on the isotherm monolayer study of headgroup region and bilayer study of hydrocarbon chain region, there is no significant difference can be obtained. However, comparing with 2OHOA-incorporated DPPC membrane, 2OHOA-incorporated SM showed stronger negative surficial potential, indicating the interaction with SM molecule induced higher dissociation degree of 2OHOA. In addition, only in SM lipid membrane, the interfacial hydration state showed obvious sensitivity to pH condition and salt concentration.

In chapter IV, the influence of incorporation of Resveratrol (RES) on lipid membranes with different phase states was evaluated by utilizing membrane-binding fluorescent

probes. The binding of RES lead to the membrane polarities decreasing slightly, regardless of the phase states of the membrane, while the membrane fluidities decreased only in the case of liquid-disordered phase. In each model membrane system, the incorporation of RES dramatically dehydrated the membrane surface. This dehydration effect at surface region was attributed to remove water species by hydrogen bonding formed with hydroxyl group of RES. It was been clarified that this effect of RES within lipid membrane could prevent the permeation of water-soluble materials, like ROS, and showed synergistic anti-oxidant effect.

In chapter V, it has known the hydration state of biomaterial surface play important roles in modulating biomolecular structure and function. Polyamidoamine amphiphilic dendrons (AD) contains multiple amide and amine groups, which is expected to achieve control of surficial hydration shell modification of membrane. In this chapter, coassemblies (lipid-AD) were designed by different generation and composition ratio of AD, and the surficial hydration shell was confirmed by modification with AD.

In chapter VI, the method to prepare lipid membrane targeted SADDS with various structure was proposed. The aryl carboxylic acid Oxaprozin (Oxa), a primary non-steroidal anti-inflammatory agent, was selected as a model molecule to design fatty acid-like Oxa-lipid. This prodrug design strategy achieved control of the drug self-assembly behavior, changing from micelle to fiber to solid based on pH conditions and molecular concentration.

Through investigating the membrane properties variation caused by incorporating with several guest molecules, the pattern for multi-level hydration state modification of lipid bilayer structure were proposed. From the hydrocarbon chain region to surface region, there are four main pathways to regulate the membrane hydration state: regulating the alkyl chain packing density; hydrogen bonding network at interfacial region; regulation the transfer of water species at the surface region; formation of hydration shell at the surface layer. In addition, by overall considering the GP_{340} value for both Laurdan and Prodan, it is possible to give a brief guidance for judging the pattern for hydration state modification. At the last chapter, the prodrug was designed focusing on regulating the pack density of SADDS to achieve membrane targeted self-assembly drug design.

Suggestions for Future Works

1. Importance of surficial hydration state for drug delivery system design

As shown in this study, the hydration state at the surficial and interfacial region of lipid membrane showed effect on membrane permeability and stability. It has been known that the surficial hydration state will show significant influence on the interaction between membrane. Lipid molecules with different headgroup molecular structure will has different hydration state at the surficial region. Such as diacylglycerophosphocholine (PC) known as lecithin, possesses both negatively charged phosphate group and positively charged choline group. The zwitterionic head groups are strongly hydrated hydrogen bonds with solvent water. Phosphoethanolamine (PE) has a small head group which preferentially provide a flat membrane surface almost no curvature. The interaction between membrane with different hydration properties would be different, it is necessary to investigate if the hydration would be one of the driving forces to facilitate or inhibit the membrane fusion or endocytosis with cell membrane.

In chapter 5, polyamidoamine amphiphilic dendrons (ADs) with multiple amide and amine groups were utilized to form the hydration shell on lipid membrane surface. The interaction of the designed AD/lipid membrane with lipid membrane could be investigated. It is can be expected that this study will put new insight to design reasonable drug delivery carrier.

2. Establish the membranome therapy method

The relevance between self-assembly structure and bioactivity have discussed in general introduction part. The phenomena have withdrawn much attention from researcher to design drug carrier and control the permeability or release from the drug carrier, its accumulation to the disease site and the retention time in the blood vessel. However, it is worth to point out that the uptake step, which can be regard as a “membrane-membrane” or “molecule-membrane” interaction process usually be ignored. In addition, the membrane properties are known to affect the “membrane-related” behavior, it is expected that the understanding of these membrane properties can contribute to the control of the membrane-related behaviors. In conclusion, it has shown critical potential to achieve ideal therapeutic effect by modifying the physicochemical properties of self-assembly structure and properties. For designed Oxa-

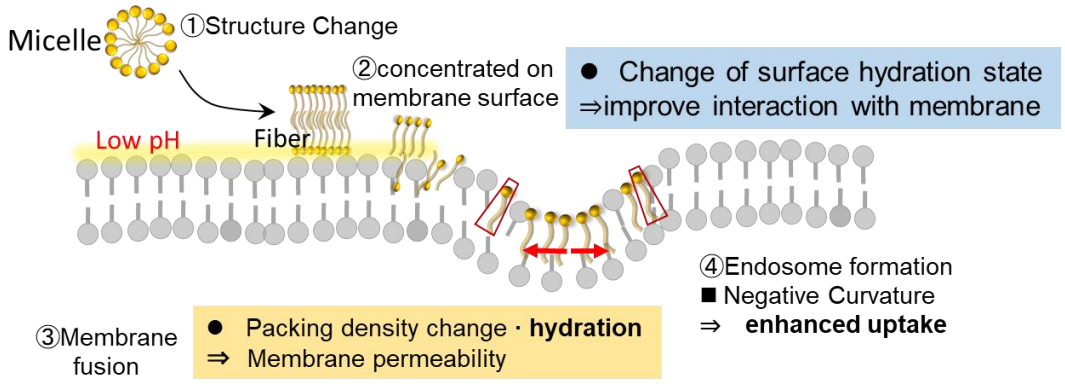

Fig. 7-1 Membrane targeted self-assembly drug molecule design from the viewpoint of "hydration".

lipids prodrugs in chapter 6, the plausible mechanism by regulating the membrane properties was shown in **Fig. 7-1**.

Therefore, based on the basic concept of the lipid-membrane therapy, further evolve membrane lipid therapy can be proposed here: (1) properly design (2) understand the nano- and meso-scopic physicochemical properties of the vesicle membrane itself, which is the molecular assembly itself, (2) design it appropriately, (3) demonstrate the therapeutic effect through delivery and fusion (Membranome therapy) can be proposed (**Scheme 7-1**). The major purpose of the applicant is to synthesize drug-linked amphipathic molecules and design the vesicle structure to form the Smart Prodrug Vesicle (SPV) to develop the improved drug delivery system based Membranome therapy approach. Here, the method to modify the headgroup structure was proposed shown as **Fig. 7-2**, the headgroup possessed positive charge is expected to show stronger disturbation when interact with lipid membrane.

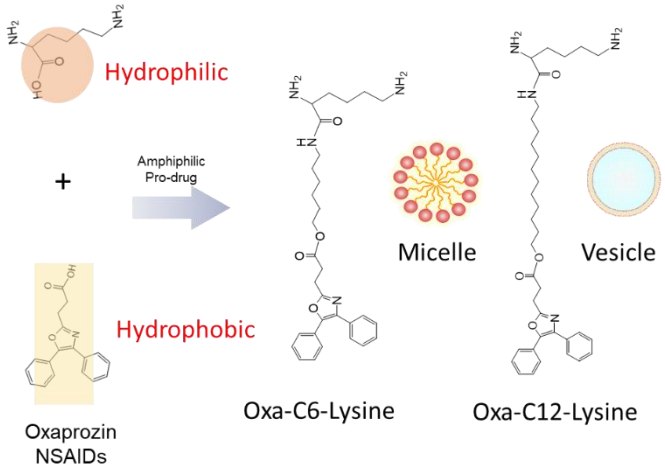

Fig. 7-2 The approach to modify the headgroup structure of Oxa prodrugs

Nomenclatures

Kp	= partition coefficient	[-]
A	= absorbance of UV-Vis light	[a.u.]
P	= Fluorescence polarization of probes imbedded in membranes	[-]
$1/P$	= membrane fluidity	[-]
G	= correction factor	[-]
G	= Gibbs free energy	[J]
GP_{340}	= general polarization calculated at exciting light at 340 nm	[-]
I	= fluorescence intensity	[a.u.]
π	= Surface pressure	*mN/m*
A	= surface Area	$Å^2$
Cs	= Compression modulus	*mN/m*
OD_{400}	= turbidity at 400 nm	[-]
R	= packing density of lipid membrane	[-]
ε	= relative dielectric constant	[-]
Θ	= CD peak (molar ellipticity)	[deg cm^2/dmol]
pK_a	= acidity constant	[-]

List of Abbreviations

CAC	Critical Aggregate concentration
CD	Circular dichroism
Ch	Cholesterol
CMC	Critical Micelle Concentration
DLS	Dynamic light scattering
DLPC	1,2-Dilauroyl-sn-glycero-3-phosphocholine
DMPC	1,2-Dimyristoyl-*sn*-glycero-3-phosphocholine
DNA	Deoxyribonucleic acid
DOPC	1,2-Dioleoyl-*sn*-glycero-3-phosphocholine
DPH	1,6-Diphenyl-1,3,5-hexatriene
DPPC	1,2-Dipalmitoyl-*sn*-glycero-3-phosphocholine
DPPH	2,2-diphenyl-1-picrylhydrazyl
HPLC	High-performance liquid chromatography
Laurdan	6-Lauroyl-2-dimethylamino naphthalene
NMR	Nuclear magnetic resonance
POPC	1-Palmitoyl-2-oleoyl-*sn*-glycero-3-phosphocholine
eggSM	egg sphingomyelin
TEMPO	2,2,6,6-Tetramethylpiperidine 1-oxyl free radical
T_m	Phase transition temperature
UV-vis	Ultraviolet-visible
l_d	Liquid disordered
l_o	Liquid ordered
s_o	Solid ordered

References

Alemany, R.; Vögler, O.; Terés, S.; Egea, C.; Baamonde, C.; Barceló, F.; Delgado, C.; Jakobs, K. H.; Escribá, P. V. Antihypertensive Action of 2-Hydroxyoleic Acid in SHRs via Modulation of the Protein Kinase A Pathway and Rho Kinase. J. Lipid Res. 2006, 47 (8), 1762–1770.

Aron-Wisnewsky, J.; Doré, J.; Clement, K. The Importance of the Gut Microbiota after Bariatric Surgery. Nat. Rev. Gastroenterol. Hepatol. 2012, 9 (10), 590–598.

Arora, A.; Byrem, T. M.; Nair, M. G.; Strasburg, G. M. Modulation of Liposomal Membrane Fluidity by Flavonoids and Isoflavonoids. Arch. Biochem. Biophys. 2000, 373 (1), 102–109.

Athar, M.; Back, J. H.; Kopelovich, L.; Bickers, D. R.; Kim, A. L. Multiple Molecular Targets of Resveratrol: Anti-carcinogenic Mechanisms. Arch. Biochem. Biophys. 2009, 486, 95-102.

Ball, P. Water as an Active Constituent in Cell Biology. Chem. Rev. 2008, 108 (1), 74–108.

Barceló, F.; Prades, J.; Funari, S. S.; Frau, J.; Alemany, R.; Escribá, P. V. The Hypotensive Drug 2-Hydroxyoleic Acid Modifies the Structural Properties of Model Membranes. Mol. Membr. Biol. 2004, 21 (4), 261–268.

Bertelli, A. A. E.; Ferrara, F.; Diana, G.; Fulgenzi, A.; Corsi, M.; Ponti, W.; Ferrero, M. E.; Bertelli, A. Resveratrol, a Natural Stilbene in Grapes and Wine, Enhances Intraphagocytosis in Human Promonocytes: A Co-factor in Antiinflammatory and Anticancer Chemopreventive Activity. Int. J. Tissue React. 1999, 21, 93-104.

Borst, J. W.; Visser, N. V.; Kouptsova, O. Oxidation of Unsaturated Phospholipids in Membrane Bilayer Mixtures Is Accompanied by Membrane £uidity Changes. Biochim. Biophys. Acta 13.

Borst, J. W.; Visser, N. V.; Kouptsova, O.; Visser, A. J. W. G. Oxidation of Unsaturated Phospholipids in Membrane Bilayer Mixtures is Accompanied by Membrane Fluidity Changes. Biochim. Biophys. Acta, Mol. Cell Biol. Lipids 2000, 1487, 61-73.

Bompard, J.; Rosso, A.; Brizuela, L.; Mebarek, S.; Blum, L. J.; Trunfio-Sfarghiu, A.-M.; Lollo, G.; Granjon, T.; Girard-Egrot, A.; Maniti, O. Membrane Fluidity as a New Means to Selectively Target Cancer Cells with Fusogenic Lipid Carriers. Langmuir 2020, 36, 5134–5144.

Brittes, J.; Lúcio, M.; Nunes, C.; Lima, J. L. F. C.; Reis, S. Effects of Resveratrol on Membrane Biophysical Properties: Relevance for Its Pharmacological Effects.

Chem. Phys. Lipids 2010, 163, 747-754.

Bui, T. T.; Suga, K.; Umakoshi, H. Roles of Sterol Derivatives in Regulating the Properties of Phospholipid Bilayer Systems. Langmuir 2016, 32 (24), 6176–6184.

Bulbake, U.; Doppalapudi, S.; Kommineni, N.; Khan, W. Liposomal Formulations in Clinical Use: An Updated Review. Pharmaceutics 2017, 9 (4), 12.

Caldorera-Moore, M.; Guimard, N.; Shi, L.; Roy, K. Designer Nanoparticles: Incorporating Size, Shape and Triggered Release into Nanoscale Drug Carriers. Expert Opin. Drug Deliv. 2010, 7 (4), 479–495.

Cao, Y.; Liu, X.; Peng, L. Molecular Engineering of Dendrimer Nanovectors for SiRNA Delivery and Gene Silencing. Front. Chem. Sci. Eng. 2017, 11 (4), 663–675.

Cevc, G.; Membrane electrostatics. Biochim. Biophys. Acta, Rev. Biomembr. 1990, 1031, 311−382.

Chachaj-Brekiesz, A.; Wnętrzak, A.; Lipiec, E.; Dynarowicz-Latka, P. Surface Interactions Determined by Stereostructure on the Example of 7-Hydroxycholesterol Epimers – The Langmuir Monolayer Study. Biochim. Biophys. Acta BBA - Biomembr. 2019, 1861 (7), 1275–1283.

Cheetham, A. G.; Chakroun, R. W.; Ma, W.; Cui, H. Self-Assembling Prodrugs. Chem Soc Rev 2017, 46 (21), 6638–6663.

Cheetham, A. G.; Zhang, P.; Lin, Y.; Lock, L. L.; Cui, H. Supramolecular Nanostructures Formed by Anticancer Drug Assembly. J. Am. Chem. Soc. 2013, 135 (8), 2907–2910.

Chen, C.; Tian, C.; Chiu, C. The Effects of Alkyl Chain Combinations on the Structural and Mechanical Properties of Biomimetic Ion Pair Amphiphile Bilayers. Bioengineering 2017, 4 (4), 84.

Chen, S.; Jiang, H.; Wu, X.; Fang, J. Therapeutic Effects of Quercetin on Inflammation, Obesity, and Type 2 Diabetes. Mediators Inflamm. 2016, 2016, 1–5.

Chulkov, E. G.; Ostroumova, O. S. Phloretin Modulates the Rate of Channel Formation by Polyenes. Biochim. Biophys. Acta BBA - Biomembr. 2016, 1858 (2), 289–294.

Coutinho, P. J. G.; Castanheira, E. M. S.; Céu Rei, M.; Real Oliveira, M. E. C. D. Nile Red and DCM Fluorescence Anisotropy Studies in C 12 E 7 /DPPC Mixed Systems. J. Phys. Chem. B 2002, 106 (49), 12841–12846.

De Almeida, R. F. M.; Loura, L. M. S.; Fedorov, A.; Prieto, M. Lipid Rafts Have Different Sizes Depending on Membrane Composition: A Time-resolved Fluorescence Resonance Energy Transfer Study. J. Mol. Biol. 2005, 346, 1109−1120.

de Athayde Moncorvo Collado, A.; Dupuy, F. G.; Morero, R. D.; Minahk, C. Cholesterol Induces Surface Localization of Polyphenols in Model Membranes Thus Enhancing Vesicle Stability against Lysozyme, but Reduces Protection of Distant Double Bonds from Reactive-Oxygen Species. Biochim. Biophys. Acta BBA - Biomembr. 2016,

1858 (7), 1479–1487.

de Granada-Flor, A.; Sousa, C.; Filipe, H. A. L.; Santos, M. S. C. S.; de Almeida, R. F. M. Quercetin Dual Interaction at the Membrane Level. Chem. Commun. 2019, 55 (12), 1750–1753.

de la Arada, I.; González-Ramírez, E. J.; Alonso, A.; Goñi, F. M.; Arrondo, J.-L. R. Exploring Polar Headgroup Interactions between Sphingomyelin and Ceramide with Infrared Spectroscopy. Sci. Rep. 2020, 10 (1), 17606.

Disalvo, E. A.; Lairion, F.; Martini, F.; Tymczyszyn, E.; Frías, M.; Almaleck, H.; Gordillo, G. J. Structural and Functional Properties of Hydration and Confined Water in Membrane Interfaces. Biochim. Biophys. Acta BBA - Biomembr. 2008, 1778 (12), 2655–2670.

Dong, Y.; Lam, J. W. Y.; Qin, A.; Liu, J.; Li, Z.; Tang, B. Z.; Sun, J.; Kwok, H. S. Aggregation-Induced Emissions of Tetraphenylethene Derivatives and Their Utilities as Chemical Vapor Sensors and in Organic Light-Emitting Diodes. Appl. Phys. Lett. 2007, 91 (1), 011111.

Escribá, P. V. Membrane-Lipid Therapy: A Historical Perspective of Membrane-Targeted Therapies — From Lipid Bilayer Structure to the Pathophysiological Regulation of Cells. Biochim. Biophys. Acta BBA - Biomembr. 2017, 1859 (9), 1493–1506.

Escribá, P. V. Membrane-lipid therapy: A New Approach in Molecular Medicine. Trends Mol. Med. 2006, 12, 34-43.

Escribá, P. V.; Busquets, X.; Inokuchi, J.; Balogh, G.; Török, Z.; Horváth, I.; Harwood, J. L.; Vígh, L. Membrane Lipid Therapy: Modulation of the Cell Membrane Composition and Structure as a Molecular Base for Drug Discovery and New Disease Treatment. Prog. Lipid Res. 2015, 59, 38–53.

Escriba, P. V.; Ozaita, A.; Ribas, C.; Miralles, A.; Fodor, E.; Farkas, T.; Garcia-Sevilla, J. A. Role of Lipid Polymorphism in G Protein-Membrane Interactions: Nonlamellar-Prone Phospholipids and Peripheral Protein Binding to Membranes. Proc. Natl. Acad. Sci. 1997, 94 (21), 11375–11380.

Escribá, P. V.; Sánchez-Dominguez, J. M.; Alemany, R.; Perona, J. S.; Ruiz-Gutiérrez, V. Alteration of Lipids, G Proteins, and PKC in Cell Membranes of Elderly Hypertensives. Hypertension 2003, 41 (1), 176–182.

Escribá, P. V.; Wedegaertner, P. B.; Goñi, F. M.; Vögler, O. Lipid-protein interactions in GPCR-associated signaling. Biochem. Biophys. Acta, Biomembr. 2007, 1768, 836-852.

Fearon, I. M.; Faux, S. P. Oxidative Stress and Cardiovascular Disease: Novel Tools Give (free) Radical Insight. J. Mol. Cell. Cardiol. 2009, 47, 372–381.

Feng, Z.; Wang, H.; Chen, X.; Xu, B. Self-Assembling Ability Determines the Activity of

Enzyme-Instructed Self-Assembly for Inhibiting Cancer Cells. J. Am. Chem. Soc. 2017, 139 (43), 15377–15384.

Ferrreira, J. V. N.; Grecco, S. dos S.; Lago, J. H. G.; Caseli, L. Ultrathin Films of Lipids to Investigate the Action of a Flavonoid with Cell Membrane Models. Mater. Sci. Eng. C 2015, 48, 112–117.

Fox, C. B.; Uibel, R. H.; Harris, J. M. Detecting Phase Transitions in Phosphatidylcholine Vesicles by Raman Microscopy and Self-Modeling Curve Resolution. J. Phys. Chem. B 2007, 111 (39), 11428–11436.

Gehm, B. D.; McAndrews, J. M.; Chien, P.-Y.; Jameson, J. L. Resveratrol, a Polyphenolic Compound Found in Grapes and Wine, is an Agonist for the Estrogen Receptor. Proc. Natl. Acad. Sci. U. S. A. 1997, 94, 14138-14143.

Gontsarik, M.; Mohammadtaheri, M.; Yaghmur, A.; Salentinig, S. PH-Triggered Nanostructural Transformations in Antimicrobial Peptide/Oleic Acid Self-Assemblies. Biomater. Sci. 2018, 6 (4), 803–812.

Grassmé, H.; Riehle, A.; Wilker, B.; Gulbins, E. Rhinoviruses Infect Human Epithelial Cells via Ceramide-Enriched Membrane Platforms. J. Biol. Chem. 2005, 280 (28), 26256–26262.

Han, J.; Suga, K.; Hayashi, K.; Okamoto, Y.; Umakoshi, H. Multi-Level Characterization of the Membrane Properties of Resveratrol-Incorporated Liposomes. J. Phys. Chem. B 2017, 121 (16), 4091–4098.

Hayashi, K.; Iwai, H.; Kamei, T.; Iwamoto, K.; Shimanouchi, T.; Fujita, S.; Nakamura, H.; Umakoshi, H. Tailor-Made Drug Carrier: Comparison of Formation-Dependent Physicochemical Properties within Self-Assembled Aggregates for an Optimal Drug Carrier. Colloids Surf. B Biointerfaces 2017, 152, 269–276.

Hayashi, K.; Walde, P.; Miyazaki, T.; Sakayama, K.; Nakamura, A.; Kameda, K.; Masuda, S.; Umakoshi, H.; Kato, K. Active Targeting to Osteosarcoma Cells and Apoptotic Cell Death Induction by the Novel Lectin Eucheuma Serra Agglutinin (ESA) Isolated from A Marine Red Alga. J. Drug Delivery 2012, 842785.

He, Y.; Park, K. Effects of the Microparticle Shape on Cellular Uptake. Mol. Pharm. 2016, 13 (7), 2164–2171.

Hendrich, A. B. Flavonoid-Membrane Interactions: Possible Consequences for Biological Effects of Some Polyphenolic Compounds1. Acta Pharmacol. Sin. 2006, 27 (1), 27–40.

Hinman, S. S.; Ruiz, C. J.; Cao, Y.; Ma, M. C.; Tang, J.; Laurini, E.; Posocco, P.; Giorgio, S.; Pricl, S.; Peng, L.; Cheng, Q. Mix and Match: Coassembly of Amphiphilic Dendrimers and Phospholipids Creates Robust, Modular, and Controllable Interfaces. ACS Appl. Mater. Interfaces 2017, 9 (1), 1029–1035.

Hong, Y.; Lam, J. W. Y.; Tang, B. Z. Aggregation-Induced Emission: Phenomenon, Mechanism and Applications. Chem. Commun. 2009, No. 29, 4332.

Huang, J.; Feigenson, G. W. A Microscopic Interaction Model of Maximum Solubility of Cholesterol in Lipid Bilayers. Biophys. J. 1999, 76, 2142–2157.

Ibarguren, M.; López, D. J.; Encinar, J. A.; González-Ros, J. M.; Busquets, X.; Escribá, P. V. Partitioning of Liquid-Ordered/Liquid-Disordered Membrane Microdomains Induced by the Fluidifying Effect of 2-Hydroxylated Fatty Acid Derivatives. Biochim. Biophys. Acta BBA - Biomembr. 2013, 1828 (11), 2553–2563.

Jin, Y.; Tong, L.; Ai, P.; Li, M.; Hou, X. Self-Assembled Drug Delivery Systems. Int. J. Pharm. 2006, 309 (1–2), 199–207.

Kanicky, J. R.; Shah, D. O. Effect of Premicellar Aggregation on the p K a of Fatty Acid Soap Solutions. Langmuir 2003, 19 (6), 2034–2038.

Kessi, J.; Poiree, J.-C.; Wehrli, E.; Bachofen, R.; Semenza, G.; Hauser, H. Short-Chain Phosphatidylcholines as Superior Detergents in Solubilizing Membrane Proteins and Preserving Biological Activity. Biochemistry 1994, 33 (35), 10825–10836.

Khmelinskaia, A.; Ibarguren, M.; de Almeida, R. F. M.; López, D. J.; Paixão, V. A.; Ahyayauch, H.; Goñi, F. M.; Escribá, P. V. Changes in Membrane Organization upon Spontaneous Insertion of 2-Hydroxylated Unsaturated Fatty Acids in the Lipid Bilayer. Langmuir 2014, 30 (8), 2117–2128.

Kitamura, K.; Goto, T.; Kitade, T. Second Derivative Spectrophotometric Determination of Partition Coefficients of Phenothiazine Derivatives between Human Erythrocyte Ghost Membranes and Water. Talanta 1998, 46 (6), 1433–1438.

Kitamura, K.; Imayoshi, N.; Goto, T.; Shiro, H.; Mano, T.; Nakai, Y. Second Derivative Spectrophotometric Determination of Partition Coefficients of Chlorpromazine and Promazine between Lecithin Bilayer Vesicles and Water. Anal. Chim. Acta 1995, 304 (1), 101–106.

Klibanov, A. L.; Maruyama, K.; Torchilin, V. P.; Huang, L. Amphipathic Polyethyleneglycols Effectively Prolong the Circulation Time of Liposomes. FEBS Lett. 1990, 268 (1), 235–237.

Komizu, Y.; Matsumoto, Y.; Ueoka, R. Membrane Targeted Chemotherapy with Hybrid Liposomes for Colon Tumor Cells Leading to Apoptosis. Bioorg. Med. Chem. Lett. 2006, 16 (23), 6131–6134.

Kubota, M.; Haga, H.; Takeuchi, Y.; Okuno, K.; Yoshioka, H.; Yoshioka, H. Effect of tea catechins on the structure of lipid membrane and beta-ray induced lipid peroxidation. J. Radioanal. Nucl. Chem. 2007, 272, 571-574.

Kuikka, M.; Ramstedt, B.; Ohvo-Rekilä, H.; Tuuf, J.; Slotte, J. P. Membrane Properties of D-Erythro-N-Acyl Sphingomyelins and Their Corresponding Dihydro Species.

Biophys. J. 2001, 80 (5), 2327–2337.

Laage, D.; Elsaesser, T.; Hynes, J. T. Water Dynamics in the Hydration Shells of Biomolecules. Chem. Rev. 2017, 117 (16), 10694–10725.

Lairion, F.; Disalvo, E. A. Effect of Dipole Potential Variations on the Surface Charge Potential of Lipid Membranes. J. phys. chem. B. 2009, 113 (6), 1607-1614

Lee, A. G. How Lipids Affect the Activities of Integral Membrane Proteins. Biochim. Biophys. Acta BBA - Biomembr. 2004, 1666 (1–2), 62–87.

Leekumjorn, S.; Sum, A. K. Molecular Studies of the Gel to Liquid-Crystalline Phase Transition for Fully Hydrated DPPC and DPPE Bilayers. Biochim. Biophys. Acta BBA - Biomembr. 2007, 1768 (2), 354–365.

Lentz, B. R. Membrane "Fluidity" as Detected by Diphenylhexatriene Probes. Chem. Phys. Lipids 1989, 50 (3–4), 171–190.

Leonard, S. S.; Xia, C.; Jiang, B.-H.; Stinefelt, B.; Klandorf, H.; Harris, G. K.; Shi, X. Resveratrol Scavenges Reactive Oxygen Species and Effects Radical-induced Cellular Responses. Biochem. Biophys. Res. Commun. 2003, 309, 1017–1026.

Levy, Y.; Onuchic, J. N. Water Mediation in Protein Folding and Molecular Reorganization. Annu. Rev. Biophys. Biomol. Struct. 2006, 35 (1), 389–415.

Lin, Y.; Wang, A.; Qiao, Y.; Gao, C.; Drechsler, M.; Ye, J.; Yan, Y.; Huang, J. Rationally Designed Helical Nanofibers via Multiple Non-Covalent Interactions: Fabrication and Modulation. Soft Matter 2010, 6 (9), 2031.

Liu, X.; Liu, C.; Catapano, C. V.; Peng, L.; Zhou, J.; Rocchi, P. Structurally Flexible Triethanolamine-Core Poly(Amidoamine) Dendrimers as Effective Nanovectors to Deliver RNAi-Based Therapeutics. Biotechnol. Adv. 2014, 32 (4), 844–852.

Liu, Z.; Ren, Z.; Zhang, J.; Chuang, C.-C.; Kandaswamy, E.; Zhou, T.; Zuo, L. Role of ROS and Nutritional Antioxidants in Human Diseases. Front. Physiol. 2018, 9, 477.

Longo, E.; Ciuchi, F.; Guzzi, R.; Rizzuti, B.; Bartucci, R.; Resveratrol Induces Chain Interdigitation in DPPC Cell Membrane Model Systems. Colloids Surf., B 2016, 148, 615-621.

Lu, J.; Hu, J.; Liang, Y.; Cui, W. The Supramolecular Organogel Formed by Self-Assembly of Ursolic Acid Appended with Aromatic Rings. Materials 2019, 12 (4), 614.

Lúcio, M.; Ferreira, H.; Lima, J. L. F. C.; Reis, S. Use of Liposomes to Evaluate the Role of Membrane Interactions on Antioxidant Activity. Anal. Chim. Acta 2007, 597, 163–170.

Luzardo, M. del C.; Amalfa, F.; Nunez, A. M.; Diaz, S.; Biondi de Lopez, A. C.; Disalvo, E. A. Effect of Trehalose and Sucrose on the Hydration and Dipole Potential of Lipid Bilayers. Biophys. J. 2000, 78(5), 2452-2458.

MacDonald, R. C.; MacDonald, R. I.; Menco, B. P. M.; Takeshita, K.; Subbarao, N. K.; Hu, L.-r. Small-volume Extrusion Apparatus for Preparation of Large, Unilamellar Vesicles. Biochim. Biophys. Acta, Biomembr. 1991, 1061, 297−303.

MacDonald, R. C.; MacDonald, R. I.; Menco, B. Ph. M.; Takeshita, K.; Subbarao, N. K.; Hu, L. Small-Volume Extrusion Apparatus for Preparation of Large, Unilamellar Vesicles. Biochim. Biophys. Acta BBA - Biomembr. 1991, 1061 (2), 297–303.

Maestrelli, F.; Cecchi, M.; Cirri, M.; Capasso, G.; Mennini, N.; Mura, P. Comparative Study of Oxaprozin Complexation with Natural and Chemically-Modified Cyclodextrins in Solution and in the Solid State. J. Incl. Phenom. Macrocycl. Chem. 2009, 63 (1–2), 17–25.

Malhotra, B.; Gandelman, K.; Sachse, R.; Wood, N.; Michel, M. The Design and Development of Fesoterodine as a Prodrug of 5-Hydroxymethyl Tolterodine (5-HMT), the Active Metabolite of Tolterodine; 2009; Vol. 16.

Mao, W.; Mao, D.; Yang, F.; Ma, D. Transformative Supramolecular Vesicles Based on Acid-Degradable Acyclic Cucurbit[n]Uril and a Prodrug for Promoted Tumoral-Cell Uptake. Chem. - Eur. J. 2019, 25 (9), 2272–2280.

Márquez-Miranda, V.; Araya-Durán, I.; Camarada, M. B.; Comer, J.; Valencia-Gallegos, J. A.; González-Nilo, F. D. Self-Assembly of Amphiphilic Dendrimers: The Role of Generation and Alkyl Chain Length in SiRNA Interaction. Sci. Rep. 2016, 6 (1), 29436.

Marsh, D. Equation of State for Phospholipid Self-Assembly. Biophys. J. 2016, 110 (1), 188–196.

Martínez, J.; Vögler, O.; Casas, J.; Barceló, F.; Alemany, R.; Prades, J.; Nagy, T.; Baamonde, C.; Kasprzyk, P.; Terés, S.; Saus, C.; Escribá, P. V. Membrane Structure Modulation, Protein Kinase Cα Activation, and Anticancer Activity of Minerval. Mol. Pharmacol. 2005, 67, 531–540.

Mendes, A. C.; Baran, E. T.; Reis, R. L.; Azevedo, H. S. Self-Assembly in Nature: Using the Principles of Nature to Create Complex Nanobiomaterials: Self-Assembling in Nature. Wiley Interdiscip. Rev. Nanomed. Nanobiotechnol. 2013, 5 (6), 582–612.

Mikirova, N.; Riordan, H. D.; Jackson, J. A. Erythrocyte Membrane Fatty Acid Composition in Cancer Patients. P. R. Health Sci. J. 2004, 23 (2), 107-113.

Mineev, K. S.; Nadezhdin, K. D.; Goncharuk, S. A.; Arseniev, A. S. Characterization of Small Isotropic Bicelles with Various Compositions. Langmuir 2016, 32 (26), 6624–6637.

Mintzer, M. A.; Grinstaff, M. W. Biomedical Applications of Dendrimers: A Tutorial. Chem Soc Rev 2011, 40 (1), 173–190.

Morita-Imura, C.; Imura, Y.; Kawai, T.; Shindo, H. Recovery and Redispersion of Gold

Nanoparticles Using the Self-Assembly of a pH Sensitive Zwitterionic Amphiphile. Chem Commun 2014, 50 (85), 12933–12936.

Movahed, A.; Yu, L.; Thandapilly, S. J.; Louis, X. L.; Netticadan, T. Resveratrol Protects Adult Cardiomyocytes Against Oxidative Stress Mediated Cell Injury. Arch. Biochem. Biophys. 2012, 527, 74-80.

Movileanu, L.; Neagoe, I.; Flonta, M. L. Interaction of the Antioxidant Flavonoid Quercetin with Planar Lipid Bilayers. Int. J. Pharm. 2000, 205 (1–2), 135–146.

Nagarajan, R. Molecular Packing Parameter and Surfactant Self-Assembly: The Neglected Role of the Surfactant Tail †. Langmuir 2002, 18 (1), 31–38.

Nasa, P.; Phougat, P. Prodrug: A Novel Approach of Drug Delivery. No. 32, 4.

Neves, A. R.; Lúcio, M.; Lima, J. L. C.; Reis, S. Resveratrol in Medicinal Chemistry: A Critical Review of its Pharmacokinetics, Drug-Delivery, and Membrane Interactions. Curr. Med. Chem. 2012, 19, 1663-1681.

Neves, A. R.; Lúcio, M.; Martins, S.; Lima, J. L. C.; Reis, S. Novel Resveratrol Nanodelivery Systems Based on Lipid Nanoparticles to Enhance Its Oral Bioavailability. Int. J. Nanomed. 2013, 8, 177-187.

Neves, A. R.; Nunes, C.; Amenitsch, H.; Reis, S. Effects of Resveratrol on the Structure and Fluidity of Lipid Bilayers: A Membrane Biophysical Study. Soft Matter 2016, 12, 2118-2126.

Neves, A. R.; Nunes, C.; Reis, S. New Insights on the Biophysical Interaction of Resveratrol with Biomembrane Models: Relevance for Its Biological Effects. J. Phys. Chem. B 2015, 119, 11664-11672.

Neves, A. R.; Nunes, C.; Reis, S. Resveratrol Induces Ordered Domains Formation in Biomembranes: Implication for Its Pleiotropic action. Biochim. Biophys. Acta, Biomembr. 2016, 1858, 12–18.

Okamoto, Y.; Kishi, Y.; Suga, K.; Umakoshi, H. Induction of Chiral Recognition with Lipid Nanodomains Produced by Polymerization. Biomacromolecules 2017, 18 (4), 1180–1188.

Orendorff, C. J.; Ducey, M. W.; Pemberton, J. E. Quantitative Correlation of Raman Spectral Indicators in Determining Conformational Order in Alkyl Chains. J. Phys. Chem. A 2002, 106 (30), 6991–6998.

Orsu, P.; Murthy, B. V. S. N.; Akula, A. Cerebroprotective Potential of Resveratrol Through Anti-oxidant and Anti-inflammatory Mechanisms in Rats. J. Neural Transm. 2013, 120, 1217-1223.

Panche, A. N.; Diwan, A. D.; Chandra, S. R. Flavonoids: An Overview. J. Nutr. Sci. 2016, 5, e47.

Papahadjopoulos, D.; Poste, G.; Schaeffer, B. E. Fusion of mammalian-cells by

unilamellar lipid vesicles – influence of lipid surface charge, fluidity and cholesterol. Biochim. Biophys. Acta 1973, 323, 23-42.

Parasassi, T.; Krasnowska, E. K.; Bagatolli, L.; Gratton, E. Laurdan and Prodan as Polarity-sensitive Fluorescent Membrane Probes. J. Fluoresc. 1998, 8, 365−373.

Patra, J. K.; Das, G.; Fraceto, L. F.; Campos, E. V. R.; Rodriguez-Torres, M. del P.; Acosta-Torres, L. S.; Diaz-Torres, L. A.; Grillo, R.; Swamy, M. K.; Sharma, S.; Habtemariam, S.; Shin, H.-S. Nano Based Drug Delivery Systems: Recent Developments and Future Prospects. J. Nanobiotechnology 2018, 16 (1), 71.

Pawlikowska-Pawlęga, B.; Dziubińska, H.; Król, E.; Trębacz, K.; Jarosz-Wilkołazka, A.; Paduch, R.; Gawron, A.; Gruszecki, W. I. Characteristics of Quercetin Interactions with Liposomal and Vacuolar Membranes. Biochim. Biophys. Acta BBA - Biomembr. 2014, 1838 (1), 254–265.

Pawlikowska-Pawlęga, B.; Gruszecki, W. I.; Misiak, L. E.; Gawron, A. The Study of the Quercetin Action on Human Erythrocyte Membranes. Biochem. Pharmacol. 2003, 66 (4), 605–612.

Pawlikowska-Pawlęga, B.; Ignacy Gruszecki, W.; Misiak, L.; Paduch, R.; Piersiak, T.; Zarzyka, B.; Pawelec, J.; Gawron, A. Modification of Membranes by Quercetin, a Naturally Occurring Flavonoid, via Its Incorporation in the Polar Head Group. Biochim. Biophys. Acta BBA - Biomembr. 2007, 1768 (9), 2195–2204.

Peetla, C.; Stine, A.; Labhasetwar, V. Biophysical Interactions with Model Lipid Membranes: Applications in Drug Discovery and Drug Delivery. Mol. Pharm. 2009, 6 (5), 1264–1276.

Puskas, L. G.; Kitajka, K.; Nyakas, C.; Barcelo-Coblijn, G.; Farkas, T. Short-Term Administration of Omega 3 Fatty Acids from Fish Oil Results in Increased Transthyretin Transcription in Old Rat Hippocampus. Proc. Natl. Acad. Sci. 2003, 100 (4), 1580–1585.

Ramstedt, B.; Slotte, J. P. Sphingolipids and the Formation of Sterol-Enriched Ordered Membrane Domains. Biochim. Biophys. Acta BBA - Biomembr. 2006, 1758 (12), 1945–1956.

Rendón, A.; Carton, D. G.; Sot, J.; García-Pacios, M.; Montes, L.-R.; Valle, M.; Arrondo, J.-L. R.; Goñi, F. M.; Ruiz-Mirazo, K. Model Systems of Precursor Cellular Membranes: Long-Chain Alcohols Stabilize Spontaneously Formed Oleic Acid Vesicles. Biophys. J. 2012, 102 (2), 278–286.

Romano, B.; Pagano, E.; Montanaro, V.; Fortunato, A. L.; Milic, N.; Borrelli, F. Novel Insights into the Pharmacology of Flavonoids: PHARMACOLOGY OF FLAVONOIDS. Phytother. Res. 2013, 27 (11), 1588–1596.

Rothwell, J. A.; Day, A. J.; Morgan, M. R. A. Experimental Determination of

Octanol−Water Partition Coefficients of Quercetin and Related Flavonoids. J. Agric. Food Chem. 2005, 53 (11), 4355–4360.

Sagisaka, M.; Koike, D.; Mashimo, Y.; Yoda, S.; Takebayashi, Y.; Furuya, T.; Yoshizawa, A.; Sakai, H.; Abe, M.; Otake, K. Water/supercritical CO2 Microemulsions with Mixed Surfactant Systems. Langmuir 2008, 24, 10116-10122.

Sagnella, S. M.; Gong, X.; Moghaddam, M. J.; Conn, C. E.; Kimpton, K.; Waddington, L. J.; Krodkiewska, I.; Drummond, C. J. Nanostructured Nanoparticles of Self-Assembled Lipid Pro-Drugs as a Route to Improved Chemotherapeutic Agents. Nanoscale 2011, 3 (3), 919–924.

Saha, S., Panieri, E., Suzen, S., and Saso, L.; The interaction of flavonols with membrane components: potential effect on antioxidant activity. J. Membr. Biol. 2020, 253, 57–71.

Saija, A.; Scalese, M.; Lanza, M.; Marzullo, D.; Bonina, F.; Castelli, F. Flavonoids as Antioxidant Agents: Importance of Their Interaction with Biomembranes. Free Radic. Biol. Med. 1995, 19 (4), 481–486.

Salentinig, S.; Sagalowicz, L.; Glatter, O. Self-Assembled Structures and pKa Value of Oleic Acid in Systems of Biological Relevance. Langmuir 2010, 26 (14), 11670–11679.

Sanver, D.; Murray, B. S.; Sadeghpour, A.; Rappolt, M.; Nelson, A. L. Experimental Modeling of Flavonoid–Biomembrane Interactions. Langmuir 2016, 32 (49), 13234–13243.

Sarpietro, M. G.; Spatafora, C.; Tringali, C.; Micieli, D.; Castelli, F. Interaction of Resveratrol and Its Trimethyl and Triacetyl Derivatives with Biomembrane Model Studied by Differential Scanning Calorimetry. J. Agric. Food Chem. 2007, 55, 3720-3728.

Seto, H.; Yamada, T. Quasi-Elastic Neutron Scattering Study of the Effects of Metal Cations on the Hydration Water between Phospholipid Bilayers. Appl. Phys. Lett. 2020, 116 (13), 133701.

Shaham-Niv, S.; Adler-Abramovich, L.; Schnaider, L.; Gazit, E. Extension of the Generic Amyloid Hypothesis to Nonproteinaceous Metabolite Assemblies. Sci. Adv. 2015, 1 (7), e1500137.

Sharma, N. K.; Singh, M.; Bhattarai, A. Hydrophobic Study of Increasing Alkyl Chain Length of Platinum Surfactant Complexes: Synthesis, Characterization, Micellization, Thermodynamics, Thermogravimetrics and Surface Morphology. RSC Adv. 2016, 6 (93), 90607–90623.

Sinha, R.; Gadhwal, M. K.; Joshi, U. J.; Srivastava, S.; Govil, G. Interaction of Quercetin with DPPC Model Membrane : Molecular Dynamic Simulation, DSC and

Multinuclear NMR Studies. J Indian Chem Soc 2011, 88, 9.

Slotte, J. P. The Importance of Hydrogen Bonding in Sphingomyelin's Membrane Interactions with Co-Lipids. Biochim. Biophys. Acta BBA - Biomembr. 2016, 1858 (2), 304–310.

Smith, M. C.; Crist, R. M.; Clogston, J. D.; McNeil, S. E. Zeta Potential: A Case Study of Cationic, Anionic, and Neutral Liposomes. Anal. Bioanal. Chem. 2017, 409 (24), 5779–5787.

Solovyev, M. M.; Kashinskaya, E. N.; Izvekova, G. I.; Glupov, V. V. pH Values and Activity of Digestive Enzymes in the Gastrointestinal Tract of Fish in Lake Chany (West Siberia). J. Ichthyol. 2015, 55 (2), 251–258.

Steinkühler, J.; Sezgin, E.; Urbančič, I.; Eggeling, C.; Dimova, R. Mechanical Properties of Plasma Membrane Vesicles Correlate with Lipid Order, Viscosity and Cell Density. Commun. Biol. 2019, 2 (1), 337.

Suga, K.; Kitagawa, K.; Taguchi, S.; Okamoto, Y.; Umakoshi, H. Evaluation of Molecular Ordering in Bicelle Bilayer Membranes Based on Induced Circular Dichroism Spectra. Langmuir 2020, 36 (12), 3242–3250.

Suga, K.; Kondo, D.; Otsuka, Y.; Okamoto, Y.; Umakoshi, H. Characterization of Aqueous Oleic Acid/Oleate Dispersions by Fluorescent Probes and Raman Spectroscopy. Langmuir 2016, 32 (30), 7606–7612.

Suga, K.; Otsuka, Y.; Okamoto, Y.; Umakoshi, H. Gel-Phase-like Ordered Membrane Properties Observed in Dispersed Oleic Acid/1-Oleoylglycerol Self-Assemblies: Systematic Characterization Using Raman Spectroscopy and a Laurdan Fluorescent Probe. Langmuir 2018, 34 (5), 2081–2088.

Suga, K.; Umakoshi, H. Detection of Nano-sized Sized Ordered Domains in DOPC/DPPC and DOPC/Ch Binary Lipid Mixture Systems of Large Unilamellar Vesicles Using a TEMPO Quenching. Langmuir 2013, 29 (15), 4830–4838.

Suga, K.; Yokoi, T.; Kondo, D.; Hayashi, K.; Morita, S.; Okamoto, Y.; Shimanouchi, T.; Umakoshi, H. Systematical Characterization of Phase Behaviors and Membrane Properties of Fatty Acid/Didecyldimethylammonium Bromide Vesicles. Langmuir 2014, 30 (43), 12721–12728.

Takahashi, T.; Kono, K.; Itoh, T.; Emi, N.; Takagishi, T. Synthesis of Novel Cationic Lipids Having Polyamidoamine Dendrons and Their Transfection Activity. Bioconjug. Chem. 2003, 14 (4), 764–773.

Teres, S.; Llado, V.; Higuera, M.; Barcelo-Coblijn, G.; Martin, M. L.; Noguera-Salva, M. A.; Marcilla-Etxenike, A.; Garcia-Verdugo, J. M.; Soriano-Navarro, M.; Saus, C.; Gomez-Pinedo, U.; Busquets, X.; Escriba, P. V. 2-Hydroxyoleate, a Nontoxic Membrane Binding Anticancer Drug, Induces Glioma Cell Differentiation and

Autophagy. Proc. Natl. Acad. Sci. 2012, 109 (22), 8489–8494.
Tiwari, G.; Tiwari, R.; Bannerjee, S.; Bhati, L.; Pandey, S.; Pandey, P.; Sriwastawa, B. Drug Delivery Systems: An Updated Review. Int. J. Pharm. Investig. 2012, 2 (1), 2.
Tobe, Y.; Utsumi, N.; Kawabata, K.; Nagano, A.; Adachi, K.; Araki, S.; Sonoda, M.; Hirose, K.; Naemura, K. M -Diethynylbenzene Macrocycles: Syntheses and Self-Association Behavior in Solution. J. Am. Chem. Soc. 2002, 124 (19), 5350–5364.
Tree-Udom, T.; Seemork, J.; Shigyou, K.; Hamada, T.; Sangphech, N.; Palaga, T.; Insin, N.; Pan-In, P.; Wanichwecharungruang, S. Shape Effect on Particle-Lipid Bilayer Membrane Association, Cellular Uptake, and Cytotoxicity. ACS Appl. Mater. Interfaces 2015, 7 (43), 23993–24000.
Ulrih, N. P.; Maričić, M.; Ota, A.; Šentjurc, M.; Abram, V. Kaempferol and Quercetin Interactions with Model Lipid Membranes. Food Res. Int. 2015, 71, 146–154.
Umakoshi, H.; Tanabe, T.; Suga, K.; Bui, H. T.; Shimanouchi, T.; Kuboi, R. Oxidative Stress Can Affect the Gene Silencing Effect of DOTAP Liposome in an In Vitro Translation System. Int. J. Biol. Sci. 2011, 7 (3), 253–260.
van Dijk, C.; Driessen, A. J. M.; Recourt, K. The Uncoupling Efficiency and Affinity of Flavonoids for Vesicles. Biochem. Pharmacol. 2000, 60 (11), 1593–1600.
Vögler, O.; Casas, J.; Capó, D.; Nagy, T.; Borchert, G.; Martorell, G.; Escribá, P. V. The Gβγ Dimer Drives the Interaction of Heterotrimeric Gi Proteins with Nonlamellar Membrane Structures. J. Biol. Chem. 2004, 279 (35), 36540–36545.
Walde, P.; Blöchliger, E. Circular Dichroic Properties of Phosphatidylcholine Liposomes. Langmuir 1997, 13 (6), 1668–1671.
Wang, H.; Xie, H.; Wang, J.; Wu, J.; Ma, X.; Li, L.; Wei, X.; Ling, Q.; Song, P.; Zhou, L.; Xu, X.; Zheng, S. Self-Assembling Prodrugs by Precise Programming of Molecular Structures That Contribute Distinct Stability, Pharmacokinetics, and Antitumor Efficacy. Adv. Funct. Mater. 2015, 25 (31), 4956–4965.
Watanabe, N.; Suga, K.; Umakoshi, H. Comparison of Physicochemical Membrane Properties of Vesicles Modified with Guanidinium Derivatives. J. Phys. Chem. B 2017, 121 (39), 9213–9222.
Watanabe, N.; Goto, Y.; Suga, K.; Nyholm, T. K. M.; Slotte, J. P.; Umakoshi, H. Solvatochromic Modeling of Laurdan for Multiple Polarity Analysis of Dihydrosphingomyelin Bilayer. Biophys. J. 2019, 116 (5), 874–883.
Wesołowska, O.; Kuzdzał, M.; Štrancar, J.; Michalak, K. Interaction of the Chemopreventive Agent Resveratrol and Its Metabolite, Piceatannol, with Model Membranes. Biochim. Biophys. Acta, Biomembr. 2009, 1788, 1851−1860.
Wiseman, H.; Quinn, P.; Halliwell, B. Tamoxifen and Related Compounds Decrease Membrane Fluidity in Liposomes: Mechanism for the Antioxidant Action of

Tamoxifen and Relevance to Its Anticancer and Cardioprotective Actions? FEBS Lett. 1993, 330 (1), 53–56.

Wu, J. M.; Wang, Z. R.; Hsieh, T. C.; Bruder, J. L.; Zou, J. G.; Huang, Y. Z. Mechanism of Cardioprotection by Resveratrol, a Phenolic Antioxidant Present in Red Wine. Int. J. Mol. Med. 2001, 8, 3-17.

Yang, Q.; Alemany, R.; Casas, J.; Kitajka, K.; Lanier, S. M.; Escribá, P. V. Influence of the Membrane Lipid Structure on Signal Processing via G Protein-Coupled Receptors. Mol. Pharmacol. 2005, 68 (1), 210–217.

Yao, J.; Wang, J.-Y.; Liu, L.; Li, Y.-X.; Xun, A.-Y.; Zeng, W.-S.; Jia, C.-H.; Wei, X.-X.; Feng, J.-L.; Zhao, L.; Wang, S.-L. Anti-oxidant Effects of Resveratrol on Mice with DSS-induced Ulcerative Colitis. Arch. Med. Res. 2010, 41, 288-294.

Yeagle, P. L., Ed.; The Structure of Biological Membranes, 2nd ed.; CRC Press: Boca Raton, FL, 2005.

Yu, T.; Liu, X.; Bolcato-Bellemin, A.-L.; Wang, Y.; Liu, C.; Erbacher, P.; Qu, F.; Rocchi, P.; Behr, J.-P.; Peng, L. An Amphiphilic Dendrimer for Effective Delivery of Small Interfering RNA and Gene Silencing In Vitro and In Vivo. Angew. Chem. Int. Ed. 2012, 51 (34), 8478–8484.

Zhang, C.; Jin, S.; Xue, X.; Zhang, T.; Jiang, Y.; Wang, P. C.; Liang, X.-J. Tunable Self-Assembly of Irinotecan-Fatty Acid Prodrugs with Increased Cytotoxicity to Cancer Cells. J. Mater. Chem. B 2016, 4 (19), 3286–3291.

List of Publications

[Publications]

1. Jin Han, Keishi Suga, Keita Hayashi, Yukihiro Okamoto, Hiroshi Umakoshi, Multi-Level Characterization of the Membrane Properties of Resveratrol-Incorporated Liposomes. J. Phys. Chem. B, 2017, 121, 4091–4098.

2. Jin Han, Keita Hayashi, Keishi Suga, Yukihiro Okamoto, Hiroshi Umakoshi. Characterization of PH-Responsive Self-Assembly Behaviors of Fatty Acid-Functionalized Prodrug. Biochem. Eng. J. 2020, 164, 107794.

3. Jin Han, Yosuke Iimure, Yukihiro Okamoto, Keishi Suga, Hiroshi Umakoshi. Structure and Properties Characterization of Amphiphilic Dendrons Modified Lipid Membrane. Chem. Lett. 2021, 50, 187-190.

4. Jin Han, Misaki Amau, Yukihiro Okamoto, Keishi Suga, Hiroshi Umakoshi. Investigation of Quercetin interaction behaviors with lipid bilayers: toward understanding its antioxidative effect within biomembrane. J. Biosci. Bioeng. in press.

[Relating Papers / Relating Proceeding]

1. Jin Han, Nozomi Watanabe, Keishi Suga, Tonya Kuhl, Hiroshi Umakoshi. Hydrogen bonding induced different interaction of 2OHOA with DPPC and SM lipid membrane, to be submitted.

2. Huanhuan Chen, Guangzu Wang, Jin Han, Mengyu Xu, Yongqiang Zhao, Huanjian Xu. Copper-Catalyzed Csp3–O Cross-Coupling of Unactivated Alkyl Halides with Organic Peroxides. Tetrahedron 2014, 70 (2), 212–217.

[Article]

1. Keita Hayashi, Jin Han, Hiroshi Umakoshi, Membranome Therapy: Next Generation DDS by Utilizing Designed Vesicle Membranes，Kagaku Kogaku 83（7）, 394-397 (2019)

[International Conference / Symposium]

1. Jin Han, Madoka Kiriishi, Keita Hayashi, Keishi Suga, Yukihiro Okamoto, Hiroshi Umakoshi, “Investigation of Fatty Acid Ketohydrazone Modified Liposome Properties as a Drug Carrier”, 10th Conference of Aseanian Membrane Society (AMS10), Nara, Japan, Jul. 26th-29th (2016)

2. Jin Han, Keishi Suga, Keita Hayashi, Yukihiro Okamoto, Hiroshi Umaokshi, “Multi-Level Characterization of the Membrane Properties of Resveratrol-Incorporated Liposomes”, Int'l Seminar on Biophys. Chem. Biol. Biomembrane and Lipid Bilayers, Osaka, Japan, Oct 9th-10th (2017)

3. Jin Han, Keishi Suga, Keita Hayashi, Yukihiro Okamoto, Hiroshi Umakoshi, “Synergistic Anti-Oxidation Effect of Resveratrol at Lipid Membrane Surface”, AIChE 2018, Pittsburgh, PA, USA, Oct 28th-Nov 2nd (2018)

4. Jin Han, Keishi Suga, Keita Hahayashi, Yukihiro Okamoto, Hiroshi Umakoshi, “Control of Drug Self-Assembly Behaviors by Designed pH-Responsible Pro-Drug Molecules”, APCChE 2019, Hokkaido, Japan, Sep 23th-27th (2019)

5. Jin Han, Keita Hayashi, Yukihiro Okamoto, Keishi Suga, Hiroshi Umakoshi, “Development of pH-Responsible Self-Assembling Prodrug”, AIChE 2020, San Fransisco, CA, USA, Nov. 16th-20th (2020)

Acknowledgements

The author is deeply grateful to Prof. Dr. Hiroshi Umakoshi (Division of Chemical Engineering, Graduate School of Engineering Science, Osaka University) for his insightful comments, guidance, and warm encouragement throughout this work. The author is thankful to Prof. Dr. Nobuyuki Matsubayashi, Prof. Dr. Tomoo Mizugaki (Division of Chemical Engineering, Graduate School of Engineering Science, Osaka University), and Assoc. Prof. Dr. K. Hayashi (Nara College) for a number of valuable comments and suggestions during the completion of this thesis. The author would like to express her gratitude to Prof. Dr. Yukihiro Okamoto (Department of Chemical Engineering, Graduate School of Engineering, Tohoku University) for his enormous encouragements on my research. The author expresses her sincere thanks to Prof. Dr. T. Kuhl (Department of Chemical Engineering, University of California Davis) for enormous supports. The author also would like to express the greatest appreciation to Assoc. Prof. Dr. Keishi Suga (Department of Chemical Engineering, Graduate School of Engineering, Tohoku University) and Assist. Prof. Dr. Nozomi Watanabe (Division of Chemical Engineering, Graduate School of Engineering Science, Osaka University) for her valuable comments and helpful advises. The author would like to offer one's special thanks to Ms. Keiko Fukumoto for her kind support during this work.

The author is thankful to Prof. Dr. Y. Okano, Prof. Dr. M. Nakano, Prof. Dr. T. Hirai, Prof. Dr. N. Nishiyama, Prof. Dr. S. Sakai and all the staff of Division of Chemical Engineering, Graduate School of Engineering Science, Osaka University for their kind cooperation during my research.

The author wishes to thank Prof. Dr. N. P. Atul (Department of Chemical Engineering, University of California, Davis), Prof. Dr. J. P. Slotte (Faculty of Science and Engineering, Abo Akademi University), Prof. Dr. Ho-Sup Jung (Department of Food Science and Biotechnology, Seoul National University), Prof. Dr. D. Nagao (Graduate School of Engineering, Tohoku University), and Assoc. Prof. Dr. A. Kuzume (Institute of Innovative Research, Tokyo Institute of Technology) for their comments and suggestions during this work. The author is grateful for the encouragement given by Prof. Dr. H. Ishii (Yamaguchi University), T. Shimanouchi (Graduate School of Environmental and Life Science, Okayama University), Dr. H. Sugaya (Toray Industries, inc.), and Dr. Y. Yamada (Kao corporation), Assist. Prof. Dr. S. Taguchi (University of Hyogo).

The author is particularly grateful for the assistance given by Y. Iimure and S. Amau. Special thanks are given to following colleagues for their experimental collaboration: F. Iwasaki, M. Hirose, B., Y. Kishi, K. Akizaki, Y. Higashie, T. Ikeda, Y. Otsuka, Y. Shinozuka, S. Sugisaki, A. Tauchi, D. Wada, B. R. Ito, T. Wakita, R. Kawakami, R. Nishino, K. Yoshida, K. Tanimura, K. Kitagawa, Y. Murata, Y. Goto, K. Kojima, B. T. Tham, F. Miftah, M. S. Chern, N. Izza, H. Takase, N. Ikushima, R. Ueno, D. Matsui, R. Murazawa, A. Ajaikumar, W. Wakileh, T. Ozawa, Y. Suzaki, A. Suzuta, K. Hamaguchi, S. Watase, N. Ito, S. Sogabe, J. Nakamura, Y. Nagamura, Y. Niwa, Y. Seno, S. Matsushita, Y. -C. Lai, H. J. Kim, Diyana, A., C. Rifda and all members in Bio-Inspired Chemical Engineering (B-ICE) Laboratory.

The author would like to express deepest appreciation to her parents Chanyi Han and Yilin Li and her siblings Yu Han for their continuous encouragements and great support throughout this work.

The author gratefully acknowledges the financial support of this work by the fellowship of the Japan Society for the Promotion of Science (JSPS).